

**Identifying Vestibular and Visual Cortical Response during Circular
Vection among People with Different Susceptibility to Motion Sickness**

by

ZHAO Yue

A Thesis Submitted to
The Hong Kong University of Science and Technology
in Partial Fulfillment of the Requirements for
the Degree of Doctor of Philosophy
in Industrial Engineering and Logistics Management

March 2017, Hong Kong

Authorization

I hereby declare that I am the sole author of the thesis.

I authorize the Hong Kong University of Science and Technology to lend this thesis to other institutions or individuals for the purpose of scholarly research.

I further authorize the Hong Kong University of Science and Technology to reproduce the thesis by photocopying or by other means, in total or in part, at the request of other institutions or individuals for the purpose of scholarly research.

A handwritten signature in cursive script, reading "Zhao Yue", is positioned above a horizontal line.

ZHAO Yue

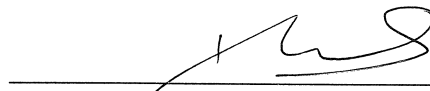
06 March 2017

**Identifying Vestibular and Visual Cortical Response during Circular
Vection among People with Different Susceptibility to Motion Sickness**

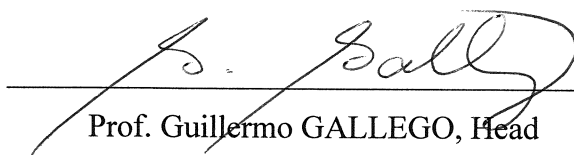
by

ZHAO Yue

This is to certify that I have examined the above PhD thesis
and have found that it is complete and satisfactory in all respects,
and that any and all revisions required by
the thesis examination committee have been made.



Prof. Richard Hau Yue SO, Supervisor



Prof. Guillermo GALLEGO, Head
Department of Industrial Engineering and Logistics Management

06 March 2017

Acknowledgments

My foremost gratitude goes to my supervisor, Prof. Richard SO, for his generous support and help through the whole process. I thank him for his profound knowledge of ergonomics, and rich research experience that helped to shape my research skills. His visionary thoughts and rigorous working attitude have influenced me greatly. In addition, he always encourages and supports me in my decisions on the future career development.

I would like to express my sincere appreciation to the thesis committee members, including Prof. QI Xiangtong and Prof. CHEN Ying-ju in the IELM department, Prof. Michael WONG in the physics department. In particular, my sincere thanks go to Prof. Paul Andrews from St George's University of London for serving as the external examiner. I would also like to thank to Prof. CAI Ning for serving as my preliminary defense committee.

Besides, I would like to thank professors in the IELM department for the courses they offered, which impacted and motivated my research. In addition, I express my sincere thanks to Ms. Fona Wong for her devotion to student affairs.

Last but not least, I would like to thank my family and fellow PGs for their generous support and warm encouragement along the way.

TABLE OF CONTENTS

Title.....	i
Authorization.....	ii
Signature.....	iii
Acknowledgments	iv
Table of Contents	v
List of figures	ix
List of tables	xvi
Abstract.....	xix
CHAPTER 1: INTRODUCTION.....	1
1.1 Background.....	1
1.2 General introduction to the visual system, the vestibular system and their interactions	3
1.3 Motion sickness	6
1.4 Visually induced motion sickness	7
1.5 Illusion of self-motion and vection.....	8
1.6 Near-infrared spectroscopy	10
1.7 Motivation and research gaps	13
1.8 An overview of the research.....	14
1.9 Thesis outline.....	15
CHAPTER 2: LITERATURE REVIEW.....	17
2.1 Cortical area responsive to vestibular functions.....	17
2.2 Review of brain areas activated by different types of vestibular stimulation	18
2.2.1 Brain areas evoked by caloric stimulation.....	19
2.2.2 Brain areas evoked by galvanic stimulation	21
2.2.3 Brain areas evoked by neck vibration	22
2.2.4 Medical cases studies identifying the vestibular areas.	23

2.3 Cortical response during sensory conflicts between visual and vestibular input ..	24
2.4 Visual-vestibular interaction	27
2.5 Motion sickness adaptation	28
CHAPTER 3: STUDY ONE - EFFECTS OF PHYSICAL MOTION ON REGIONAL	
BRAIN HEMODYNAMIC RESPONSES IN HUMAN	31
3.1 Introduction	31
3.2 Objective and hypotheses	31
3.3 Methods	32
3.4 Data analysis and result	39
3.4.1 Data analysis	39
3.4.2 Result	41
3.5 Discussion	47
3.5.1 Brain activation in different condition	47
3.6 Summary	49
CHAPTER 4: STUDY TWO - VERIFICATION OF MOTION ARTIFACT USING	
MANIKIN	50
4.1 Introduction	50
4.2 Objective and hypothesis	50
4.3 Design of experiment	51
4.4 Data analysis	53
4.5 Results and discussion	54
4.6 Summary	55
CHAPTER 5: STUDY THREE - CROSS VALIDATION ON VIMS SUSCEPTIBILITY	
MEASUREMENTS	56
5.1 Introduction	56
5.2 Objective	58
5.3 Design of experiment	58
5.3.1 Subject	58
5.3.2 Experiment procedure	59
5.4 Data analysis	63

5.5 Discussion.....	66
5.6 Summary.....	68
CHAPTER 6: STUDY FOUR - BRAIN HEMODYNAMIC RESPONSES DURING	
VECTION: EFFECTS OF VIMS SUSCEPTIBILITY	69
6.1 Introduction	69
6.2 Experiment 4A – Pilot test on stability of vection onset/offset	70
6.2.1 Subjects.....	70
6.2.2 Stimulus and conditions	70
6.2.3 Data analysis.....	72
6.2.4 Result.....	73
6.3 Experiment 4B –Brain hemodynamic response during vection: effects of VIMS	
susceptibility.....	74
6.3.1 Subjects.....	74
6.3.2 Stimuli and conditions.....	75
6.3.3 Apparatus.....	77
6.3.4 Optodes location	77
6.4 Data analysis.....	79
6.4.1 Subject grouping.....	79
6.4.2 Data processing	80
6.5 Result.....	81
6.6 Discussion.....	86
6.7 Summary.....	88
CHAPTER 7: STUDY FIVE – EXPLORATORY STUDY ON EFFECTS OF	
ADAPTATION ON VIMS SUSCEPTIBILITY AND REGIONAL BRAIN	
HEMODYNAMIC RESPONSES	89
7.1 Introduction	89
7.2 Materials and methods.....	89
7.2.1 Subjects.....	89
7.2.2 Experiment procedure	90
7.2.3 Stimuli	91

7.2.4 Data processing	93
7.3 Result.....	96
7.3.1 Adaptation training result.....	96
7.3.2 Vection behavioral change	97
7.3.3 Hemodynamic change	98
7.4 Discussion.....	101
7.5 Summary.....	102
CHAPTER 8: CONCLUSION	103
Bibliography	107
APPENDIX A: NEAR-INFRARED SPECTROSCOPY MEASUREMENT SYSTEM	121
APPENDIX B: MOTION SIMULATOR	123
APPENDIX C: MSSQ-SHORT	125
APPENDIX D: CONSENT FORM.....	127
APPENDIX E: DATA ANALYZE PROCEDURE	128

LIST OF FIGURES

<i>Number</i>	<i>Page</i>
Figure 1.1 An illustration of vestibular system and its pathways (the picture is downloaded from https://otorrinos2do.files.wordpress.com/2009/12/4.jpg on 10:40pm, UTC+8, Jan 10 st 2017). This figure shows the basic vestibular structure and also some of the neural pathways related with vestibular organ. The vestibular nucleus is composed of superior, lateral, inferior and medial vestibular nucleus (explanation of S/L/D/M shown in the picture). The purpose of the figure is to illustrate how signals received from the eyes and inner ears are integrated in vestibular nucleus.	5
Figure 1.2 This figure illustrates the necessity of visual and real motion as input to generate motion sickness, VIMS andvection. It also shows the differences in symptoms among motion sickness, VIMS andvection.....	9
Figure 1.3 Absorption spectra for oxygenated hemoglobin (HbO), deoxygenated hemoglobin (Hb), cytochrome oxidase, melanin, and water over wavelengths in NIR range from Murkin and Arango (2009). The main purpose of this figure is to show the difference in absorption coefficient of HbO and HB in the near-infrared (NIR) region. It is this difference enables the use of NIR to estimate the HbO and Hb levels.	10
Figure 1.4 An illustration of near-infrared light path way in human brain. Picture source: http://www.iss.com/biomedical/instruments/imagent.html , downloaded on Oct 20 th , 2014. The purpose of this figure is to illustrate the imaginary ‘banana shape’ near-infrared light pathway in human brain. This figure also shows that the near-infrared light comes out from the light transmitter and received by the light detector.	12
Figure 3.1 The flow chart of overall experiment procedure in the experiment investigating the effects of physical motion on cortical responses (Study one). Subjects were allowed to drop out at any time during the exposure, in this experiment,	

none of the subjects dropped out during three sessions of different motion conditions.	33
Figure 3.2 The figure illustrates international 10-20 system used in dividing the surface of a skull with anatomical references. Picture source: http://www.bem.fi/book/13/13.htm , downloaded on Feb 11 th 2017. This picture aims at illustrating some specific locations in the 10-20 system which are T4, C4, O1 and O2. These locations were utilized as references in our experiments for placing the NIR transmitter sources and detectors.....	37
Figure 3.3 An illustration of the locations of the NIR detectors and transmitter sources. The red dots are the detector location, blue dots are the sources location and the dots circled in yellow are extra scalp markers. (The model for the brain is downloaded from http://i2.photobucket.com/albums/y20/MatrixNAN/RealisticMaleHead_06.jpg , on 10:30pm, UTC+8, May, 17 th 2014).....	39
Figure 3.4 Main effect plots of treatment factor for all activated NIR channels (6, 7, 8, 11, and 12). Data from these channels represent signals measured on the nearby cortical areas of temporal parietal region (6), motor/sensory motor areas (7&8) and intraparietal region (11&12). Results of three-way ANOVA show HbO levels were higher in the presence of motion. Data also indicate that HbO change differently in the four conditions (fore-and-aft, lateral, sway and no motion). Data of 12 subjects.....	43
Figure 3.5 Significant changes ($p<0.05$) in HbO levels measured in channel 6 and 8 (corresponding to the cortical areas of temporal parietal region and sensory motor areas) due to the presence of lateral motion in the three repeated sessions (0, 1, 2). Data of 12 subjects. Locations of the channels are shown in Table 3.2	44
Figure 4.1 Photos of experiment set up in control experiment (study two) with a manikin and in experiment (study one) with human subject. As seen from the photo, we tried to replicate the set-up in the manikin experiment to be same with human subject experiment.....	51

Figure 4.2 Photos of NIRS transmitter sources and detectors on the manikin (control study) and a human subject (study one) from the front view.	53
Figure 5.1 The items and levels used in the MSSQ questionnaire. Each subject needs to fill in twice : one for childhood and one for adult period. Total score are calculated by summarizing the childhood score and adult score. For detailed explanation of MSSQ questionnaire, please refer to appendix C.....	57
Figure 5.2 An illustration of vection stimuli and dots rotation direction. The purpose of this figure is to give an illustration of the vection-generating stimulus and show the rotating direction of all black and red dots. The detailed description of the stimulus could be found in the following paragraph.....	60
Figure 5.4 7-point nausea rating adopted from Golding and Kerguelen (Golding and Kerguelen, 1992). This rating shows how nausea level is defined according to the scale. In our experiments, any subjects who reached nausea level of 5 were asked to terminate stimulus exposure and take rest.....	62
Figure 5.7 The scatter plot between MSSQ scores and nausea rating after 20 minutes exposure to circular vection stimuli. Although the correlation was significant ($p < 0.05$), the R-square was 0.32. After removing two ‘outlier’ data points, the R-square improved to 0.62	65
Figure 5.8 The linear correlation between nausea rating after 20 minutes circular vection exposure and nausea rating after 20 minutes game video exposure. No linear correlation could be found between the nausea rating after 20 minutes CV and nausea rating after 20 minutes game video.	66
Figure 6.1 An illustration of vection stimuli in one block. Grey background with the fixation point in the center of the screen was presented for 5s at the very beginning. Then random moving dots were presented for 20 seconds, followed by 30 seconds during which all the dots moved in an co-ordinated direction (roll) while keeping the same speeds when they were moving in random direction. The 20s random moving and the 30s roll rotating sessions were repeated three times. The fixation point was shown in the center of the screen during the entire stimulus period.	72

Figure 6.2 A photograph illustrating the experimental setup with the LCD screen, chin rest and the subject mounted with NIRS transmitters and detectors. A black curtain was temporarily removed for the photo taking.	76
Figure 6.3 An illustration of the NIR detectors and transmitters placement. The red dots represent detector location, blue dots represent transmitters location and the dots circled in yellow are extra scalp markers (taking C _z , C ₄ , T ₄ and O ₂ from the 10/20 system). The image in the lower middle illustrates the locations of the measurement channels in this experiment (The model for the brain is downloaded from http://i2.photobucket.com/albums/y20/MatrixNAN/RealisticMaleHead_06.jpg , on 10:30pm, UTC+8, May, 17 th 2014).....	79
Figure 6.4 The interaction effects of vection (with: condition 0 and without: condition 2) and susceptibility to motion sickness (susceptible: green and resistive: blue) on changes of HbO levels measured in channels 6, 7 (motor/somatosensory area), 10 , 11 and 12 (middle temporal lobe to posterior parietal region). Data from 18 subjects.	82
Figure 6.5 The interaction effects of vection (with: condition 0 and without: condition 2) and susceptibility to motion sickness (susceptible: green and resistive: blue) on changes of HbO levels measured on channels 2, 3 and 4 (corresponding to occipital lobe). All three channels are located at the occipital part of the brain. Exact location of the three channels with reference to 10/20 system could be read from Figure 6.3.	83
Figure 6.6 The interaction effects of vection (with: condition 0 and without: condition 2) and susceptibility to motion sickness (susceptible: green and resistive: blue) on changes of HbO level measured on channel 8 (corresponding to intraparietal area). Motion sickness susceptible group shows significant increases in HbO concentration change while motion sickness non-susceptible group shows significant reduction in HbO concentration changes. The interaction effects were significant. Data from 18 subjects.	84

Figure 7.1 A photograph illustrating subjects with NIRS equipment during pilot testings. The experimental setting in this experiment was the same as that in experiment 4B.	92
Figure 7.2 An illustration of detectors and light transmitters placement. The red dots represent detector location, blue dots represent light transmitters location and the dots circled in yellow are extra scalp markers. The image in the middle illustrates the locations of the channels in this study (The model for the brain is downloaded from http://i2.photobucket.com/albums/y20/MatrixNAN/RealisticMaleHead_06.jpg , on 10:30pm, UTC+8, May, 17 th 2014).....	93
Figure 7.3 An illustration of the changes in the cortical hemodynamic before and after adaptation for subject D. blue dots represent the location of NIR light transmitter and red dots represent the location of NIR detectors. Channels highlighted in red represent HbO level increases in cortical area covered by the channels. Channels highlighted in blue represent HbO level decreases in the cortical area covered by the channels. The purpose of this graph is to illustrate the cortical hemodynamic change before and after adaptation training for motion sickness susceptible subject D.	99
Figure 7.4 An illustration of the changes in the cortical hemodynamic before and after adaptation for subject A. blue dots represent the location of NIR light transmitter and red dots represent the location of NIR detectors. Channels highlighted in Red represent HbO level increases in cortical area covered by the channels. Channels highlighted in blue represent HbO level decreases in the cortical area covered by the channels. Channels not marked in red or blue represent no significant changes were found in the cortical area covered by the channels. The purpose of this graph is to illustrate the cortical hemodynamic change before and after adaptation training for motion sickness susceptible subject A.....	100
Figure 8.1 A graphical summary of hemodynamic changes in response to the presence of vection in Study 1 and Study 4B in this thesis. The brain picture on the top	

righthand corner is adopted from Lopez and Blanke (2011). Red dots on the top righthand corner indicate brain areas which were found to be responsive to caloric stimuli blue dots are those responsive to galvanic stimuli, and yellow dots indicates those responsive to neck vibration. Brodmann area is also shown on the top righthand corner. The purpose of this graph is to illustrate and compare the cortical areas activated in earlier studies (as reported in Lopez and Blanke (2011) and in our studies (Study 1: top lefthand corner; study 4B: lower left and right hand corners). 104

Figure A.1 Imagent ISS: near-infrared spectroscopy system. The Imagent ISS was adopted for NIRS measurement in all our experiments. The system has 4 NIR detectors and 8 pairs of NIR transmitters (one pair contains transmitters of two wavelengths). 121

Figure B.1 A photo of the motion simulator used in the study. The motion simulator could move along the fore-and-aft axis (x) and lateral axis (y). It is designed and built in house at HKUST. The actuation is electromagnetic. 123

Figure E.1 The raw discrete time history a single wavelength near-infra red (NIR) light intensity data measured by the detector ('O4') when transmitter X8 was emitting NIR of 830nm wavelength. Data were plotted in the HomER analysis software. The Purpose is to illustrate what the raw data look like. The diagram on the right illustrate the relative location of channels. 129

Figure E.2 This figure shows the heart rate pattern look-alike wave forms as observed in the raw NIR light intensity data. The purpose of the figure is to illustrate how the heart rate signals were picked up by the NIR raw data. If a channel did not have heart rate signal, we concluded that the channel is dead. The most possible reason was hair blockage. 130

Figure E.3 An illustration of the artifact detection procedure for one single channel. The top figure shows the raw light intensity data and the figure below shows the moving standard deviation (SD). As the SD value went above the threshold as represented by the horizontal line represents the threshold calculated from the raw data. The points raised above the threshold are treated as artifact

contaminated sampling points. The threshold was data driven and was set at 2.5 times of the average SD within a time window of 2s. A sensitivity analysis was conducted on using a threshold of 2 times SD, 1.5 times SD and the main finding did NOT change. 132

Figure E.4 The blocks could be disabled from HomER software directly. Those blocks would not be taken into average in further calculation steps (meanwhile those blocks could be shown in the plots of raw sampling points). The purpose of this figure is to show HomER illustration of raw sampling points and how the channel is excluded from the further calculation in HomER 133

Figure E.5 An illustration of averaged change of HbO across all blocks excluding motion artifact contaminated blocks. Time 0 in the horizontal axis represents stimulus onset. The unit in the horizontal axis is in seconds. The different color curves represent data from different channels. 134

LIST OF TABLES

<i>Number</i>	<i>Page</i>
Table 2.1 Stimulation sites and operations of vestibular stimulation. The purpose of this table is to highlight the various cortical locations previously identified to be associated with vestibular stimulations. This information will be used in later chapters to determine where to put the sensing probes	19
Table 3.1 This table summarizes the tapering modulation function of the motion platform over the first and the last 2 seconds period of each motion stimuli lasting 14 seconds. Motion platform could move in the horizontal plane. It has a displacement driving mechanism. Its motion trace was defined by displacement input along x and y axis. During the starting of motion, motion simulator moved gradually from origin ($x = 0, y = 0$) to the circular trace. This ensured a smooth change in acceleration. During this 2s period, a tapering function was applied and its function is shown in the table. In the motion ending period, motion simulate moved back from circular trace to origin by applying a reverse sequence of (x, y) as in the first 2 second period.	35
Table 3.2 Descriptive statistics of treatment effect (motion) and channel location of three-way ANOVA. This p-values indicate the level of significance between HbO levels measured in the presence and absence of motion (two-level factor, thus degree of freedom is one). Data were measured in Channels 6, 7, 8, 11 and 12 corresponding to the cortical areas of temporal parietal region (channel 6), motor/sensory motor area (channel7 and 8) and intraparietal regions (channel 11 and 12).	42
Table 4.1 Statistical result from three-way ANOVA test in manikin experiment. Results of the ANOVA test show no significant main effect of repeated session (3 repeated sessions, condition (4 moving conditions) and motion (yes/no). None of the two-way interactions was significant.	54

Table 6.1	The statistics table on the difference between vection onset/offset time and reference on/off set time. Onset time difference was calculated by using the difference between onset time and reference onset time in the second and third blocks, while offset time difference was calculated by taking the difference between the offset time and reference offset time in the second and third blocks.....	74
Table 6.2	Significance level for each channel using Kolmogorov-Smirnov normality test. Data failed Kolmogorov-Smirnov normality test if the p-value is less than 0.05. Channels 2, 8 and 10 failed normality test according to the results in the table.	84
Table 7.1	The MSSQ and MSSS score of the subjects in this experiment. This table lists the MSSQ score for both childhood and adult. Subject A had motion sickness in his childhood but never had motion sickness since adult. Subject D was not motion sickness susceptible as a child however became motion sickness susceptible since adult. Subject B and C experienced motion sickness in both childhood and adult period.	94
Table 7.2	The summary of exposure minutes and nausea rating of every subject. The number listed in below table is in the form of exposure minutes (nausea rating). For example, subject A exposed to vection stimuli for 45 minutes and his nausea rating after 45 minutes exposure was 0 in day 1. Subject D reached nausea level of 6 after 6 minutes exposure and he would not continue exposure in day 1. Multiple record on one day means subject took rest between exposures on the same day (generally because subject reported high nausea level).	95
Table 7.3	The vection occurrence and duration for each subject before and after adaptation training. Occurrence refers how many blocks that subject reported vection out of a total number of 15 blocks before and after training. Duration refers to how long could subject feel vection on average before and after training. For example, subject A had vection in all 15 blocks and the average vection period was 15.124s before training. After training, he could feel	

vection in 2 blocks out of total 15 blocks and his average vection period
reduced to 5.494s.....98

Identifying Vestibular and Visual Cortical Response during Circular Vection among People with Different Susceptibility to Motion Sickness

by

ZHAO Yue

Department of Industrial Engineering & Logistics Management
The Hong Kong University of Science and Technology

ABSTRACT

Humans perceive motion information using vestibular and visual organs. Conflicts in motion information perceived from the two systems have been investigated as the major cause of visually induced motion sickness (VIMS). However little is known in the brain hemodynamics responses associated with VIMS provoking stimuli. In particular, whether these brain responses differ between people with different susceptibility to motion sickness is unknown. Indeed, cortical brain response to real physical movement is also poorly documented. This study uses Near-infrared spectroscopy (NIRS) to study the cortical hemodynamic responses to circular vection when watching VIMS provoking stimuli. The research comprises three parts and five studies. First, the cortical areas responding to real physical motion are

investigated. The purpose was to identify the cortical areas sensitive to vestibular stimuli. Results of studies 1 and 2 indicate that different cortical hemodynamics were found in response to different motion conditions (lateral, fore-aft and sway motion) and circular swaying motion produced the strongest hemodynamic responses. The relationships between VIMS susceptibility and patterns in brain hemodynamic responses duringvection were studied in the second part. Results of studies 3 and 4 indicate that the upper lateral area in the right hemisphere and the occipital region of the brain were oxygenated during circularvection, while regions around intraparietal cortex were found to be significantly and consistently affected by motion sickness susceptibility. This is partially consistent with the reciprocal inhibition theory between the visual and vestibular cortices (Brandt *et al.*, 1998). The third part of the research was a pilot study to examine the effects of adaptation on VIMS susceptibility and the regional brain hemodynamic responses. After 7-days desensitization training, the cortical hemodynamic responses of the motion sickness susceptible participant converged to those of non-susceptible participants in the cortical areas which have been identified to be significantly affected by motion sickness susceptibility. In summary, this thesis investigated human cortical regions which could respond to real physical motion and identified cortical responses which are highly correlated with motion sickness susceptibility.

CHAPTER 1: INTRODUCTION

1.1 Background

Visual vestibular interaction functions during everyone's life time and has become a widely studied topic in both medical and academic research (Dichgans and Brandt., 1971; Joseph *et al.*, 1993). Generally speaking, it allows each human to receive visual information and motion signals simultaneously, separate them into independent input sources, and perceive self-motion and object-motion to help control the balance and detect movement (Dichgan and Brandt 1978). In ancient times, this function contributed significantly to locating one-self and objects during hunting and farming. In modern life, it never loses its importance. For instance, one needs to know which direction to go accurately when driving and be aware of the exact paths of the vehicles coming towards him.

Detection of motion in human relies on both visual and vestibular systems. To be more specific, human visual and vestibular systems can perform varieties of functions. On one hand, in addition to gathering static information such as color and shape from our environment, the visual system is able to get motion information about objects in our surroundings. Humans have built up the ability to be aware of self-motion based on other object motions. On the other hand, the vestibular system could directly perceive rotational and linear acceleration of head. Detection of human motion relies on both visual and vestibular systems. Therefore, after combing the input from the proprioceptive system such as muscle and joints, one can control the posture and balance as well. Visual vestibular interaction is the key to maintaining human balance. The human brain has built up a well-developed network for visual and vestibular systems to work in a coordinated way to maintain visual acuity and achieve balance control. These two systems generally work in coordination in our

daily life as above. However, problem occurs when the information from both systems does not match.

Some people will have symptoms, including but not limited to headache, nausea and sweating when they are subjected to mismatched motion information between visual and vestibular system. The symptoms range from slight to severe, and vary quite a lot among individuals (Reason, 1968). One important category of such symptoms is called motion sickness, which refers to the sickness feeling in human caused by conflict between the senses of motion from visual and vestibular system. Motion sickness can further be categorized into car sickness, sea sickness and air sickness.

Due to the commonality and severity of the motion sickness in humans, understanding the mechanism of how the brain works during motion sickness is of practical and theoretical importance. Sensory conflicting theory(Reason, 1978; Oman, 1990; Bles *et al.*, 1998) is one of the theories trying to explain how visual and vestibular system interact under information mismatch, but brain functioning mechanisms are still poorly documented due to technical limitations. This study focuses on studying how our brain coordinates between the visual and vestibular system when mismatched information is perceived. As the brain cortices are the most detailed function center for human, our study investigates on the cortical metabolism activity of human brain during processing mismatched information between the two systems. The stimulus adopted in this study is either real physical motion or visually induced motion sickness, during which the sensation of motion is completely triggered by solely the vestibular system or visual system while the other system receives no information.

1.2 General introduction to the visual system, the vestibular system and their interactions

Understanding the function of visual and vestibular system is the fundamental basis for understanding their interactions. Both visual and vestibular systems are important perception systems of humans and play crucial roles in detecting motion.

Collection and processing information from environment is a fundamental basis function for visual system. Another important capability for visual system is to detect object motion, and in advance, to monitor self-motion (Simpson *et al.*, 1988). It is composed of the eyes, the connecting neural pathways, the visual cortical structures, and other vision related brain structures. Eyes are the main sensory organ which is in charge of receiving light information. Light signal gathered from environment is transferred by neural firing and finally processed in the cortical structure. Based on the information from the visual system, humans are able to detect the color, size, distance, and motion information of objects in attention (Rokszin *et al.*, 2010). Given the basic visual information, the human brain integrates other brain structures to accomplish the object identification, categorization, location and self-motion detection. The visual system is composed of functional specific cortices and visual information is divided into two pathways, one of which processes the location and motion information while the other processes the shape, color information (Grill - Spector and Malach, 2004). It is also one of the most well studied cortical systems. When human moves from one place to another, the displacement of visual features is terminated as optical flow. Optical flow is the most important source people use to get motion information. In the meanwhile, ambiguity and incompleteness are generally found in the motional information derived from visual system due to latency of information perception and irrelevant information processing (Werkhoven *et al.*, 1992).

The vestibular system is located inside the inner ear, and is composed of semicircular canal system and otolith organs. The vestibular system receives and

processes information about head position and body orientation. It cooperates with the visual system and proprioception system to report back information to decide the head position and body orientation. The vestibular system is particularly important in sensing linear and angular acceleration due to its peripheral organ structure located inside the inner ear. Three semicircular canals sense the angular acceleration in different axis, thus they detect rotational movement. The semicircular canals are approximately orthogonal to each other. They detect head rotation by detecting the movement of fluid in the canals. The otolith structure of vestibular organ is composed of two otolith organs, utricle and saccule. The two organs could detect linear acceleration in all directions and trigger eye movement and muscle response. All vestibular organs transduce motion signal to neural signal via triggering hair cells. And neural signals are further projected to cerebellum, cranial nerves, thalamus, spinal cord, reticular and ventral pathways (Bear *et al.*, 2007). A simple illustration of the signal pathways connecting eyes, inner ears (vestibular) via the vestibular nucleus for the purpose of balancing and motion sickness is shown in Figure 1.1.

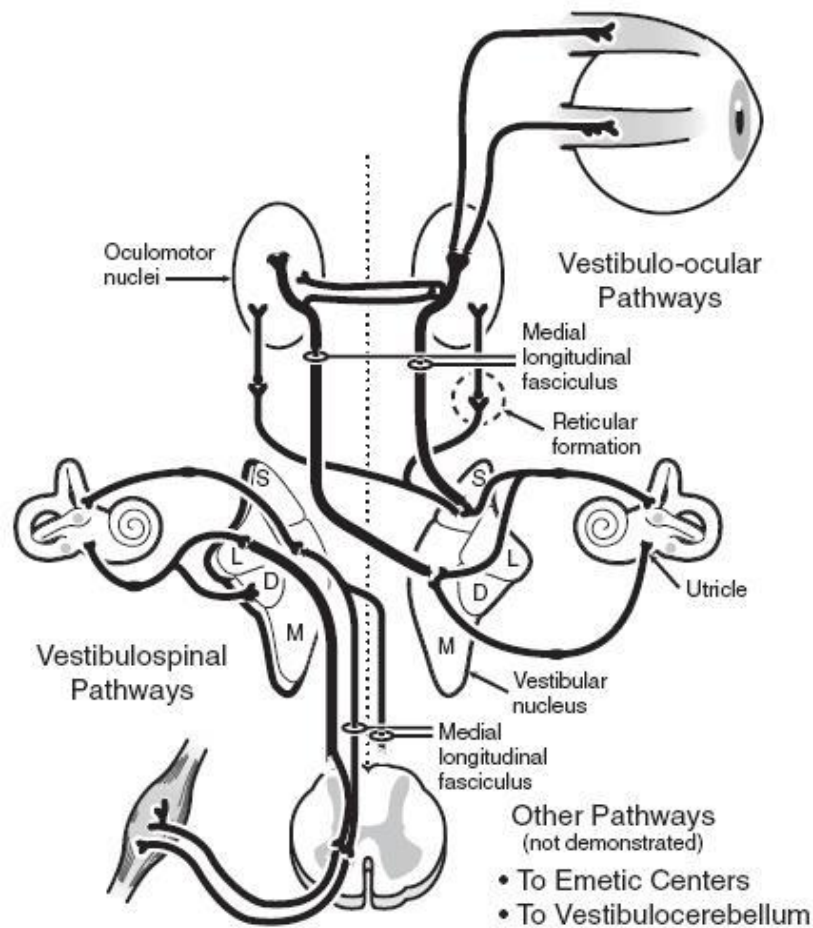


Figure 1.1 An illustration of vestibular system and its pathways (the picture is downloaded from <https://otorrinos2do.files.wordpress.com/2009/12/4.jpg> on 10:40pm, UTC+8, Jan 10st 2017). This figure shows the basic vestibular structure and also some of the neural pathways related with vestibular organ. The vestibular nucleus is composed of superior, lateral, inferior and medial vestibular nucleus (explanation of S/L/D/M shown in the picture). The purpose of the figure is to illustrate how signals received from the eyes and inner ears are integrated in vestibular nucleus.

Comparing the functions of visual and vestibular systems, the visual system is considered as a more direct and comprehensive perceptive system, while the vestibular system detects only relative values of velocity. Therefore vestibular system requires a higher level of information integration and processing from other

sources. Given that the acceleration detected by the vestibular system is considered to be relatively ambiguous to give a whole picture of motion, the perceived motion is relatively dominated by the visual cues.

Visual-vestibular interaction happens all the time in determining magnitude and velocity of transaction, tile, axis and amplitude of self-rotation. Besides the independent functional control of visual and vestibular systems, there is also a functional interaction between these two systems. One of the most well-known visual vestibular interactions is commonly known as vestibular-ocular reflex (VOR). Eye movement can be elicited by stimulating the vestibular system only, and VOR stabilizes the image in the visual field. VOR is an accurate and fast process which is crucial in maintaining gaze stability during motion and independent of visual input (Crane and Demer, 1997).

Visual and vestibular systems generally work in a coordinated way in people's daily life. However, people can suffer from motion sickness when the information from the two systems mismatches. Dizziness, fatigue and nausea are the most common symptoms of motion sickness. Motion sickness happens quite frequently when people travel in cars, airplanes and ships. Based on where the motion sickness happens, people further categorize motion sickness into car sickness, air sickness and sea sickness.

1.3 Motion sickness

Motion sickness is a general term for a constellation of symptoms and signs due to exposure to abrupt, periodic, or unnatural accelerations (Uliano *et al.*, 1986). Dizziness, fatigue, and nausea are the most common symptoms of motion sickness. It is claimed that almost everyone could feel motion sickness with a functioning vestibular system. Existing studies also show that people without functioning vestibular system are immune to motion sickness (Golding, 2006). The motion

sickness caused by a certain type of stimuli would be finally eliminated or significantly lightened after exposing to the same exposure repeated times (Reason, 1978). Motion sickness is also found to be significant varied in susceptibility and adaptation among individuals. Ethnic origin and gender are shown to have an impact on susceptibility (Klosterhalfen *et al.*, 2005). To sum up, motion sickness is a common syndrome and an individualized experience.

Motion sickness is commonly believed to be caused by the conflict of information between visual and vestibular system (Benson, 2002). It could happen during any condition when the conflict of visual and vestibular information input exists. For example, when people sit inside an airplane and do not watch outside the window, motion is sensed only by the vestibular system while no motion is detected by the visual system. According to different motion types, motion sickness is further categorized as air sickness, car sickness and sea sickness. Motion sickness does not necessarily require physical motion. Visual cues which cause people feeling moving could also trigger motion sickness. People are found to be motion sick while watching films, videos and playing computer games. Motion sickness during visual stimuli is more frequently found nowadays with a wider application of virtual reality technologies.

One of the most widely adopted theories is sensory conflict theory. However, there's no agreement on the conflicting source of motion sickness. Conflicting between visual and vestibular system, expected motion and actual motion, and expected and sensed vertical difference have all been proposed as the root cause of motion sickness (Money, 1969; O'Hanlon and McCauey, 1973; Bos and Bles, 1998).

1.4 Visually induced motion sickness

A specific type of motion sickness is called visually induced motion sickness (VIMS), which describes the motion sickness triggered by exposure to visual input only. It

could occur in a large variety of daily environments like cinemas, video games and simulators (So and Ujike, 2010). Motion sickness under VIMS could be purely triggered by visual input, while physical motion could be totally absent in the whole procedure. The symptoms of VIMS are the same as general motion sickness. The sensory conflicting theory is currently adopted to explain the mechanism of VIMS. The conflicts happen when visual system detects moving while vestibular system detects no motion at the same time.

Given the proposed similar root cause and syndromes of VIMS and motion sickness, VIMS generally contains certain types of involuntary eye movement which is called optokinetic nystagmus. Several studies claim that the stimulation of the Vagus nerves from eye movement is the possible cause of motion sickness (Ebenholtz *et al.*, 1994; Gupta, 2005).

1.5 Illusion of self-motion and vection

Illusion of self-motion refers to a phenomenon that occurs when people feel like they are moving when no movement is actually taking place. Vection is a specific type of illusion of self-motion. It describes the illusion of self-motion when it is triggered by a large field of visual movement.

Vection could be triggered in different axes given the proper stimuli. It is generally categorized into linear vection and circular vection. Linear vection usually refers to the self-illusion of moving along one single axis, and circular vection refers to the illusion of self-rotation along one axis. Both linear vection and circular vection could be experienced in daily life. For example, people would generally feel themselves moving when they sit inside a train and watch the train on the next railway pulling in or out. People would also feel themselves rotating or tilting when watching 3D films or using virtual reality instruments. A specific type of involuntary eye movement, nystagmus, is also frequently found during vection.

In addition to visual cues, auditory cues could also trigger vection feeling (Riecke *et al.*, 2005). In this thesis, vection specifically refers to the illusion of self-motion triggered by visual stimuli.

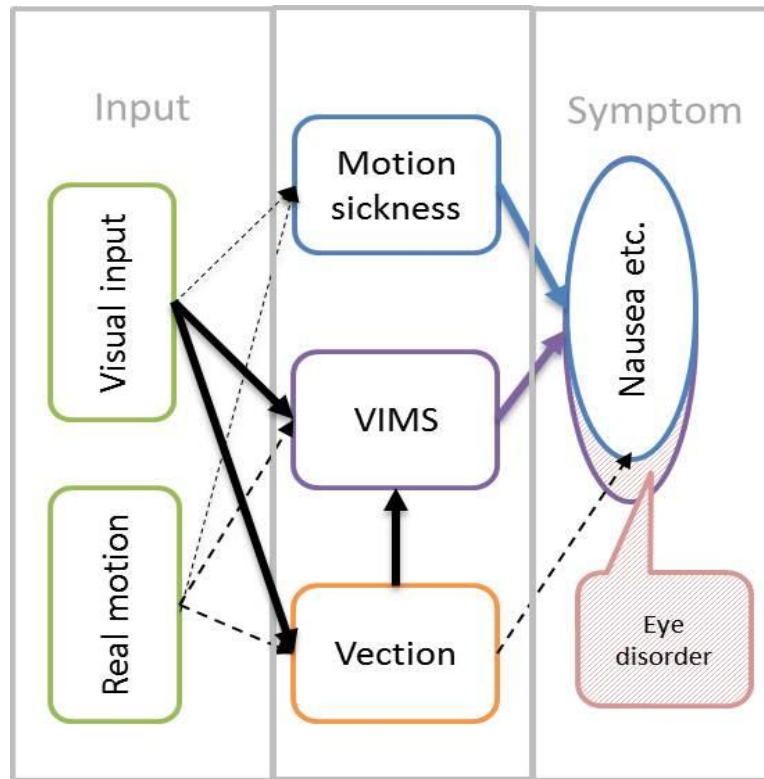


Figure 1.2 This figure illustrates the necessity of visual and real motion as input to generate motion sickness, VIMS and vection. It also shows the differences in symptoms among motion sickness, VIMS and vection.

Figure 1.22 shows a simple illustration of the relationship between motion sickness, visual induced motion sickness, and vection. Visually input is necessary to trigger VIMS and vection, but is not necessary to trigger motion sickness. Real physical motion is not a pre-requisite to any of motion sickness, VIMS or vection. In terms of symptoms, most common symptoms such as nausea, dizziness and fatigue could be found in motion sickness, VIMS and vection. Eye disorders could also be found in VIMS and vection. In advance, Some previous studies claims that vection is a pre-requisite of VIMS (Smart *et al.*, 2002).

1.6 Near-infrared spectroscopy

Near-infrared spectroscopy (NIRS) is a non-invasive functional brain imaging technology which monitors the hemodynamic changes in the brain cortical regions (Jobsis 1977; Chance *et al.*, 1993). Dating back to 1977, near-infrared light was first found to be able to penetrate brain and myocardial tissues with high transparency (Jobsis, 1977). A cerebral oximetry study was later conducted using NIRS measurement in 1985 (Ferrari *et al.*, 1985). NIRS utilizes the light in the near-infrared region (650 nm to 950 nm) to conduct brain activity measurement. Human tissues, including the skull, are relatively transparency in the near-infrared light region.

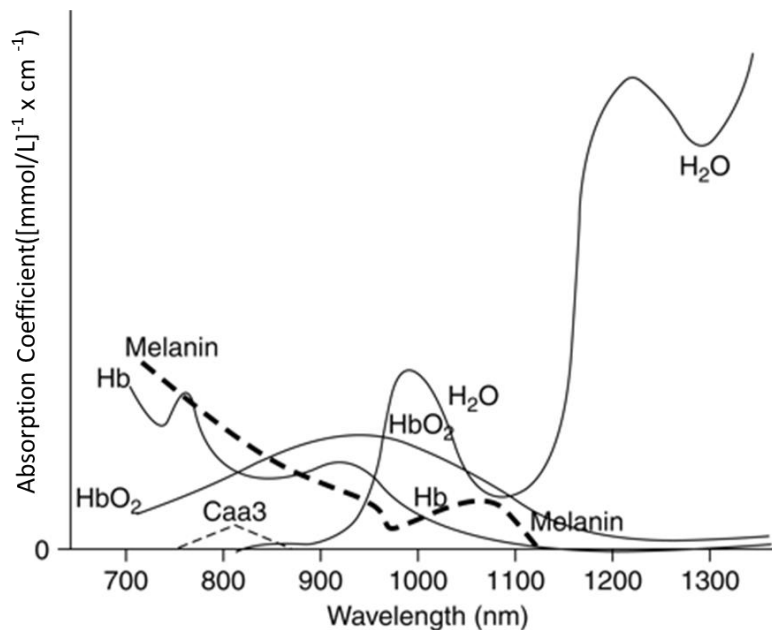


Figure 1.3 Absorption spectra for oxygenated hemoglobin (HbO₂), deoxygenated hemoglobin (Hb), cytochrome oxidase, melanin, and water over wavelengths in NIR range from Murkin and Arango (2009). The main purpose of this figure is to show the difference in absorption coefficient of HbO₂ and Hb in the near-infrared (NIR) region. It is this difference enables the use of NIR to estimate the HbO₂ and Hb levels.

Oxy-hemoglobin (HbO) and Deoxy-hemoglobin (Hb) are the main tissue absorbers in the near-infrared region. Water, fat and cytochrome oxidase also have an impact on the near-infrared light absorption, but relatively not as significant as can be seen from Figure 1.32. Melanin could also absorb light strongly in the near infrared region. Therefore extra carefulness needs to be taken to remove the hair from the measurement site while taking the NIRS measurement.

Both experimental and simulation results illustrate a 'banana-shape' pathway of near-infrared light transmission in human tissues. Given that the near-infrared light power from the light transmitter is constant, the depth of penetration is predominately determined by the distance of light transmitter and detector. The mean depth of photon penetration is proved to be approximately one third of the transmitter /detector separation (Germon *et al.*, 1999). So if the distance between the transmitter and detector is short, NIRS could be able to measure the superficial tissues only. The major safety concern on NIRS technology is the burning injuries (Bozkurt *et al.*, 2005). The safety considerations are specifically related with the power of the light sources.

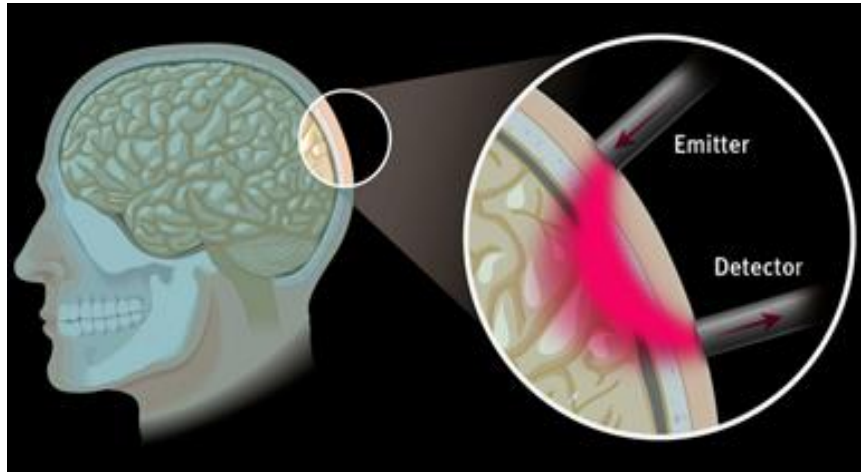


Figure 1.4 An illustration of near-infrared light path way in human brain. Picture source: <http://www.iss.com/biomedical/instruments/imagent.html>, downloaded on Oct 20th, 2014. The purpose of this figure is to illustrate the imaginary ‘banana shape’ near-infrared light pathway in human brain. This figure also shows that the near-infrared light comes out from the light transmitter and received by the light detector.

Compared with existing brain imaging technologies, such as positron emission tomography (PET), computerized axial tomography (CT) and functional magnetic resonance imaging (fMRI), NIRS is especially suitable to be applied in studying the brain response to physical movement due to its portability. NIRS has another advantage of high temporal resolution compared with above mentioned technologies. By monitoring the light intensity changes in the targeted brain regions, NIRS could reveal the local hemodynamic responses and thus could further indicate the neural activities via neurovascular coupling. NIRS has been widely applied to brain imaging studies in the last more than twenty years (Kato *et al.*, 1993; Strangman *et al.*, 2002; Huppert *et al.*, 2006; Hofmann *et al.*, 2008; Boban *et al.*, 2014). On the other side, the spatial resolution of NIRS is generally considered to be less than that of fMRI (Gagnon *et al.*, 2012). And due to the penetration depth limitation of the near-infrared light, the sensitivity of NIRS measurement is limited to superficial level (1 cm) of the cerebral cortex (Boas *et al.*, 2004).

1.7 Motivation and research gaps

Motion sickness is a common syndrome in human beings. Most of the studies agree that mismatched information between visual and vestibular systems is the major cause of motion sickness. There is a large inter-subject variability in motion sickness susceptibility. Both ethnicity and gender have been proven to have impact on susceptibility. For the same exposure to sickness provoking stimuli, there exists people who do not feel motion sick and people who report different severity levels of motion sickness. Most past studies on motion sickness have been behavioral studies. There are relatively few studies looking into brain hemodynamics of visual and vestibular cortices under motion sickness among people with different susceptibility to motion sickness.

This study investigates what are the differences in brain signatures among people with different susceptibility to motion sickness. In particular, the thesis addresses the following research gaps:

The first research gap is that the cortical brain response to real physical movement is still poorly studied. And the research identifies the cortical representation of vestibular cortex using real physical motion.

The second research gap is that visual-vestibular cortical responses during sensory conflict among people with different susceptibility to motion sickness have not been specifically studied. This research investigates whether the brain signatures tovection in motion sickness susceptible groups are different from non-susceptible group.

The third research gap is that the visual-vestibular cortical responses changes after desensitization training to visually induced motion sickness have received little attention. This study investigates what would be the brain hemodynamic change after adaptation training among people with different susceptibility.

1.8 An overview of the research

In order to fill the three research gaps, six studies have been conducted. As motion sickness mainly involves vestibular and visual system, this research will investigate the cortical hemodynamic within the scope of these two systems. The first study serves as the basis for the next studies because it determines the cortical areas which respond to real physical motion. Few brain imaging studies have used real physical motion in locating vestibular cortices due to the requirement of a stationary subject. In this study, three different motion conditions were utilized as motion stimulus including sway, lateral, and fore-and-aft. Brain hemodynamic responses were studied under different motion conditions.

The second study uses a manikin to investigate the possible impact of motion artifact on NIRS measurement in the presence of physical motion. This purpose of this study is to investigate whether motion artifact could significantly impact NIRS measurement under the current experiment set up.

The third study presents a cross validation examination of VIMS measurements. Motion sickness susceptibility survey, motion sickness susceptibility questionnaire and pre-recorded video game were tested as criteria of VIMS susceptibility measurements. Although MSSQ is widely applied in measuring subject motion sickness susceptibility, whether it could serve as the standard to distinguish Asian people among visually induced motion sickness was in doubt. As MSSQ study was originated from non-Asian people and ethnic origin was found to be significantly affecting the motion sickness susceptibility. The purpose of this study was to verify the optimal approach to measuring VIMS susceptibility among MSSS, MSSQ and pre-recorded video game. The optimal approach will be applied in Study 5.

Based on the areas found to be responsive to real physical motion and the results of preliminary experiments, cortical hemodynamic response during vection among people with different motion sickness susceptibility are examined in Study 5. Since

the cortical area around intraparietal region was found to respond differently among people with different susceptibility to motion sickness - a pilot study (study 4) on the stability of vection onset/offset time was also conducted to assist parameter choice before Study 5.

The final study investigates whether the cortical area around intraparietal region could illustrate change in hemodynamic response to VIMS provoking stimuli after adaptation training. This study is a pilot exploratory study into the hemodynamic response before and after adaptation. The result shows the potential change in cortical hemodynamics before and after adaptation training indicatively.

1.9 Thesis outline

Chapter 1 summaries the background of this research and presents a general introduction of visual system, vestibular system and their interactions. It also contains a detailed introduction of motion sickness, visually induced motion sickness, vection and near-infrared spectroscopy. The research gaps, thesis outline of this study are also briefly introduced in this chapter. Specifically, the main research question of this study is: is there brain cortical response difference in human with different motion sickness susceptibility? The other two research questions are: where is cortical representation of vestibular cortex and will the brain cortical response change after motion sickness adaption?

Chapter 2 presents a comprehensive literature review of existing studies related to the research gaps. The first part gives an introduction on the cortical areas which are found to be activated by vestibular stimulation of different categories. The second part reviews past studies of brain hemodynamic response to visual and vestibular stimulations. The third part reviews past literature on motion sickness adaptation.

Chapter 3 reports the results of the first experiment conducted to study the effects of real physical motion on cortical brain hemodynamic responses. Physical motions in

different axes (fore-and-aft, lateral and sway motion) were presented as stimuli and brain hemodynamics in the vestibular related cortical areas were studied in this experiment.

Chapter 4 reports the second experiment which was conducted using a manikin. The objective of the experiment is to verify the potential impacts of motion artifact and instrumental noise during NIRS measurement in the presence of physical motions.

Chapter 5 reports the third experiment conducted to cross validate the use of motion sickness susceptibility questionnaire, motion sickness susceptibility survey, and video game to measure the susceptibility of visually induced motion sickness.

Chapter 6 reports the fourth and fifth experiments conducted to determine the effects of susceptibility to visually induced motion sickness on brain hemodynamic responses during circularvection.

Chapter 7 reports the sixth experiment, a pilot attempt to examine the cortical hemodynamic changes before and after VIMS adaptation. The adaptation procedure lasted for seven days during which participants regularly exposed tovection every day. Hemodynamics measured by NIRS before and after training was taken into comparison to illustrate the change.

Chapter 8 presents an overall discussion, the concluding remarks, and future research opportunities.

Technical details concerning major apparatus used in this thesis are presented in the appendices. The most important instruments used in this research are the Imagent ISS NIRS measurement system and the motion simulator. Details of questionnaires and ratings used to measure the susceptibility to motion sickness and symptoms of motion sickness are also presented in the appendices.

CHAPTER 2: LITERATURE REVIEW

2.1 Cortical area responsive to vestibular functions

Understanding human balancing and motion perception has been a topic of interest for many years. With a fast development in brain imaging techniques, the mechanism of how the brain processes the motion information is attracting more and more attention (Guldin and Grüsser 1998; Sunaert *et al.*, 1999, Pelphrey *et al.*, 2003; Blake and Shiffrar 2007; Grosbras *et al.*, 2012). The knowledge of how the brain reacts to motion not only provides fundamentals to understanding brain neural network, but also forms a solid basis for medical therapy. However, due to the difficulty in combining real physical motion and brain imaging techniques such as Functional Magnetic Resonance Imaging (fMRI), Positron Emission Topography (PET), and brain response to real physical motion are still poorly documented. On the other hand, study human response to motion widely applies alternative methods in current studies to trigger the vestibular system as vestibular system is acknowledged as the key system which plays a central part in receiving and processing information about motion perception, head position and body orientation (Brandt and Dieterich 1999). These alternative methods used to evoke the vestibular system mainly include caloric stimulation (CVS), galvanic stimulation (GVS), neck vibration and auditory stimulation. These stimuli function by stimulating a particular part of the vestibular organs, then the fMRI or PET is generally applied to identify the activated brain areas (Lobel *et al.*, 1998; Bottini *et al.*, 2001; Suzuki *et al.*, 2001; Stephan *et al.*, 2005; Marcelli *et al.*, 2009). For example caloric stimulation works by injecting cold/warm water or gas into the ear canal of the subjects, the vestibular system is considered to be triggered by the injection, and the resulting brain activation map is taken by fMRI or PET to be the functional mapping of

vestibular organ (Fasold *et al.*, 2002; Stephan *et al.*, 2009). In spite of the significant multisensory inputs caused by the stimuli, the way in which the vestibular system is evoked deviates from the general path where the vestibular system is generally triggered by real physical motion in the real world.

In previous studies, the vestibular brain response was proved to be widely spread. Insula area, superior temporal lobe, temporoparietal region, anterior part of occipital lateral gyrus, precentral and postcentral gyrus, precentral sulcus, dorsolateral prefrontal cortex, thalamus, and cerebellum are the responsive regions most frequently found in CVS and GVS studies (Fasold *et al.*, 2002; Suzuki *et al.*, 2001; Stephan *et al.*, 2005; Marcelli *et al.*, 2009). The activated brain areas found by neck vibration are within the active brain regions in CVS and GVS studies (Bottini *et al.*, 2001). As multimodality input is caused in these studies, the brain responding regions could not be elicited only for vestibular system. Apart from alternative stimuli to vestibular system, medical studies using intracranial electrode stimuli directly link cortical regions and human response to get the cortices function (Borchers *et al.*, 2011). A lateral cortical temporoparietal area was defined as temporo-peri-Sylvian vestibular cortex (TPSVC) from an intracranial electric stimulation study which was conducted on 260 patients with partial epilepsy (Kahane *et al.*, 2003). The vestibular symptoms, especially the rotatory sensation could be elicited from this area. Stimulation of parietal operculum and superior and middle temporal gyrus could also elicits sensations of pitch and yaw plane. Most studies showed a right hemispheric dominance of brain response in right handed subjects (Dieterich *et al.*, 2003; Philbeck *et al.*, 2006).

2.2 Review of brain areas activated by different types of vestibular stimulation

While the vestibular system is mainly responsive for perceiving linear and angular motion, most the existing studies which aim at studying the cortical representation of

vestibular system mainly adopt caloric stimulation, galvanic stimulation, neck vibration, auditory stimulation to evoke the particular part in the vestibular organs, due to the limitation of existing brain imaging technologies. The remaining studies on the vestibular system are generally part of medical case study which utilized intracranial electrode stimuli or comparison studies between a particular type of patient and normal people. This part will first give a detailed review of selected studies using particular stimuli, then the summary and comments will be given in the later parts.

The most widely accepted methods of vestibular stimulation are caloric stimulation and galvanic stimulation, there are also some studies using neck vibration to evoke the vestibular system. The stimulation site and the basic operations are listed in Table 2.1.

Table 2.1 Stimulation sites and operations of vestibular stimulation. The purpose of this table is to highlight the various cortical locations previously identified to be associated with vestibular stimulations. This information will be used in later chapters to determine where to put the sensing probes

Stimuli category	Part of organ stimulated	Operation of stimulation
Caloric stimulation	The horizontal semicircular canal.	Injection of hot/cold water/gas into the external ear canal.
Galvanic stimulation	The whole afferent nerve including three semicircular canals and two otolith organs	Alternative current or direct current stimuli on the mastoid bone.
Neck vibration	Neck muscles	Vibration on the posterior neck muscles

2.2.1 Brain areas evoked by caloric stimulation

Caloric stimulation is a widely applied method to evoke the vestibular system. The stimulation operation is injecting hot/cold water/gas into the external canal of

subject's ear. After the caloric stimulation, the evoked brain areas are generally examined by brain imaging technologies such as functional Magnetic Resonance Imaging (fMRI) and Positron Emission Topography (PET). It is already proved that both cortical and sub-cortical structures could be activated in response to the caloric stimuli.

In caloric stimulation studies, there was no uniform standard for stimuli parameters such as water/gas temperature, amount of water/gas injected and injection time, resulting in a variety of stimulation which combines different parameters in such studies. As a result, a network of cortical and subcortical structures were found to be activated in these studies, meanwhile, differences in activated areas exist between different studies.

Cold nitrogen injection (5-7°C, 60s) was applied in an fMRI study examining cortical representation of vestibular system. The brain activation could be described as a cortical network with right hemispheric dominance. The brain areas activated included insula area, temporoparietal region, anterior part of occipital lateral gyrus, precentral and postcentral gyri, precentral sulcus and dorsolateral prefrontal cortex. Individual differences were also reported in cluster size and configuration of some activated areas (Fasold *et al.*, 2002). Short injection of cold water (5ml at 4°C in 1.5s) was adopted in an fMRI study aiming at both cortical and sub-cortical regions responding to caloric stimulation. Unilateral caloric stimuli were applied to the subject's left ear for a single trial. The activated brain areas include right insula, the thalamus, the cerebellum and the brainstem (Marcelli *et al.*, 2009). Another cold water injection (15ml at 4°C in 30s) was applied in the fMRI study. The insula, intraparietal, cingulate and superior temporal gyrus, hippocampus and thalamus were activated regions found according to the stimulation (Suzuki *et al.*, 2001). Relatively longer injection of iced water (30ml in hippocampus, 60s) was applied in a PET study to study the cortical regions activated by caloric stimulation. The brain areas activated include inferior and dorsal frontal gyrus, insula region, temporoparietal junction, thalamus, and cerebellum (Bottini *et al.*, 2001).

Apart from the differences in the operations and materials during caloric stimuli, the injection of water or gas will generally induce sound and even pain in some studies, and subject could be quite alert to such injection. Even after the injection, subject will generally go through a certain period of nystagmus period. All of the evoked response listed above could contribute to the brain signal monitored afterwards. Thus they could bring noise to the brain signal and make the activation of brain areas less comparable between different studies. The multi-modalities responses are quite synchronized and it is very hard to separate them using experiment design.

2.2.2 Brain areas evoked by galvanic stimulation

Galvanic stimulation refers to the electric stimulation exerted on the mastoid bone. It is applied to stimulate the whole vestibular nerve rather than the organ. The current utilized in galvanic stimulation could be either alternative current (AC-GVS) or direct current (DC-GVS). The response evoked by different type of current is different. The response also differs with different stimulation time, current frequency and current density (Stephan *et al.*, 2005).

The type of current exerted could influence the subject response directly. During the DC-GVS, the onset and offset of the stimuli could trigger strong vestibular sensation while the sensation was weaker in-between the onset and offset. On the other hand, subjects under AC-GVS experienced vestibular sensation during the whole stimulation period. Subjective decay was reported by subjects in galvanic stimulation, especially when the subject is stimulated by DC current in the supine position. AC-GVS will generate perceived movement change, which can be avoided by DC-GVS. DC-GVS excited a subset of cortical areas activated by AC-GVS (Stephan *et al.*, 2009).

Sinusoidal stimulation current with different frequencies was carried out to investigate whether the frequency will have an influence on different brain areas. It is reported that the frequency of AC-GVS could influence the amplitude of activation

but have no influence on the activated cortical regions. The regions activated in this study include supramarginal gyrus, posterolateral thalamus, cerebellar vermis, posterior insular and hippocampal region (Stephan *et al.*, 2005).

Unlike most of the galvanic studies, insula was not reported to be activated in another fMRI study published in 1998. In this study, the temporoparietal junction, intraparietal sulcus and pre-motor regions of the frontal lobe are found to be activated by galvanic stimulation. Also in this study, temporoparietal junction activation was found in the left hemisphere rather than the right hemisphere using right-handed subjects, which was also contradictory to the right hemispheric dominance found in other studies. (Fasold *et al.*, 2002, Dieterich *et al.*, 2003)

The difference between the caloric and galvanic stimulation could be concluded from a large variety of aspects although there are some overlapping between the activated brain areas. Apart from the stimulated part of organ and the material summarized in Table 2.1, caloric stimuli could be unilateral, while the galvanic stimulation is generally bilateral. The sensations are also different, galvanic stimulation generally introduces ocular torsion, and the sensation changed according to different parameters of stimulation meanwhile caloric stimuli generally introduce horizontal nystagmus. Compared with caloric stimulation, galvanic stimulation generally has a shorter response time, and shorter duration of evoked vestibular symptoms. Both caloric and galvanic stimuli could evoke multi-modal input, apart from the sound and pain in caloric stimulation, galvanic stimulation could also introduce pain due to the heat of electrode on the mastoid bone (Lobel *et al.*, 1998).

2.2.3 Brain areas evoked by neck vibration

The utilization of neck vibration as a vestibular stimuli originate from classical anatomical studies that signals from vestibular and neck muscle converge in the vestibular nuclei.

Vibration at 80 Hz with 0.4mm amplitude was conducted on the left posterior neck muscles through an experimental vibrator. The neck vibration caused subjects to have illusion of horizontal movement of a fixed point of light. Insula area, somatosensory area were proved to be activated responding to this vibration. Activation in superior temporal lobe and in other subcortical regions was also reported (Bottini *et al.*, 2001).

2.2.4 Medical cases studies identifying the vestibular areas.

The medical case study is also a very important aspect in studying and understanding the functional brain regions which response to a certain system. Medical cases could provide the advantages of stimulation result comparison between normal people and patients with diseases related to vestibular disorders, and in some cases, directly stimulation on the brain cortical or sub-cortical regions is needed as for pre-surgery examination. These cases are of special value to identify the inversed control mechanism of stimulating brain areas. However, considering the connection and pathology changes in the brain of the patients, the generalization of results from the medical cases should be carefully demonstrated.

A comparison caloric stimulation study was conducted to identify the brain regions which could respond. The comparison was made between six healthy people and six patients who underwent the removal of a tumor from the right cerebello pontine angle. The vestibular function was lost among the patients. Iced water (30ml at 0 °C in 60s) was injected into the external acoustic meatus, and brain signals collected by PET. The comparison result between healthy people and patients showed that no difference was found in the left-sided CVS stimuli, however difference was found in the right-sided CVS. The differences are in inferior parietal lobe, temporoparietal junction, transverse temporal gyri and superior temporal gyri (Emri *et al.*, 2003).

Intracranial application of electrical current to the cortex is another important category of stimulation which has been used as a standard technique to examine the

function of brain areas in brain surgeries on tumors or epilepsy for years. Unlike other types of stimulation such as caloric and galvanic stimulation mentioned previously which bear the limitation of unclear or uncertain stimulation-response mechanism, it is very intuitive to link the response and the relative stimulate site up during the intracranial stimulation. Although there is argument that the physiology of such kind of stimulation is still poorly understood, and high variability exists in the behavioral response (Borchers *et al.*, 2003), studies in this category are still valued in cognitive neuroscience.

A lateral cortical temporoparietal area was defined as temporo-peri-Sylvian vestibular cortex (TPSVC) from an intracranial electric stimulation study which was conducted on 260 patients with partial epilepsy. The vestibular symptoms, especially the rotatory sensation could be elicited from this area. Stimulation on parietal operculum and superior and middle temporal gyri could also elicits sensations of pitch and yaw plane (Kahane *et al.*, 2003).

2.3 Cortical response during sensory conflicts between visual and vestibular input

Motion perception and balance control for humans requires a good coordination of the visual system and vestibular system. The visual system and vestibular system work in accordance to detect motion and the orientation relative to gravity. Visual system detects the motion direction via optical flow when the person moves from one place to another. Motion perception through visual system has inadequacy and ambiguity due to latency and incompleteness of visual information processing. The vestibular system detects acceleration of the head. The two systems provide complementary information to each other and realize posture control, motion perception and eye movement control. Other systems contributing to human motion perception includes the auditory system and somatosensory system as well.

Incongruent information perceived by the two systems could cause motion sickness in susceptible populations (Owen *et al.*, 1998). And most of the researchers agree that motion sickness is primarily due to the incongruence of sensory information perceived from visual and vestibular system (Rine *et al* 1999). One of the most well adopted explanations to motion sickness is the sensory conflict theory (Kohl R L, 1983; Oman CM, 1990), which states that the conflicting between sensory perceptions is the source of motion sickness. Vestibular system is proven to be essential in motion sickness as it was found that people without functional vestibular system are immune to either motion sickness or visually induced motion sickness (Cheung *et al.*, 1991, Golding 2006). During decades of debate on the mechanism of motion sickness, motion status derived from visual information is also shown to be an important source to provoke the feeling of motion sickness (Bles *et al.*, 1998). With the wide application of visual reality technology, it is found that motion sickness happens when people watches moving scenes in stationary posture (Ujike H, 2009). Motion sickness is proved to be most provocative by visual stimulus (Eyeson-Annan *et al.*, 1996). Under certain circumstances, such as viewing objects moving towards one direction from a large screen, people could feel themselves moving instead of the objects moving. The illusion of self-motion in these cases is termed asvection. Motion sickness triggered by visual stimuli is termed as visual induced motion sickness (VIMS). Most studies claimvection is the necessary component for VIMS at the early stage (Keshavarz *et al.*, 2015). The visual and vestibular information conflict, which is believed to be the possible source of motion sickness, is also functioning throughvection or VIMS. This provides a unique chance to study and understand how the sensory systems work under sensory conflict. In advance, understanding the brain mechanism of motion sickness is of vital importance to the prevention and therapy of related diseases and syndromes.

Brain activities during motion sickness induced by real physical motion are not intensively studied because the existing brain imaging technologies such as fMRI and PET are strictly intolerant to real physical motion. Different visual patterns which

could trigger vection or VIMS were widely adopted by most of studies exploring the brain response, as those patterns could introduce the similar sensory conflict compared with motion sickness triggered by physical motion based on sensory conflict theory.

A PET study on brain response of visual and vestibular system was conducted using large field circular vection which is composed of coherently moving dots in same angular speed. During the period of circular vection, bilaterally medial parieto-occipital visual areas were found to be activated, and parieto-insular vestibular cortexes were deactivated in the meanwhile (Brandt *et al.*, 1998). Reciprocal inhibitory interaction between the visual and vestibular system was proposed from this study, claiming that brain redistributes sensorial weight between different sensory cortices by self-modulation. The theory was further tested by another study, in which one of the conditions used a similar kind of stimulus but at a higher speed, and the similar activation and deactivation of brain areas was reported (Deutschlander *et al.*, 2002). The difference of activity between visual and vestibular brain areas was also found in vestibular stimulation studies (Wenzel *et al.*, 1996). One recent fMRI study revealed the different activation of left anterior cingulate cortex between the nausea-sensitive and nausea-resistant people, the more activated area among nausea-sensitive group could be due to the arousal of autonomic system (Farmer *et al.*, 2015).

The susceptibility to motion sickness varies a lot among individuals. One study reported that one third of Hong Kong Chinese people are susceptible to motion sickness (So *et al.*, 1999). However, whether the brain responds differently to motion sickness provoking stimuli among people with different susceptibility to motion sickness is not documented. This study will investigate the cortical response to motion sickness provoking stimuli among people with different susceptibility to motion sickness.

2.4 Visual-vestibular interaction

Visual vestibular interaction comes naturally in human to maintain gaze stability during daily movement (Crane and Demer 1997). The neural correlation works not only on keeping retinal image stable by making compensating eye movement against head rotational or translational movement, but also work together to determine accurate motion status. As mentioned previously, visual information is one of the important sources in motion detection, but its estimation of acceleration of target is relatively poor (Werkhoven *et al.*, 1992). Meanwhile vestibular system has the biological structure to detect head acceleration with the high accuracy,

Brandt conducted a series of experiments to prove his hypothesis that reciprocal inhibition exist between the visual and vestibular systems, the finding starts with finding the visual area, mainly represented by Brodmann area 17, 18, 19 showed significantly decrease during the caloric stimulation of human, and the cold water injection could be able to trigger a higher level of rCBF in the visual cortex compared to that of warm water (Brandt *et al.*, 1996). This deactivation could not be easily clarified to be triggered by either involuntary ocular oscillation or vestibular system, as the caloric stimuli could simultaneously evoke other sensation responses. Meanwhile, the cold water injection was shown to be able to trigger a more significant vestibular feeling.

Then it was hypothesized that the visual system and vestibular system have reciprocal inhibitory interaction in human. But from the experiment above, it is not possible to tell if the deactivation of visual system in previous experiment comes from the inhibition of the visual system or from the side effects caused by vestibular caloric stimulation like involuntary eye movement.

The next experiment comes from Brandt and his colleagues in 1998, where the large field visual motion was used as the stimulation. In that study, illusion of self-motion (vection) was used to trigger the vestibular system (Brandt *et al.*, 1998). The result

showed that the visual area was activated from the large field of visual motion, meanwhile the posterior insula and other vestibular related cortex was deactivated. This experiment also showed regional CBF changes accordingly with the perceived intensity of CV. During the large field visual stimuli, irregular rotatory nystagmus was spotted.

However as both the two studies triggered eye movement to different extents, it is hard to tell if the activation and deactivation of related cortical areas is the reflection of visual vestibular interaction. In the previous study, it was shown that the optokinetic modulation of vestibular activity is more related to ocular motor function. This means with the eye fixation, the response in the PIVC is considered to be solely related to vestibular function.

Then in 2002, four experiment conditions were used to trigger the response from the vestibular area (Brandt *et al.*, 2002). Condition A used simply caloric stimuli, condition B used counter-clockwise rotating dots, however in whichvection was not triggered, condition C mix condition A and condition B together, in which the dots in condition B are stationary under this situation. Condition D is the baseline, subjects lied supine with their eye closed. The result of this research was in line with the reciprocal inhibition theory between the visual system and vestibular system.

2.5 Motion sickness adaptation

Motion sickness is a common symptom with great individual variation in susceptibility. The most common motion sickness syndromes include nausea and vomiting. Other syndromes include, but are not limited to, pallor of different degrees, cold sweating, drowsiness and headache. People's response to motion sickness stimuli relies heavily on the provocativeness of stimulation and his or her prior experience. The difference in susceptibility has been investigated for both academic purpose and for practical usage. The stimuli triggering motion sickness could be either real physical

motion or opkinetic stimuli which could generate perceived motion (Rine *et al.*, 1999). Both motion sickness and visually induced motion sickness are known to generate similar symptoms, including sweating, nausea, and dizziness. Those syndromes could be reduced in both prevalence and severity after repeated exposure to motion sickness provoking environment or training. Continuous exposure to visually induced motion sickness is proved to be an effective approach to reduce those syndromes as well. Adaptation to motion sickness which is induced by real motion and visual environment are suggested to be similar (Welch, 1978). The release of syndromes is generally termed as habituation or adaptation. Motion sickness habituation is generally considered to be stimulus specific (Golding 2006). On one hand, it is suggested that the adaptation to one kind of motion could not be completely generalized to other kinds. A seasoned sailor who has already adapted to the motion sickness that occurred during sailing will readily become motion sick when changed to another unaccustomed environment such as an aircraft (Stroud *et al.*, 2005). And visually induced self-vection did not help to increase the tolerance to bodily rotation (Dobie *et al.*, 1991). On the other hand, research also shows that adaptation training on different types of motion provoking stimuli could help in similar environment. Visual motion sickness provoking stimuli could help to reduce nausea feeling in potentially disorienting surroundings. Simulated rotatory stimulation could be extended to virtual reality and OKN (Smither *et al.*, 2008). Vestibular-Ocular Reflex was also found to be able to be adapted across different axis (Young *et al.*, 2003).

One of the most intensively studied areas on motion sickness desensitization training is aircrew desensitization training which dates back to 1960s. The training has been provided for pilots and space workers since then (Cheung and Hofer, 2005) and helped most of people who completed the training to release motion sickness syndromes. The desensitization training initially started from rotatory table training combined with in-flight training, and the former part was gradually changed to rotatory chair training and ground based desensitization training. One air sickness desensitization study reported that a majority of the people get adapted by about the

third air experience (Deshmukh, 2007). Adaptation training is a procedure that relies heavily on the subject. Willingness to coordinate was found to be very important in subjects, as subjects with low motivation were proved to be of no help. Reduction of motion sickness has been in most of the subjects who completed the training. Prior adaptation to motion could also have an impact on the speed of visually perceived motion (Gilden and Hurst, 1995).

Similar with the air force desensitization training, other studies also found the period for adaptation will usually take two to three days. One study stated that the maximum exposure for habituation takes only a few days to occur (Golding and Stott, 1995). And an adaptation study of vection induced by a rotating drum indicated that exposure interval of two days is enough to generate the adaption, while the adaptation was not shown when the interval was greater than 4 days (Stern *et al.*, 1989). It was also proved that number of exposure is a more important factor than the exposure intervals (Howarth and Hodder, 2008).

CHAPTER 3: STUDY ONE - EFFECTS OF PHYSICAL MOTION ON REGIONAL BRAIN HEMODYNAMIC RESPONSES IN HUMAN

3.1 Introduction

This study focuses on the cortical response to different kinds of physical motion. Instead of using alternative methods to activate the vestibular system, such as galvanic or caloric stimuli, this study uses real physical motion generated by motion simulator in the horizontal plane in different directions. The study aims at finding the cortical areas that respond to real physical motion, and verifying whether the cortical regions could response differently under different moving conditions. Near-infrared spectroscopy (NIRS) was utilized as brain imaging technology in this study. . A review of literature indicates that there has been no fNIRS study measuring cortical responses during real physical motion stimulation.

3.2 Objective and hypotheses

This study focuses on studying activation of brain areas under different moving conditions. As the oxy-hemoglobin (HbO) level is a direct reflection of brain activities and could be derived from NIRS measurements, the HbO level of targeted brain areas is considered to be the dependent variable in this study. It is hypothesized that motion has a significant effect on the HbO level of targeted brain area, and motion direction has a significant effect on the HbO level of the targeted brain area.

3.3 Methods

Subjects

Twelve right-handed male subjects participated in this study with a written consent form (age: 23-28, mean 24.5). None of them had any history of neurological or psychiatric disease. Alcohol and caffeine beverages are forbidden for 24 hours before the experiment. This study was approved by the Hong Kong University of Science and Technology.

The lower threshold of number of subjects in this study was primarily determined by reviewing the publications in similar fields (Hoshi *et al.*, 1997; Okamoto *et al.*, 2004; Huppert *et al.*, 2006). Subjects were recruited from both on-line university postings and off-line recruiting, the majority of subjects were university students. There were no female subjects in this study due to the difficulty caused by hair to fix the light transmitters and detectors onto the scalp firmly. Our male participants had short hairs.

Independent variables

Independent variables in this study were number of repeated session (1-3), motion direction (sway, lateral, fore-and-aft) and presence of motion (yes / no). The three sessions are repeated measurements of brain activation taken in the same time slot but on different days. Repeatability of measurements could be examined by the session factor. Motion direction includes three different moving conditions of sway, lateral and fore-and-aft, and a control condition with no motion. Thus the level of motion conditions is considered to be four in some of the analyses. Presence of motion and no presence of motion are considered to be two levels of the last independent variable.

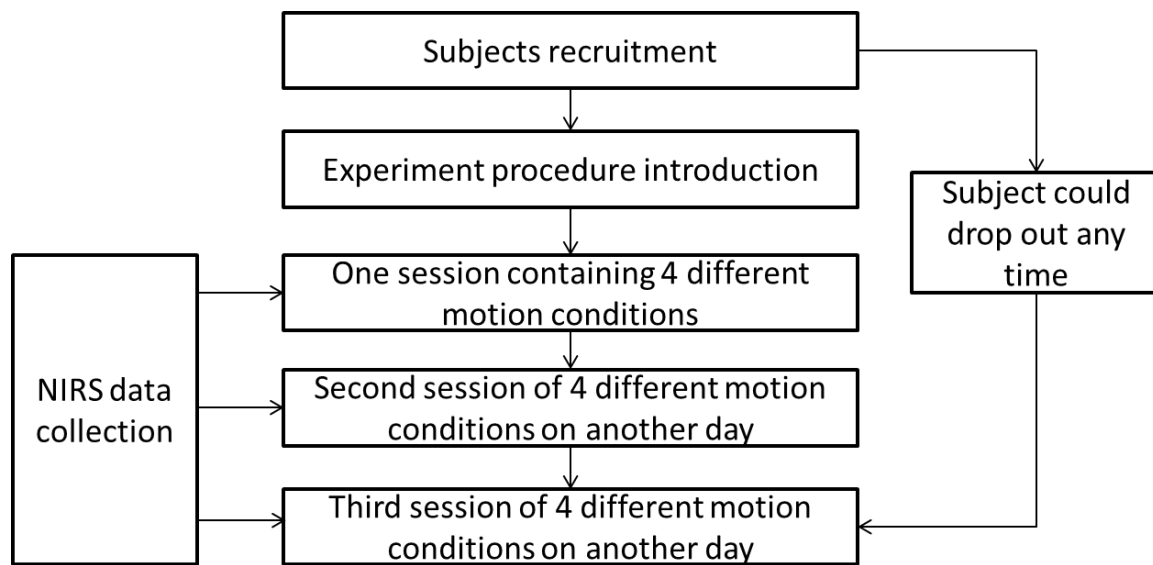


Figure 3.1 The flow chart of overall experiment procedure in the experiment investigating the effects of physical motion on cortical responses (Study one). Subjects were allowed to drop out at any time during the exposure, in this experiment, none of the subjects dropped out during three sessions of different motion conditions.

Details of four motion directions are listed in Table 3.1. In sway motion, the stimulus is the circular movement in the horizontal plane at 0.5Hz with a radius of 15mm; in lateral motion, the stimulus is a linear sinusoidal movement at 0.5Hz perpendicular to the facing direction of the subjects (i.e., lateral direction), and the amplitude is 15mm; in fore-and-aft motion, the stimulus is a linear sinusoidal movement at 0.5Hz along the facing direction of the subjects (i.e., fore-and-aft direction), the amplitude is 15mm; in the control condition, no movement is present to the subject. The detailed motion parameters are listed in the Table 3.1. The motion trace of motion simulator was defined by coordinates input file. In this study, the two axis of the moving platform follows the motion generation function listed in the condition. The coordinates of trace are modulated in the first two seconds and the last two seconds to achieve a smooth change in acceleration between rest and motion stimulus. The

modulation function is shown in Table 3.1 as well. The coordination of last two seconds was generated by reversing the coordinates during the first two seconds, such that the acceleration change for the motion ending period is smooth.

Presence of motion is directly related to the block design which is applied in presenting the motion directions to the subjects. Each block includes the presence of motion stimulus for 14 seconds and 20 seconds rest with no motion following the presence of motion, and each motion direction is composed of 10 repeats of the above block, thus each motion direction stimuli lasts for 6 minutes. A session is composed of four different motion directions sequenced in a randomized order. Rest time was allowed between different motion directions.

Within all moving directions, subjects are seated inside the moving platform with their head fixed on a chin rest, and they are instructed to fixate their eyes on a 3cm×3cm red cross presented on a black background from a distance of 1.0m. The absolute facing direction of subjects does not change under any moving direction. NIRS data is collected during all time.

Table 3.1 This table summarizes the tapering modulation function of the motion platform over the first and the last 2 seconds period of each motion stimuli lasting 14 seconds. Motion platform could move in the horizontal plane. It has a displacement driving mechanism. Its motion trace was defined by displacement input along x and y axis. During the starting of motion, motion simulator moved gradually from origin ($x = 0, y = 0$) to the circular trace. This ensured a smooth change in acceleration. During this 2s period, a tapering function was applied and its function is shown in the table. In the motion ending period, motion simulate moved back from circular trace to origin by applying a reverse sequence of (x, y) as in the first 2 second period.

Moving conditions	Motion parameters	
	Direction	Motion generation function (Period $T = 2s$)
Swaying motion (sway)	Circular movement in the horizontal plane	$x = f(t) \cos \frac{2\pi}{T} t$ $y = g(t) \sin \frac{2\pi}{T} t$ $f(t) = g(t) = \begin{cases} \lambda \left(\frac{1}{5} t^5 - \frac{T}{2} t^4 + \frac{T^2}{3} t^3 \right), & 0 \leq t \leq T \\ \lambda \left(\frac{T^5}{30} \right) = 15, & t > T \end{cases}$
Lateral motion (lateral)	Left-right motion in the horizontal plane $y = 0$ in this condition	
For-afterward motion (fore-and-aft)	For-backward motion in the horizontal plane $x = 0$ in this condition	
No motion at all (blank)	Not applicable $x = y = 0$ in this condition	

Control variables

During all conditions, temperature, environmental light and noise were under carefully controlled and physiological status of subjects recorded. The temperature was 21°C, environmental light was turned off, and ear plug was provided to block the environmental noise. Plethysmograph was taken at the ear lobe of the subject for monitoring the whole body physiological status change. The equipment used to take plethysmograph measurement was Masimo Radical-7 Monitor (PN: MAS9153). The blood pressure at the ear lobe was measured at 12.5 samples per seconds and the purpose of recording the blood pressure data was to cross check and isolate the effects of systemic changes of blood pressure on the findings.

Localization(s) of NIRS probes

The light fiber probe transmitters and detectors were placed in reference to the 10-20 system (Homan *et al.*, 1987). The 10-20 system is illustrated in Figure 3.2. Anthropometry measurements of the heads were taken from subjects with regarding to the 10-20 system. Cz, C4 and T4 are chosen as land marks in locating the light sources and detectors on the right hemisphere (see Figure 3.2). The line connecting Pz and Oz was the landmark for locating the detector on the occipital lobe. Light transmitter 4 was placed exactly at T4 location, and detector B was located exactly on the line which joining C4 and T4. As the relative location for the detectors and light sources were fixed, the locations of other detectors and light transmitters were determined with reference to C4 and T4 location.

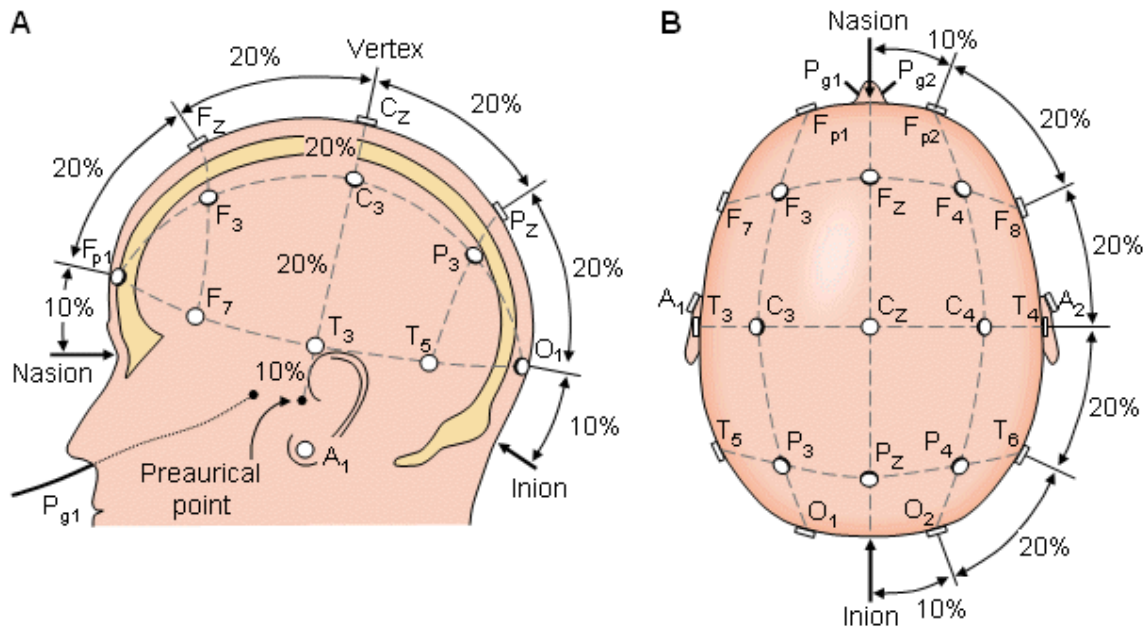


Figure 3.2 The figure illustrates international 10-20 system used in dividing the surface of a skull with anatomical references. Picture source: <http://www.bem.fi/book/13/13.htm>, downloaded on Feb 11th 2017. This picture aims at illustrating some specific locations in the 10-20 system which are T4, C4, O1 and O2. These locations were utilized as references in our experiments for placing the NIR transmitter sources and detectors.

The optical fibers were attached to a flexible, but not elastic rubber cap. An elastic cap was not used because rubber cap was used to hold light transmitters and detectors firmly onto the scalp of the subject. Elastic rubber cap may introduce shift or change of detectors and transmitters location during the experiment. The cap was fastened around subject's head snugly by nylon tape. The detectors and light transmitters from NIRS machine could be fixed firmly onto the scalp of subjects by using the flexible rubber cap. To avoid hair obstruction, hair between fibers and scalp was carefully moved away before data collection procedure, and the light transmitters and detectors were further fastened by putting black bandage around the cap.

In this study, each pair of detector and light transmitter was spaced at 3cm apart and the pair was denoted as a channel. The NIRS light estimated the level of cortical oxygenated blood flow underneath each channel (see Chapter 1 for explanation of how NIRS works). Three detectors and six light transmitters (10 channels) were placed on the targeted brain areas of right hemisphere to measure the signal responding to physical motion (Brandt and Dieterich., 1999; De Waele *et al.*, 2001). The other detector and two light sources are placed on the occipital region of the brain which aimed at providing reference control. Within the two channels placed on the occipital region, one recorded signal from visual area, and the other light transmitter was intentionally not attached to scalp, thus the detector collects signal from the brain with no light source, and this could be treated as a blank channel control from the noise of environment.

The graphical representation of light source and detector location is illustrated in Figure 3.33. The red dots indicate the location of the detectors, and the blue dots are the location of the light sources where the near-infrared light is attached to the scalp and shine into the brain. The yellow dots are the landmarks in locating the detectors and light transmitters, in this figure, T4 is overlapped with light source 4 and landmark C4 is overlapped with detector B.

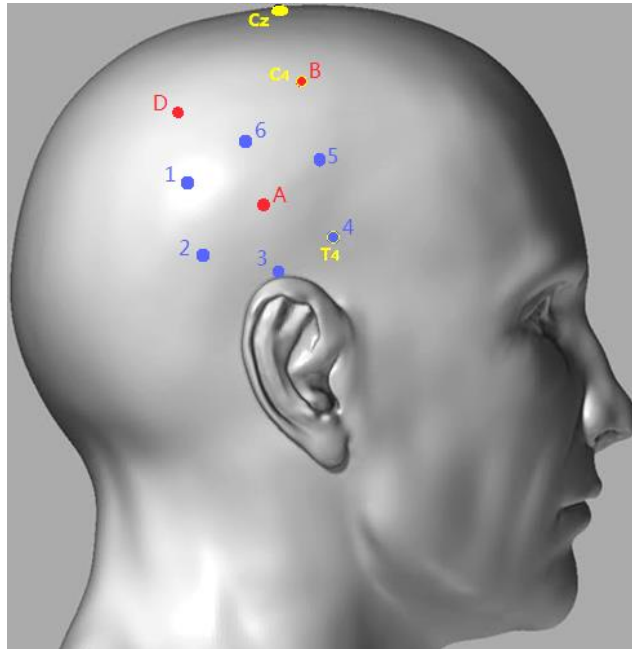


Figure 3.3 An illustration of the locations of the NIR detectors and transmitter sources. The red dots are the detector location, blue dots are the sources location and the dots circled in yellow are extra scalp markers. (The model for the brain is downloaded from http://i2.photobucket.com/albums/y20/MatrixNAN/RealisticMaleHead_06.jpg, on 10:30pm, UTC+8, May, 17th 2014)

3.4 Data analysis and result

3.4.1 Data analysis

Channel exclusion and artifact recognition was conducted first. A channel was excluded from the whole analysis procedure if the data collected by NIRS fails to show the heart rate pattern (Jasdzewski *et al.*, 2003). Artifact recognition was identified by detecting regions with high noise levels which resulted from location shift of detectors or light sources. The contamination in the data was generally triggered by the sudden movement of the subject, and the raw data had a character of synchronized sudden shift in the light intensity data among different channels. Two-sided moving standard deviation algorithm was applied to the light intensity

level to pick up the noise contaminated blocks (Scholkmann *et al.*, 2010). A block was marked as noise contaminated block if at least one artifact was detected within the block period.

After channel exclusion and artifact recognition, the data processing procedure was generally conducted by HomER (Huppert *et al.*, 2006). In order to remove the high frequency noise and very slow drift, the data went through a bandpass filter of 0.001-0.3Hz (3rd Butterworth filter), phase distortion was intentionally avoided in designing the filter (Osharina *et al.*, 2010). The light intensity level was then converted into the concentration change of oxygen hemoglobin (HbO) and deoxygen hemoglobin (Hb) through a calculation process based on the modified Beer-Lambert Law (Arridge *et al.*, 1993). Among all the valid blocks (motion artifact contaminated blocks are invalid blocks), the hemoglobin concentration change was taken in to average in reference to the stimulus start time. The final averaged hemoglobin concentration change is called grant average in this study.

The representation of concentration change with and without motion was extracted for each condition. The average concentration change of 4 seconds was extracted both from the moving period and the resting period. As the oxygen hemoglobin level will reach its peak at 5s to 8s after the stimuli onset (Blamire *et al.*, 1992; DeYoe *et al.*, 1994), the period of which the HbO concentration changes to be averaged was chosen to be 6s to 10s after the motion onset. Time period of equally length was chosen in the resting period, which was from 12s to 16s after the movement stops in each block.

After extracting HbO concentration change with and without motion for all conditions and sessions among all subjects, statistical analysis was conducted. ANOVA analysis is a widely applied method in analyzing the data from block design (Tak and Ye 2014). In this study, three-way ANOVA analysis with independent variables including session (repeated measure on three different days), condition (sway,

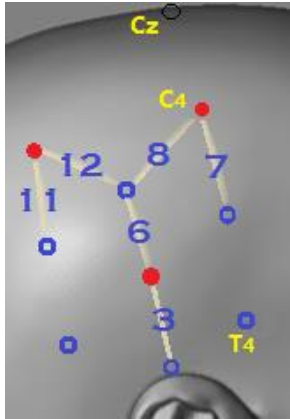
lateral, fore-and-aft and blank), and treatment (motion-on and motion-off) was conducted. According to the results shown in the three-way ANOVA, the data was further grouped by condition, each condition was considered separately. The two-way ANOVA was conducted by treating session and treatment as the independent variables. Session was treated as an independent variable in both statistical procedure to verify data repeatability and validity. Considering the natural of physiological recordings, Wilcoxon sign rank test was also conducted to further verify the significant factor to the HbO concentration level change. The detailed data analyze procedure could be found in Appendix E.

3.4.2 Result

Statistical analysis

All subjects completed the experiment in this study. The three-way ANOVA revealed a significant main effect of 'treatment' among channel 6, 7, 8, 11 and 12, indicating cortical area under these channels are responsive to the motion. The numerical result from the test demonstrates an increase in HbO level when the motion was presented. The location of the channel and the statistical result for the activated channels is listed in Table 3.2.

Table 3.2 Descriptive statistics of treatment effect (motion) and channel location of three-way ANOVA. This p-values indicate the level of significance between HbO levels measured in the presence and absence of motion (two-level factor, thus degree of freedom is one). Data were measured in Channels 6, 7, 8, 11 and 12 corresponding to the cortical areas of temporal parietal region (channel 6), motor/sensory motor area (channel 7 and 8) and intraparietal regions (channel 11 and 12).

Descriptive statistics of treatment effect					Channel location
channel	degree of freedom	Mean Square (MS)	F	P-value (Sig. < 0.05)	
6	1	27.316	5.49	0.020	
7	1	64.226	8.32	0.004	
8	1	140.576	12.75	<0.001	
11	1	42.467	5.436	0.021	
12	1	119.233	7.962	0.005	

To further demonstrate the effect of treatment, interaction plot between treatment and condition of the activated channels in three-way ANOVA are shown in Figure 3.44. In all responding channels, treatment could cause an increase in HbO concentration level. In sway condition, treatment triggered the largest increase in HbO, and blank condition is mostly flat compared to other conditions. Channel 6 and 8 both demonstrate a large increase under the lateral condition. The HbO concentration level change shows different scale under three motion conditions among channels. However, the condition does not show significance in this test.

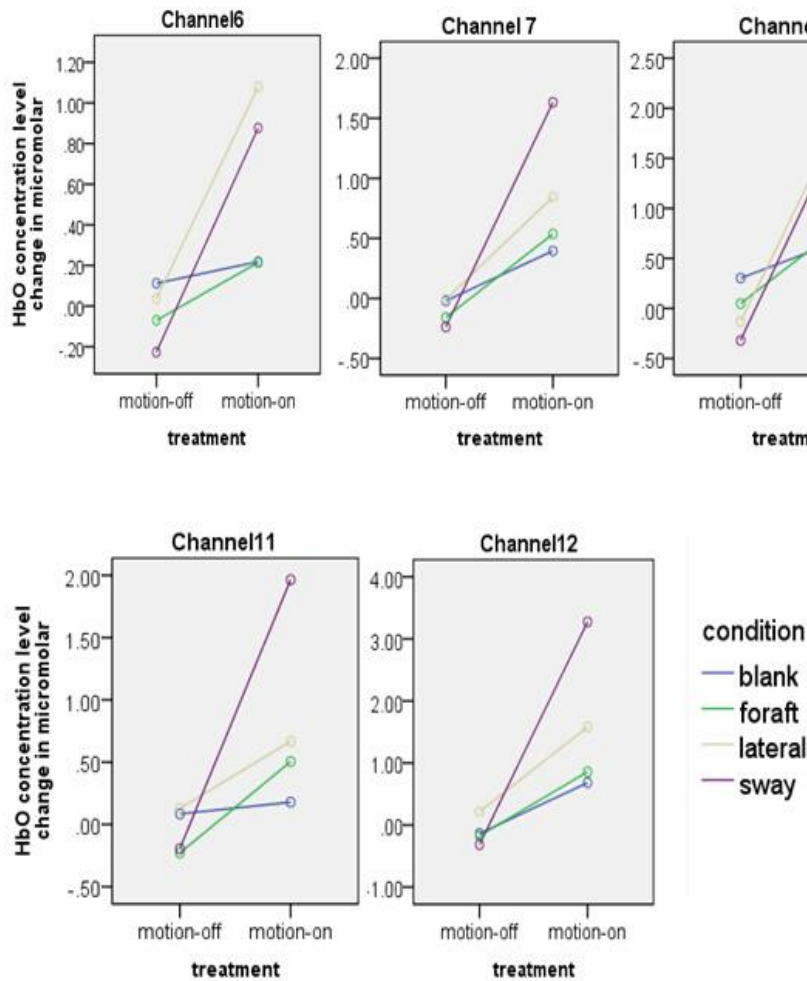


Figure 3.4 Main effect plots of treatment factor for all activated NIR channels (6, 7, 8, 11, and 12). Data from these channels represent signals measured on the nearby cortical areas of temporal parietal region (6), motor/sensory motor areas (7&8) and intraparietal region (11&12). Results of three-way ANOVA show HbO levels were higher in the presence of motion. Data also indicate that HbO change differently in the four conditions (fore-and-aft, lateral, sway and no motion). Data of 12 subjects.

From the figure above, we could see the HbO concentration change under different conditions appears to be different. However no significant condition effect could be found from the three-way ANOVA analysis. To further verify the treatment effect under different conditions, two-way ANOVA with independent variables of session

(repeated measurement on different days), and treatment (with and without motion) was conducted within each condition (sway, lateral, fore-and-aft and blank).

In blank condition where no motion was presented, no significant main effect or interaction effect was found in any channels. In fore-and-aft condition, no significant main effect or interaction effect was found in any channels either.

In lateral condition, treatment was found to be a significant effect in channel 6 ($F = 5.267$, $p = 0.025$) and also channel 8 ($F = 10.081$, $p = 0.002$) (please refer to the Table 3.2 for the location of channel 6 and channel 8). Main plot of treatment effects (grouped by session) illustrates that the motion could cause significant increase in HbO concentration level change. The plot also shows that the change across different sessions is quite similar.

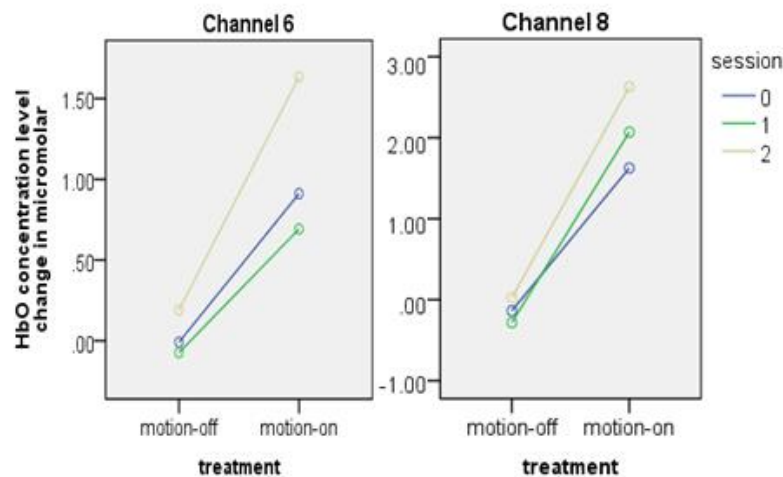


Figure 3.5 Significant changes ($p < 0.05$) in HbO levels measured in channel 6 and 8 (corresponding to the cortical areas of temporal parietal region and sensory motor areas) due to the presence of lateral motion in the three repeated sessions (0, 1, 2). Data of 12 subjects. Locations of the channels are shown in Table 3.2

In sway condition, the activated channels are channel3 ($F = 6.911$, $p = 0.011$), channel7 ($F = 5.511$, $p = 0.022$), channel8 ($F = 4.378$, $p = 0.04$), channel11 ($F =$

4.287, $p = 0.044$) and channel12 showed a marginal significance level ($F = 4.066$, $p = 0.051$). The main plot is listed in Figure 3.66 (group by sessions). The HbO concentration level in channel 3 decreased when sway condition is presented to subjects according to the plot. And the other activated channels (channel 7, 8, 11 and 12) showed a significant increase under the sway condition.

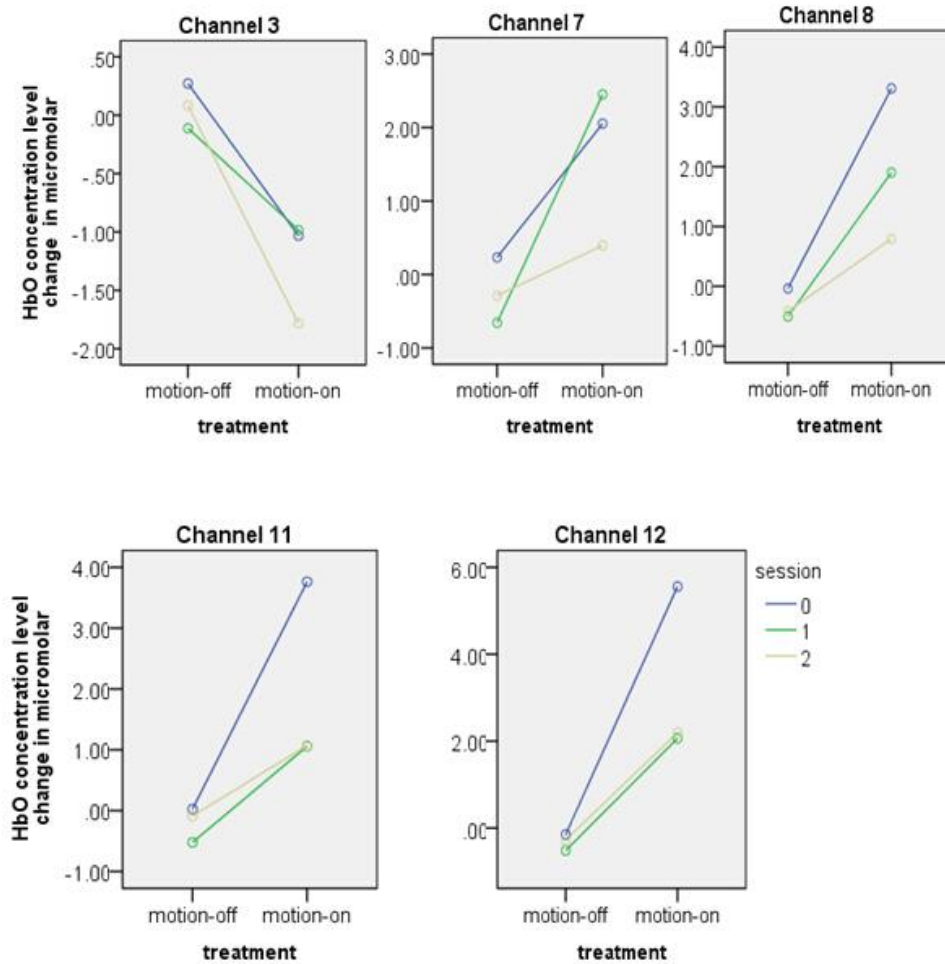


Figure 3.6 Significant changes ($p < 0.05$) of HbO levels measured in channel 3 (reduction) and channels 7, 8, 11, and 12 (increase) due to the presence of sway motion. Data from these channels represent signals measured on the nearby cortical areas of posterior temporal lobe (3), motor / sensory motor areas (7&8) and intraparietal region (11&12). Data of 12 subjects

From the two-way ANOVA analysis, the changing pattern of significance factor showed consistency between different sessions. The consistency indicates repeatability of HbO concentration level change among repeats of experiments in this study. In all the statistical analysis, the control channel placed on the occipital region of the brain and the blank control channel did not show any significant result, and the plethysmograph did not show any significant result under either. This suggests that the significant findings on HbO were not caused by systemic changes in blood pressure.

The change of hemoglobin level in human brain is generally related to non-stationary physiological status. The normality of the HbO concentration change was poor in this study. The reason for poor normality of the data could be the limited number of subjects in the experiment. To further verify the statistical result, Wilcoxon sign rank test was further conducted on the data within each condition. In blank and fore-and-aft condition, no significant result was found. In lateral condition, channel 6 ($p = 0.023$) and channel 8 ($p = 0.001$) demonstrated significant increase, and in sway condition, channel 3 ($p = 0.01$), channel 7 ($p = 0.011$), channel 9 ($p = 0.03$) channel 11 ($p = 0.024$) demonstrated significant result. A further verification also confirmed that the direction of change was consistent with the ANOVA result. The Wilcoxon sign rank test showed high consistency with the ANOVA analysis in general. However, the channel 9 which is put on the occipital lobe and treated as a control channel showed significant increase in sway condition under Wilcoxon test. And from all the channels, only channel 3 showed an opposite changing direction of HbO concentration level in sway condition.

3.5 Discussion

3.5.1 Brain activation in different condition

From the three-way ANOVA test, the brain region that was responding to physical motion could be characterized by the coverage area under channel 6, 7, 8, 11 and 12. The conclusion that the cortical area underneath the activated channels reacts quite differently in different motion conditions could be drawn from the two-way ANOVA. It was obvious that the responding brain areas to physical motion were widest in the sway condition, and the activated channels were 3, 7, 8, 11, and 12. These channels correspond to cortical areas of posterior temporal lobe, intraparietal region, and motor/sensory motor area. Within all the responding channels, hemoglobin level change of channel 3 is in an opposite direction compared to other channels. In lateral condition, the activated brain area locates underneath channel 6 and 8. However in fore-and-aft condition, no significant activated brain area was shown. The possible reason for no significant cortical hemodynamic changes were found under fore-and-aft condition could be due to human are very adaptable to fore-and-aft motion in the daily motion, it could be also due to the current detectors and transmitter location selection. In this experiment, the location of detectors and light transmitters were due to the activated cortical areas under caloric or galvanic stimulus. However those stimuli could evoke sensation of tilt or rotation. It is also possible that the cortical areas which could be activated by fore-and-aft motion were not covered in this experiment.

The fibers were located in reference to 10-20 system in this study, and the reference location between the outer scalp markers and intracranial structures have been demonstrated in previous studies (Okamoto *et al.*, 2004). According to these studies, intracranial structure underneath T4 is most likely to be around the middle to superior temporal lobe in the middle to frontal region, and C4 is most likely to be around central sulcus. According to the brain function areas, channel 7 and 8 could

be related to motor area and sensory area. Channel 3 locates posterior to C4 which indicate it could be responsive to posterior temporal lobe. Thus channel 6 is most likely to be temporal parietal region, and then the channel 7 and 8 could be most representative of intraparietal region. If the inference according to the 10-20 system is taken into account, then the brain activated area found in our study is in high consistency with the previous research on vestibular brain mapping (Bottini *et al.*, 2001; Suzuki *et al.*, 2001; Fasold *et al.*, 2002; Stephan *et al.*, 2009). And this study specifically reveals how brain cortical regions are activated under different moving conditions.

It is also worth noticing that in swaying condition, apart from channels on the right hemisphere, a significant increase of the HbO concentration level is also found in channel 9. This indicates that the brain area in the occipital part of the brain is also activated in a motion condition. On the other hand, compared to the general increasing of HbO concentration, channel 3 demonstrated a decrease in HbO level in sway condition. The synchronized phenomenon might be related to the functional inhibitory brain mechanism between the visual cortices and vestibular cortices.

Limitations

Although our motion is limited into small region with a radius or the largest point to point distance of 30mm to reduce the mechanical noise from the motion simulator. Human reaction force still comes naturally in muscles and joints when they are present to motion. This could contribute to the activation of channel 7 and 8.

Lacking of intracranial reference of the detector and light sources location introduces difficulty in comparing our result with existing brain imaging results. Although 10-20 system is universally applied in brain imaging studies, individually difference of anatomical brain structure is a crucial concern to relate the outer scalp landmarks with brain structures.

3.6 Summary

According to this study, different motion conditions of sway, lateral, for-and aft could trigger different brain cortical responses. Sway condition could trigger a most widely spread brain area covered by cortical areas located in posterior temporal lobe, intraparietal region and motor/sensory motor area. Brain region near temporal parietal and motor/sensory motor area are responsive to lateral condition according to the statistical analysis. In the meanwhile, no significant response in any channel could be found under fore-and-aft condition. According to our knowledge, this study is the first study to demonstrate brain cortical responses under different types of real physical motion.

CHAPTER 4: STUDY TWO - VERIFICATION OF MOTION ARTIFACT USING MANIKIN

4.1 Introduction

This chapter introduces a complementary experiment which aims at identifying whether motion artifact and instrumental or environmental noise could lead to any significant result in the same experimental condition in chapter 3.

It is proved that brain cortical regions could be triggered differently under sway, lateral and fore-and-aft conditions in earlier experiment. Although environmental variables were carefully controlled during experiment to prevent noise, people may argue that motion artifact might have been introduced during the stimulus period and resulted in significance. This experiment uses exactly the same set up as earlier experiment, while all measurements are set up on a manikin. This experiment serves as an indication of whether motion artifact could be introduced to the measurement under the experiment set up.

4.2 Objective and hypothesis

This experiment investigates whether different motion directions could have significant effect of NIRS measurement on manikin. The hypothesis of this experiment is that presence of motion has a significant effect on the HbO level measured from manikin.

The subject of this experiment is a manikin, and the measurement area of the manikin is made of silicone gel. The manikin is well fixed on the chin rest. Figure 4.1 illustrates the comparison between the manikin and real human subject.



Figure 4.1 Photos of experiment set up in control experiment (study two) with a manikin and in experiment (study one) with human subject. As seen from the photo, we tried to replicate the set-up in the manikin experiment to be same with human subject experiment.

4.3 Design of experiment

Independent variables

Independent variables in this study were exactly the same as earlier experiment which were: session (three repeated measurement taken on three days), motion condition (sway, lateral, fore-and aft) and presence of motion (yes/no). Sway motion was the circular movement in the horizontal plane; lateral motion was a linear sinusoidal movement in left-right direction; fore-and-aft motion was a linear sinusoidal movement along fore-and-aft direction; frequency was 0.5 and amplitude was 15mm for all motions mentioned above. In blank motion, no movement was presented to the subject. The motion trace had been calculated such that no jumps in acceleration or velocity could be introduced during the motion period (Table 3.2).

The experiment procedure followed block design, each block was composed of 14 seconds with motion presence and 20 seconds with no motion, and each stimulus was composed of 10 repeats of block, thus one stimuli for each motion condition lasted for 6 minutes. A session was composed of four different motion conditions sequenced in a randomized order. NIRS data was collected during all time from the manikin.

Control variables

Same control variables with human experiment were used in the manikin experiment. Environment settings in this experiment were same with previous experiment as well. The temperature was 21°C. Environmental light was turned off during the whole experiment procedure.

Fiber localization

Measurement was taken from the manikin to locate the 10-20 system. The detector and light transmitter was placed at channel 6 in reference to Table 3.2. Because of the limitation of manikin, only one pair of light transmitter and detector could be placed. The optical fibers were attached to a flexible, but not elastic rubber cap. The cap was fastened around subject's head snugly by nylon tape. The probes and detectors were further fastened by putting black bandage around the cap. The distance between detector and light transmitter was 3cm as well, and the measurement was taken from the right hemisphere of the manikin.

The setup of measurement on manikin and the comparison between manikin and human subject is shown in below Figure 4.2:

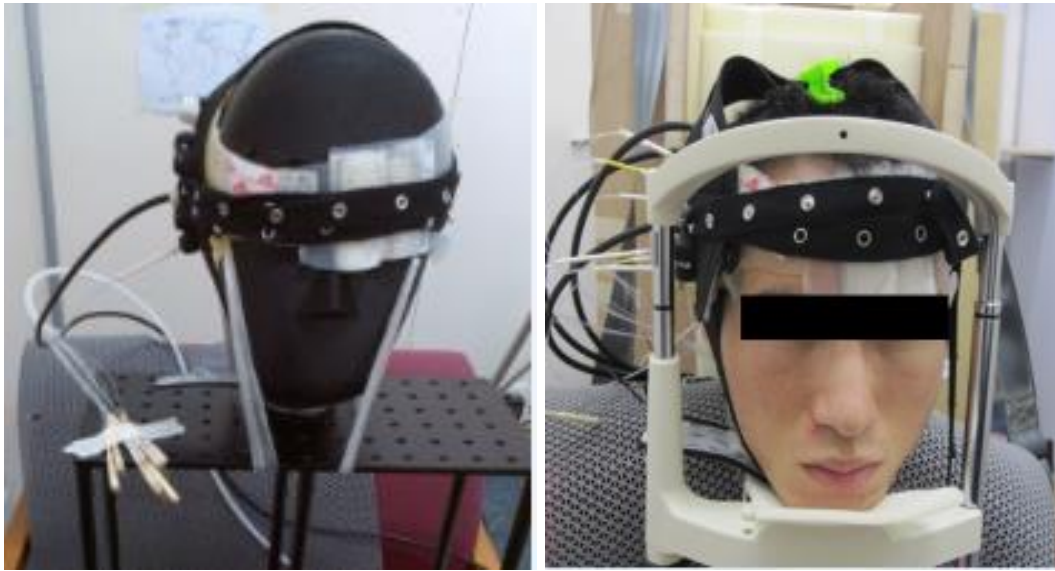


Figure 4.2 Photos of NIRS transmitter sources and detectors on the manikin (control study) and a human subject (study one) from the front view.

4.4 Data analysis

In the data analysis part, data went through artifact detection using two-sided moving standard deviation algorithm (Scholkmann *et al.*, 2010). Blocks containing artifact were removed from further analysis. Then data were analyzed in HomER (Huppert *et al.*, 2006), bandpass filter of 0.001-0.3Hz (3rd Butterworth filter) was applied to filter out slow drift and high frequency noise, phase distortion was intentionally avoided in designing the filter (Osharina *et al.*, 2010). The light intensity level was then converted into the concentration change of oxygen hemoglobin (HbO) and deoxygen hemoglobin (Hb) through a calculation process based on the modified Beer-Lambert Law (Arridge *et al.*, 1993). A grant average (explained in study 3) of hemoglobin concentration change was then calculated among the remaining blocks within a condition while the noise contaminated blocks were excluded.

The time period extracted to calculate HbO concentration for no motion and motion were using the same period as that of human subjects. The period of HbO concentration change to be averaged were chosen to be 6s to 10s after the motion onset. And rest period was taken as 12s to 16s after the movement stops in each block.

ANOVA analysis was applied in analyzing the data on manikin as well. Three-way ANOVA analysis with independent variables including session (repeated measure on three different days), condition (sway, lateral, fore-and-aft and blank), and treatment (motion-on and motion-off) was conducted on HbO level.

4.5 Results and discussion

ANOVA result showed no significant influence could be seen from any single factor or interactive factor. P-value for different factors and interactive factor are summarized in the Table 4.1 below:

Table 4.1 Statistical result from three-way ANOVA test in manikin experiment. Results of the ANOVA test show no significant main effect of repeated session (3 repeated sessions, condition (4 moving conditions) and motion (yes/no). None of the two-way interactions was significant.

Factor	Degree of freedom	F	P
session	2	1.29	0.341
condition	3	0.42	0.744
motion	1	0.37	0.567
session*condition	6	1.04	0.482
condition*motion	3	1.67	0.270
session*motion	2	2.04	0.211

Several motion artifacts was also spotted in the NIRS raw data as there could be light transmitter shift or some unpredictable movement of the manikin during the measurement. This experiment showed that no motion artifact resulted in data significance under the experiment set-up.

4.6 Summary

This experiment serves as a verification experiment which studies the potential impact of motion artifact on NIRS measurement during the experiment conducted in motion simulator. A manikin was utilized as the subject and it was tested under the paradigm of earlier experiment. The statistical result could not show any significant impact from motion artifact under existing experiment set-up.

CHAPTER 5: STUDY THREE - CROSS VALIDATION ON VIMS SUSCEPTIBILITY MEASUREMENTS

5.1 Introduction

Motion sickness is commonly known as a syndrome with individualized susceptibility (Golding, 2006). The Motion Sickness Susceptibility Questionnaire (MSSQ) has been utilized to mark the severity of motion sickness in wide varieties of research (Sang *et al.*, 2003; Meissner *et al.*, 2009; Paillard *et al.*, 2013). The questionnaire was first introduced in 1998 by Golding (Golding 1998) in the long form. Further study was conducted to prove the validity of the questionnaire (Golding 2006). Meanwhile, few studies have been done in distinguishing people among different susceptibility to VIMS to date now. This chapter verifies two possible methods in distinguishing people with different susceptibility of VIMS.

This study first verifies whether Motion Sickness Susceptibility Questionnaire and Motion Sickness Susceptibility Survey could be utilized as an effective method in distinguishing people from different susceptibility to VIMS provoking stimuli. MSSQ contains two parts which aim at evaluating motion sickness severity in the childhood and in the most recent 10 years. Subjects need to evaluate the severity of their symptoms under different motion conditions (Figure 5.1). The motion conditions and severity range are the same between childhood and most recent 10 years in the questionnaire.

	Not Applicable - Never Travelled	Never Felt Sick	Rarely Felt Sick	Sometimes Felt Sick	Frequently Felt Sick
Cars					
Buses or Coaches					
Trains					
Aircraft					
Small Boats					
Ships, e.g. Channel Ferries					
Swings in playgrounds					
Roundabouts in playgrounds					
Big Dippers, Funfair Rides					
	t	0	1	2	3

Figure 5.1 The items and levels used in the MSSQ questionnaire. Each subject needs to fill in twice : one for childhood and one for adult period. Total score are calculated by summarizing the childhood score and adult score. For detailed explanation of MSSQ questionnaire, please refer to appendix C

After collecting subject responses to the above questionnaire, total sickness scores of childhood and latest ten years were calculated and raw scores were finally calculated. In the original study, table of means and percentiles was derived from 257 subjects.

Another questionnaire, Motion Sickness Susceptibility Survey (MSSS) utilized in this study was adopted from a study conducted in 1999. The study was conducted specifically in Asian group and the questionnaire aims at collecting subjective rating of motion sickness from 'Not at all' to 'Extremely' (So *et al.*, 1999; 5 level of motion sickness self-evaluation was taken as record and analyzed further: 0- Not at all, 1- Slightly, 2-Moderately, 3- Very, 4- Extremely).

This study also investigated whether subject's nausea rating induced from other VIMS provoking stimuli could be served as a more direct measurement of subject VIMS susceptibility. The VIMS provoking stimuli was a pre-recorded game named 'Mirror Edge' (Keshavarz and Behrang, 2012). Nausea rating generated from

passive game watching was recorded to test if it could discriminate different susceptibility of visually induced motion sickness among individuals.

5.2 Objective

The motion sickness susceptibility questionnaire was developed and verified in non-Asian people and the percentile and score were induced from non-Asian people. Motion sickness is known to be affected by ethnic origin or gender (Klosterhalfen *et al.*, 2005). There's no research or verification that the motion sickness susceptibility questionnaire measurement could be extended to Asian group and the effectiveness in distinguishing VIMS susceptibility is unknown either. The objective of this research is to construct validity for using motion sickness susceptibility questionnaire to measure VIMS susceptibility.

Apart from using questionnaire to tell the subject susceptibility to VIMS, this study also investigates whether subject nausea rating to VIMS provoking stimuli could be directly utilized as the VIMS susceptibility measurement.

5.3 Design of experiment

5.3.1 Subject

18 right-handed male subjects (mean age: 24.8 years old, range from (22.5 ~ 27)) participated in this experiment with a written consent form (Appendix D). Female subject was not included in this study as gender was proved to be an important factor in motion sickness susceptibility (Klosterhalfen *et al.*, 2005), and also the sensitivity to motion sickness varies with menstrual cycle (Golding *et al.*, 2015). None of them has any history of neurological or psychiatric disease. Alcohol and caffeine beverages were forbidden for 24 hours before the experiment. None of the

subject dropped out during the experiment process. This study was approved by the Hong Kong University of Science and Technology.

5.3.2 Experiment procedure

Firstly, subjects were asked to fill in Motion Sickness Susceptibility Questionnaire and Motion Sickness Susceptibility Survey. Then they watched the experimental stimuli for one to three of minutes (each time the stimulus was presented for 2.5 minutes. Stimuli presented from 2.5 minutes to 7.5 minutes in total. Subjects did not need to watch the stimuli all the time during the period, they could describe their feelings and raise questions anytime they want during this period). An introduction to the experiment procedure and circularvection were introduced after subjects were presented with the stimuli for the first time. To be more specific, subjects were asked about if they had any feelings of motion after the first time of watching the stimulus. If subjects confirmed they feel themselves rotated, they were asked to describe the direction of rotation. If subjects confirmed they did not feel any motion, they were asked to watch the stimulus once more and they were asked specifically if they could feel any motion while watching the stimulus. In the second stimulus watching, subjects were asked to report any motion they feel in real time, including their rotating direction and the moving status of the dots. Subjects could drop anytime during the whole experiments. And they were allowed to continue experiments only when they could correctly describe the direction of their self-rotating. After the second time of watching the stimulus, a clear description ofvection (the Illusion of self-motion, and in our experiments thevection should be the self-rotating in the counter clock-wise direction) was introduced to the subjects. Subjects were suggested to watch the stimulus for another time to confirm thevection feeling.

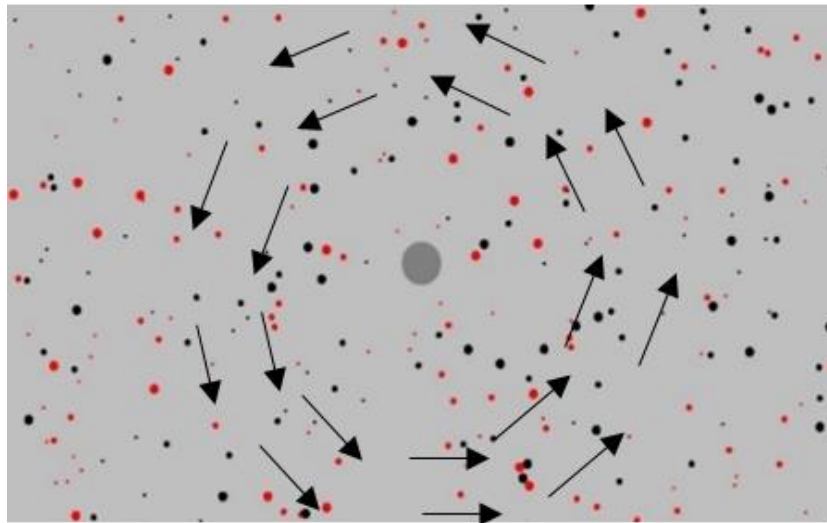


Figure 5.2 An illustration of vection stimuli and dots rotation direction. The purpose of this figure is to give an illustration of the vection-generating stimulus and show the rotating direction of all black and red dots. The detailed description of the stimulus could be found in the following paragraph.

Subjects were asked to watch the stimulus continuously for 20 minutes in this experiment. The stimulus was presented on the LCD screen (SONY KDL-46EX720), and the field of view (FOV) was 61 degree vertically by 93 degree horizontally. The stimulus contained an average of 320 circular patterns on a grey background, with half in red and half in black. The FOV for each circular pattern varied from 1 to 2 degrees. A gray fixation point was located stationary at the center of the screen all the time, with a FOV of 4 degree. The overall luminance level measured at the subject's eye location was 10lux. During the stimulus period, subjects were instructed to fix their eye on the gray fixation point in the center of the screen. All circular patterns rotated at the same angular speed of 5 rotation per minute (RPM) in the stimuli period for 20 minutes. During the experiment, the entire environment light was turned off. Environment noise was under 50db and surrounding objects were blocked from the subject visual field by a black curtain.



Figure 5.3 An illustration of a subject taking part in the experiment. Subjects will watch the stimulus with their head comfortably fixed on the chin rest. Black curtain was provided to mark off the irrelevant environment. Subjects could press the button to stop the stimulus at any time. Light were turned off during the experiment.

After watching the stimuli, subjects gave the current nausea rating according to the 7-point nausea rating adopted from Golding and Kerguelen (Golding and Kerguelen, 1992). Experiment would be terminated if any subject reached a nausea level of 5 or more, or any time they could like to pause or terminate the experiment.

- 1 = No symptoms;
- 2 = Any symptoms, however slight;
- 3 = Mild symptoms, e.g. stomach awareness but no nausea;
- 4 = Mild nausea;
- 5 = Mild to moderate nausea;
- 6 = Moderate nausea but can continue;
- 7 = Moderate nausea, want to stop.

Figure 5.4 7-point nausea rating adopted from Golding and Kerguelen (Golding and Kerguelen, 1992). This rating shows how nausea level is defined according to the scale. In our experiments, any subjects who reached nausea level of 5 were asked to terminate stimulus exposure and take rest.

All subject were called back to participate another visual stimuli exposure session after one week from the circular vection exposure. In this session, each subject was exposed to a pre-recorded video of first-person action-adventure game 'Mirror Edge'. Mirror Edge is a product of EA Digital Illusions Creative Entertainment (EA DICE). In this game, player will have the first-person view. And players need to run/jump/clime from time to time to know their current environment in the game to achieve the game mission. Along with running, jumping, climbing and other kinds of motions; players could get a strong sensation of motion. And in earlier studies, it was showedd that passive players could get sensation of motion as well (Guo *et al.*, 2013).



Figure 5.5 Screen capture of the pre-recorded video game ‘Mirror Edge’. Players’ views are in the first-person perspective. They need to jump, run and climb different buildings and obstacles while running away from an ‘enemy’. The viewpoint moved in all directions and the speed of motion varied.

The video record was displayed under the same environment as the circular vection exposure. A fixation crossing was located stationary at the center of the screen through the entire video game. Subject was instructed to fix their eyes the fixation point during the video game. Each subject watched the video for a maximum of 20 minutes, and 7-point nausea rating was recorded every 5 minutes during the period. The video was stopped whenever the subject’s nausea level reached 5 or higher in the 7 point nausea rating. A screen capture of the pre-recorded game is given in Figure 5.5.

5.4 Data analysis

Summary statistics of MSSQ survey scores comparison

Given the difference in number and ethnic origin of subject in our study and Golding's study, mean and standard deviation of adult score showed much similarity. In our study, the data range for adult score is 11.31 ± 8.94 while it shows 11.13 ± 8.78 in Golding's study.

MSSQ and MSSS

The linear regression analysis was conducted between MSSQ and MSSS score. The relationship between the MSSQ adult score and MSSS self-evaluation is showed to be correlated with P-value 0.001 and R-square 0.6471. This means that MSSQ and MSSS score are generally in accordance with each other in terms of motion sickness self-evaluation.

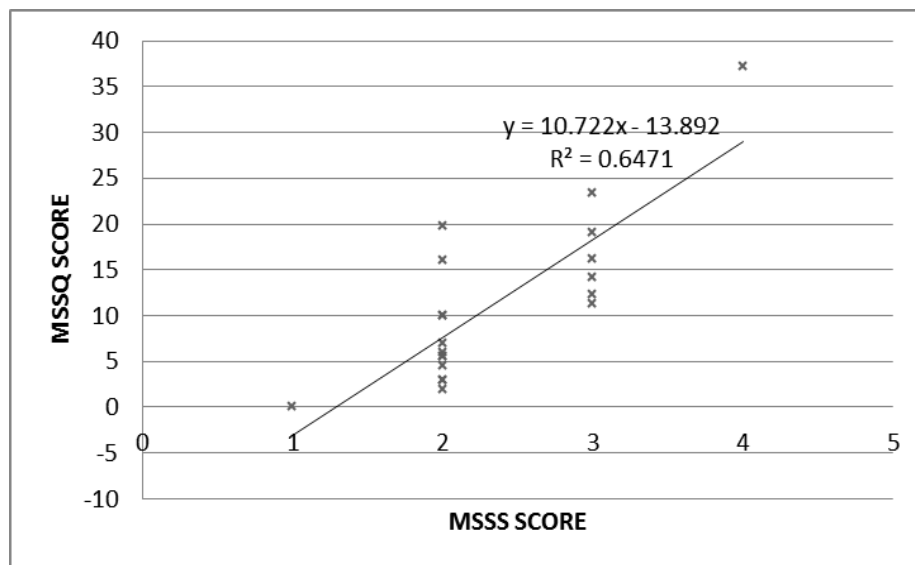


Figure 5.6 The scatter plot between MSSQ and MSSS scores. The two scores were significantly correlated ($p < 0.005$) with a R^2 of 0.64.

MSSQ score and nausea rating after circular vection exposure

Regression analysis was also conducted between subjects' nausea rating after 20 minutes circular vection exposure and MSSQ score. The nausea rating of one subject reached 5 during the exposure. The exposure was terminated by the subject during the experiment, and afterwards the subject reported his nausea rating was 6. Linear regression was conducted between the total score of MSSQ and nausea rating. From the regression result, a linear correlation was found between nausea rating and MSSQ score with P-value 0.014.

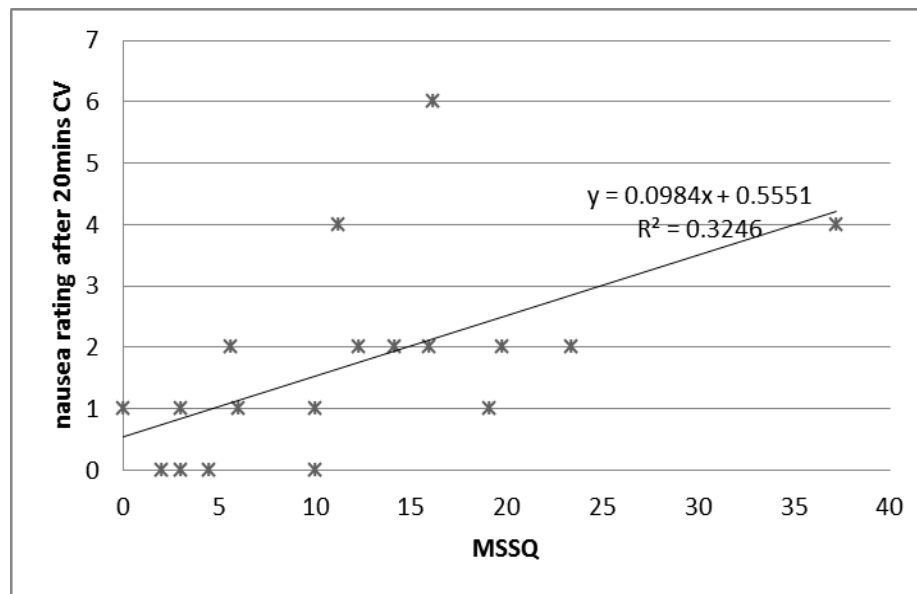


Figure 5.7 The scatter plot between MSSQ scores and nausea rating after 20 minutes exposure to circular vection stimuli. Although the correlation was significant ($p < 0.05$), the R-square was 0.32. After removing two 'outlier' data points, the R-square improved to 0.62

Nausea rating correlation between game and circular vection exposure

During the exposure of video game, one of the subjects reached 6 in 7-point nausea level during the first 5 minutes, and two other subjects reached 5 and 6 within 10

minutes after the onset of stimuli exposure. Exposure was immediately stopped when any subject reported 5 or higher in 7-point level nausea level. Regression analysis was also conducted between subjects' nausea rating after 20 minutes circular vection exposure and video game exposure. No significant relationship could be found between nausea rating after 20 minutes game video and nausea rating after 20 minutes circular vection exposure. The illustration of linear correlation between nausea rating after 20 minutes circular vection exposure and 20 minutes video game exposure is also presented in figure 5.8.

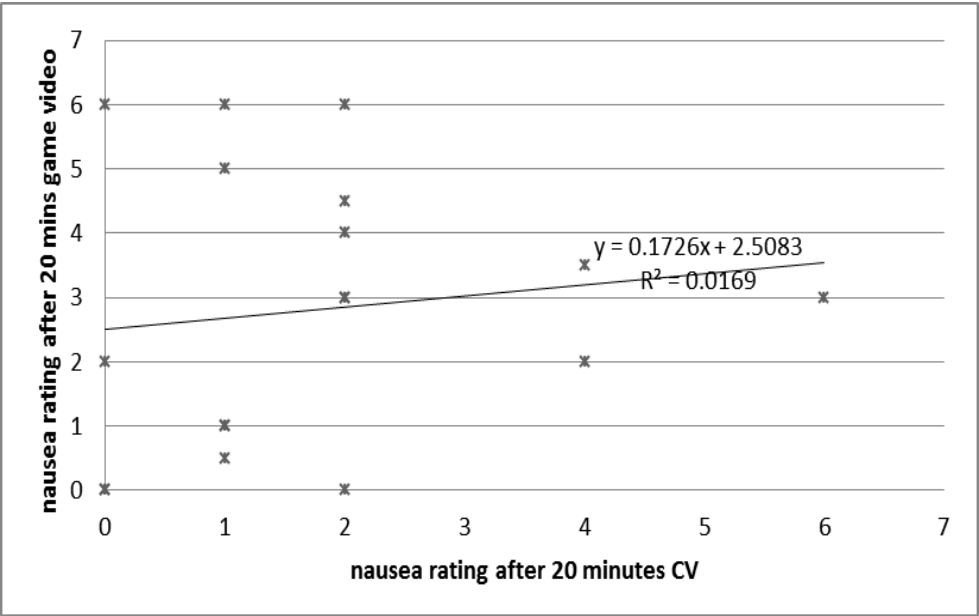


Figure 5.8 The linear correlation between nausea rating after 20 minutes circular vection exposure and nausea rating after 20 minutes game video exposure. No linear correlation could be found between the nausea rating after 20 minutes CV and nausea rating after 20 minutes game video.

5.5 Discussion

The summary statistics derived from 18 subjects in this research and 257 subjects in Golding's study showed great similarity, regardless of the differences between

subject number, ethnic origin and gender. Golding's research included both male and female, however only male subjects participated in this research. The distributions are similar between Golding's research and our study as well. Based on this experiment, MSSQ score would be utilized as the criteria to distinguish motion sickness susceptibility among subjects in our research.

Motion sickness susceptibility survey includes one question to ask subject to give a self-evaluation of motion sickness severity. The reason why motion sickness susceptibility survey was not selected as criteria in our research is that it is hard to eliminate subject bias introduced in answering only one question. While most people evaluated themselves in the middle range of motion sickness susceptibility, motion sickness susceptibility questionnaire better distinguishes the susceptibility among subjects as is shown in Figure 5.66 due to the better resolution of motion sickness susceptibility score. The linear regression analysis basically shows the evaluation from MSSS and MSSQ are in accordance with each other.

The linear collation found between nausea ratings after 20 minutes circular vection exposure and motion sickness susceptibility questionnaire shows that motion sickness susceptibility questionnaire could be a valid measure of motion sickness induced by circular vection as well.

Nausea level from the game is not significantly correlated with motion sickness induced by circular vection from our research. Some of the subjects who were motion sickness susceptible according to their self-rating did not show higher level of nausea after game exposure while other subjects who seldom feel motion sick became extremely sick during the game exposure. The reason could be that people's experience of playing video game could significantly influence the nausea level induced from game watching.

5.6 Summary

In summary, this study validated that motion sickness susceptibility questionnaire could be utilized as criteria to distinguish VIMS susceptibility among subjects. Pre-recorded game was not selected as criteria of VIMS susceptibility due to influence of prior game-playing experience.

CHAPTER 6: STUDY FOUR - BRAIN HEMODYNAMIC RESPONSES DURING VECTION: EFFECTS OF VIMS SUSCEPTIBILITY

6.1 Introduction

This study investigates the cortical response to motion sickness provoking stimuli among people with different susceptibility to motion sickness. Near-infrared spectroscopy measurement would be taken from both motion sickness susceptible and non-susceptible subjects while subjects are exposed to VIMS provoking stimuli (circular vection). We hypothesize that the visual cortical regions would be activated and the vestibular cortical regions would be deactivated during vection for people who is not susceptible to motion sickness. Meanwhile for people who are susceptible to motion sickness, the brain response follows visual activation and vestibular deactivation, but the vestibular deactivation is to a lesser degree.

Most of the earlier brain imaging studies adopted finger pressing or verbal reporting as the responding method if subjects need to make a response during the experiment. Both finger pressing and verbal reporting would trigger unwanted noise in brain imaging. A pilot study was conducted to investigate the stability of circular vection onset and offset time during short period of time.

6.2 Experiment 4A – Pilot test on stability of vection onset/offset.

6.2.1 Subjects

Seven right-handed male subjects participated in this experiment with a written consent form (age: 23-27, mean 24.7). None of them had any history of vestibular or psychological disease. The Alcohol and caffeine beverages are forbidden for 24 hours before the experiment. This study was approved by the Hong Kong University of Science and Technology.

6.2.2 Stimulus and conditions

The stimulus was presented by the LCD screen (SONY KDL-46EX720), and the field of view (FOV) is 61 degree vertically by 93 degree horizontally. The stimulus followed block design and was generated by Microsoft Visual Studio 2010. The stimulus contained an average of 320 circular patterns on a grey background, half of them were red and the other half were black. The FOV for each circular pattern varied from 1 to 2 degree. A gray fixation point was located stationary at the center of the screen all the time, with a FOV of 4 degree. The overall luminance level measured at the subject's eye location was 10lux. The trials contained discrete epochs of baseline and stimuli period. Subjects watched the stimuli at a distance of 48cm from the center of the screen.

Subjects were instructed to watch the experimental stimuli for two to three times (each time the stimulus was presented for 2.5 minutes. Stimuli presented from 5 minutes to 7.5 minutes in total. Subjects did not need to watch the stimuli all the time during the period, they could describe their feelings and raise questions anytime they want during this period). An introduction to the experiment procedure and circular vection were introduced after subjects were presented with the stimuli for the first time. To be more specific, subjects were asked about if they had any feelings of

motion after the first time of watching the stimulus. If subjects confirmed they feel themselves rotated, they were asked to describe the direction of rotation. If subjects confirmed they did not feel any motion, they were asked to watch the stimulus once more and they were asked specifically if they could feel any motion while watching the stimulus. In the second stimulus watching, subjects were asked to report any motion they feel in real time, including their rotating direction and the moving status of the dots. Subjects could drop anytime during the whole experiments. And they were allowed to continue experiments only when they could correctly describe the direction of their self-rotating. After the second time of watching the stimulus, a clear description ofvection (the Illusion of self-motion, and in our experiments thevection should be the self-rotating in the counter clock-wise direction) was introduced to the subjects. During our experiment procedure, some subjects wanted to watch the stimulus for another time after the introduction.

The experiment followed block design, where there were 3 blocks in one session and each subject needed to finish 3 sessions. The whole session started with 5 seconds presentation of grey background. One block was composed of 20s baseline and 30s stimuli and there were three repeated blocks in one trial. Circular patterns moved randomly in all directions in the baseline period, and they rotated at the same angular speed of 5 rotation per minute (RPM) in the stimuli period. Subject needed to press and hold a button whenever they started to feelvection and hold until thevection disappeared.

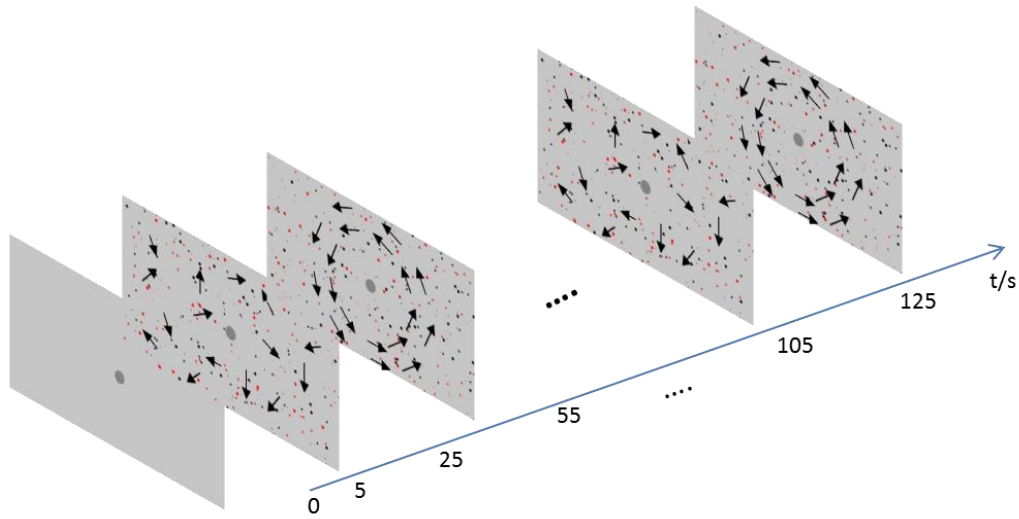


Figure 6.1 An illustration of vection stimuli in one block. Grey background with the fixation point in the center of the screen was presented for 5s at the very beginning. Then random moving dots were presented for 20 seconds, followed by 30 seconds during which all the dots moved in an co-ordinated direction (roll) while keeping the same speeds when they were moving in random direction. The 20s random moving and the 30s roll rotating sessions were repeated three times. The fixation point was shown in the center of the screen during the entire stimulus period.

6.2.3 Data analysis

The maximum vection onset and offset time in the first block of all three sessions was set as reference time for the rest of blocks. Onset time difference was calculated by using the difference between onset time and reference onset time in the second and third block, while offset time difference was calculated by taking the difference between the offset time and reference offset time in the second and third block. One of the subjects did not experience vection in all blocks, and the data from that subject was excluded from the analysis (subject 6). A within subject student-t test was conducted on the vection onset and offset time difference to see if the maximum of vection onset and offset time could cover the vection period in the rest of the blocks.

6.2.4 Result

From the statistical analysis, we could see the maximum of vection onset time among three first blocks in each trail are larger than the vection onset time in the second and third blocks for subject 1, 2, 3 and 5. Similar conclusion could not be drawn from the statistical result for subject 4 and 7. The maximum of vection offset time among three first blocks in each trail are larger than the vection offset time in the second and third blocks for the subjects. . Considering the target of this study is to verify if the maximum of vection onset/offset time could provide a better representation of vection period compared with using purely stimulus period. It was shown this method could act as the screening of vection period in general.

The result also shows the variance of vection onset time difference is smaller than that of the vection offset difference. For subject 4, the standard deviation for vection onset time difference is within 0.5 seconds. This indicates that subject 4 started to experience vection almost starting from the identical time in each block. For subject 7, it is also considered to be acceptable for using the maximum vection onset time among first three blocks as the reference of vection onset time, because the vection period for subjects generally lasts much longer.

Table 6.1 The statistics table on the difference between vection onset/offset time and reference on/off set time. Onset time difference was calculated by using the difference between onset time and reference onset time in the second and third blocks, while offset time difference was calculated by taking the difference between the offset time and reference offset time in the second and third blocks.

	Vection onset time difference(s)				Vection offset time difference(s)			
	mean	S.D	T	P-value	mean	S.D	T	P-value
sub. 1	0.90	0.70	3.14	<0.05	11.21	4.62	5.94	<0.05
sub. 2	8.91	1.49	14.67	<0.05	3.69	3.77	2.4	<0.05
sub. 3	11.41	0.87	32.15	<0.05	6.57	5.57	2.89	<0.05
sub.4	-0.057	0.47	-0.30	0.611	6.67	6.73	2.43	<0.05
sub.5	10.34	5.58	4.54	<0.05	2.095	2.32	2.21	<0.05
sub.7	0.86	1.7	1.22	0.138	5.39	5.68	2.33	<0.05

From this result, it could be concluded that the maximum of vection offset time during the first blocks of all sessions could be used as a reference as the vection offset in the remaining blocks in those sessions.

6.3 Experiment 4B –Brain hemodynamic response during vection: effects of VIMS susceptibility

6.3.1 Subjects

Twenty right-handed male subjects participated in the experiment with a written consent form (age: 23-30, mean 25.4). None of them had any history of vestibular or psychological disease. Female subjects were not included in this study is because motion sickness susceptibility has been proved to vary through menstrual cycle (Golding *et al.*, 2015). And it was also found in our earlier experiments that fixing the detectors and light transmitters firmly onto the scalp is very difficult for female

subject due to the long hair. Alcohol and caffeine beverages were forbidden for 24 hours before the experiment. This study was approved by the Hong Kong University of Science and Technology.

The set of experiment was conducted in the acoustic room where noise level was well controlled (<50dB). The experiment was composed of training session, cortical blood oxygenation measurement, and visually induced motion sickness test. In the training, subjects needed to fill in the Motion Sickness Susceptibility Questionnaire (MSSQ) and Motion Sickness Susceptibility Survey (MSSS), and needed to participate in a screening procedure which used the same type of stimuli as in the later experiment (Golding 2006). Subjects were instructed to know the experiment procedure and to make responses. Subjects who failed to follow the instruction or experience vection could not proceed with the experiment.

During the experiment, subjects equipped with near-infrared spectroscopy and plethysmograph measurement were seated comfortably in front of large screen with their heads fixed on a chin-rest. Subjects watched the stimuli at a distance of 48cm from the center of the screen. The stimuli were composed of five trials, and each trial was composed of three repeated blocks. NIRS and plethysmograph measurement were taken all the time during the brain measurement. The blood pressure at the ear lobe was measured at 12.5 samples per second and the purpose of recording the blood pressure data was to cross check and isolate the effects of systemic changes of blood pressure on the findings.

6.3.2 Stimuli and conditions

The experimental settings were exactly the same as those in pilot studies. Stimuli were presented on the same LCD screen. The stimulus contained an average of 320 circular patterns on a grey background, half of them were red and the other half was black (FOV 1-2 degree). Subjects were instructed to fix their eyes on a fixation point

located at the center of the screen. The trials contained discrete epochs of baseline and stimuli period. One block was composed of 20s baseline and 30s stimuli and there were three repeated blocks in one trial. Circular patterns moved randomly in all directions in the baseline period, and they rotated at the same angular speed of 5 rotation per minute (RPM) in the stimuli period. During the experiment, the environment light was turned off, and surrounding objects were blocked from the subject visual field by a black curtain.



Figure 6.2 A photograph illustrating the experimental setup with the LCD screen, chin rest and the subject mounted with NIRS transmitters and detectors. A black curtain was temporarily removed for the photo taking.

Five trials of stimuli were consequently presented to subjects with rest time in between. Each trial contained three blocks and lasted for 155s. Subjects were instructed to make response in the first trial by pressing the button at their right hand side once they feel vection and containing pressing until vection disappeared. During the rest two blocks, subjects did not need to make any response. Subject take rest between different trails, the rest included three minutes rest with eyes closed and three minutes rest with eyes. During the rest, subjects reported verbally if they entered vection in the second and third trial and submitted their nausea rating at the

end of visual stimuli. 7-point nausea rating was given as the standard, and no subject reported their nausea larger than 0 (no symptom).

During the above procedure, NIRS measurement was taken from the brain, and the plethymograph measurement was taken at the ear lobe at the same time. A 2.5cm by 2.5cm light sensor was placed at the right down corner of the LED screen. It was covered in black and it collected information on screen luminance change. The data collected by the light sensor with sampling rate 12.5HZ was used as the alignment standard to synchronize the NIRS measurement and the visual stimuli.

6.3.3 Apparatus

The NIRS instrument (Imagent ISS Inc., Champaign IL.) utilized in this study had 16 light sources (eight at 830nm, eight at 690nm) and four photomultiplier detectors. The light sources were transmitted through optical fibers (0.4mm core diameter), and each pair of 690nm light source and 830 light source was coupled as a combined light source. The near infrared light was modulated at a frequency of 110MHz. The AC, DC and phase data were collected. The sampling rate was set as 12.5Hz.

6.3.4 Optodes location

The optic fibers and detector in this study were placed with reference to the Cz, T4, C4 and Oz in 10-20 system (Homan and Herman, 1987). Two panels were located to a home-made rubber cap with little material flexibility. Panel1 was placed on the lateral part of the brain, while panel2 was placed on the occipital part of the brain. The graphical demonstration of the panels is shown in Figure 6.23. Blue dots indicate the placement of the light transmitters and red dots represent the detector location. The relative distances between detectors and light transmitters were fixed. Each detector could take the measurement from several light transmitters and the distance between each detector and light transmitter was 3 centimeters.

To repeatedly locate the panel placed on lateral side of the brain, the light transmitter 5 in panel1 was put exactly on T4, and the line connecting detector C, light transmitter 4 and light transmitter 5 were aligned with the line connecting T4, C4 and Cz. According to the dimensional difference of subject head in this study, detector C would be placed 8mm to 17mm lower than C4. For the panel placed on the occipital part of brain, detector D was placed on the Oz, and the line connecting light transmitter 8 and detector D were placed in alignment with the line connecting Oz and Cz. As both panels were fixed in all the experiments, the alignment procedure guaranteed the repeatability of placement. The demonstration for the panel placement could be seen from Figure 6.3.

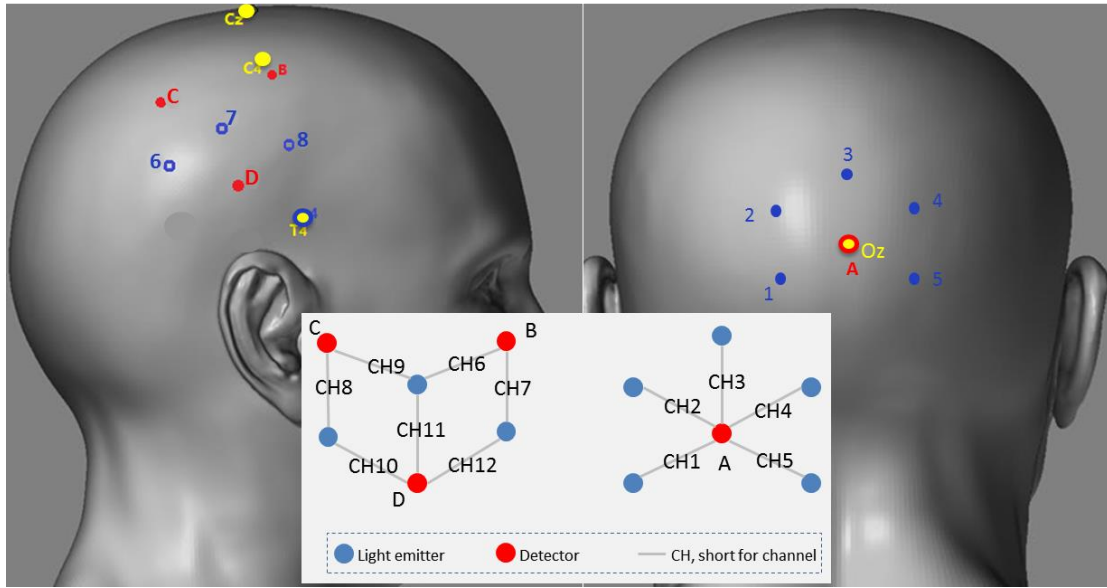


Figure 6.3 An illustration of the NIR detectors and transmitters placement. The red dots represent detector location, blue dots represent transmitters location and the dots circled in yellow are extra scalp markers (taking C_z , C_4 , T_4 and O_z from the 10/20 system). The image in the lower middle illustrates the locations of the measurement channels in this experiment (The model for the brain is downloaded from http://i2.photobucket.com/albums/y20/MatrixNAN/RealisticMaleHead_06.jpg, on 10:30pm, UTC+8, May, 17th 2014)

6.4 Data analysis

6.4.1 Subject grouping

Motion Sickness Susceptibility Questionnaire has been widely applied to distinguish between people with different susceptibility to motion sickness (Farmer *et al.*, 2015). According to our earlier experiment, the mean for MSSQ score among 20 subjects in our experiment is 11.3059, which meets the mean (11.3) in the original study (Golding, 1998). A strong linear correlation could be found between the MSSQ score and self-evaluation in MSSS (p-value = 0.001).

Thus our subjects were divided into two groups, subjects who got the MSSQ no less than 11.3 were treated as motion sickness susceptible group, and the rest were recognized as motion sickness non-susceptible group.

6.4.2 Data processing

NIRS data processing started from channel exclusion and artifact recognition. Channels failing to show heart rate pattern were excluded from the following analysis (Jasdzewski *et al.*, 2003). Artifact recognition utilized two-sided moving standard deviation algorithm as the criteria to pick up the data which was significantly contaminated by noise (Scholkmann *et al.*, 2010). This algorithm could extract the period contains abnormal shift in NIRS data, where the shift is generally triggered by sudden movement of optical fiber, detector or the subject. Blocks were marked as noise contaminated if artifact was detected by the algorithm. The noise contaminated blocks were excluded.

Afterwards, the data processing procedure was conducted through HomER package (Huppert *et al.*, 2006). High frequency noise and slow shift were filtered out by a 3rd Butterworth bandpass filter of 0.001-0.3Hz with no phase distortion (Osharina *et al.*, 2010). The changes of oxygen-hemoglobin (HbO) and deoxygen-hemoglobin (Hb) concentration were derived from NIRS measurement based on modified Beer-Lambert Law (Arridge *et al.*, 1993). A grand average of hemoglobin concentration change was then calculated by averaging the blocks.

Given that it generally takes 5s to 8s for oxygen hemoglobin level to reach its peak after stimulus onset (DeYoe *et al.*, 1994), the average hemoglobin level takes 10s to 17s within the total 20s baseline period. The average hemoglobin level of vection was determined individually by using the response time. As subjects marked their vection period by finger pressing in the first block of each trial, vection onset and

offset time was calculated separately from taking the average of onset and offset time recorded from total 5 trials.

Considering the experimental design, two-way ANOVA analysis was conducted to draw the independent and interactive effects of vection and motion sickness susceptibility. ANOVA analysis is widely utilized in block design human brain studies (Tak and Ye 2014) to identify significant factor. Normality test was conducted on hemoglobin level among all channels as well. Wilcoxon sign rank analysis was also performed on channels concerning the data normality property.

6.5 Result

The statistical analysis was conducted by IBM SPSS Statistics 19. The statistical result of two-way ANOVA shows a significant condition effect in both occipital part and right hemisphere of the brain. Channel6 ($F= 5.317$, $p= 0.028$), channel7 ($F=6.369$, $p=0.017$), channel10 ($F= 6.365$, $p=0.017$), channel11 ($F=22.791$, $p<0.001$) and channel12 ($F=6.061$, $p=0.020$) on the right hemisphere also show a significant increase in HbO concentration change during vection. Condition includes baseline and vection, which is represented by 0 and 2 in the figure (0 represents baseline and 2 represents vection).

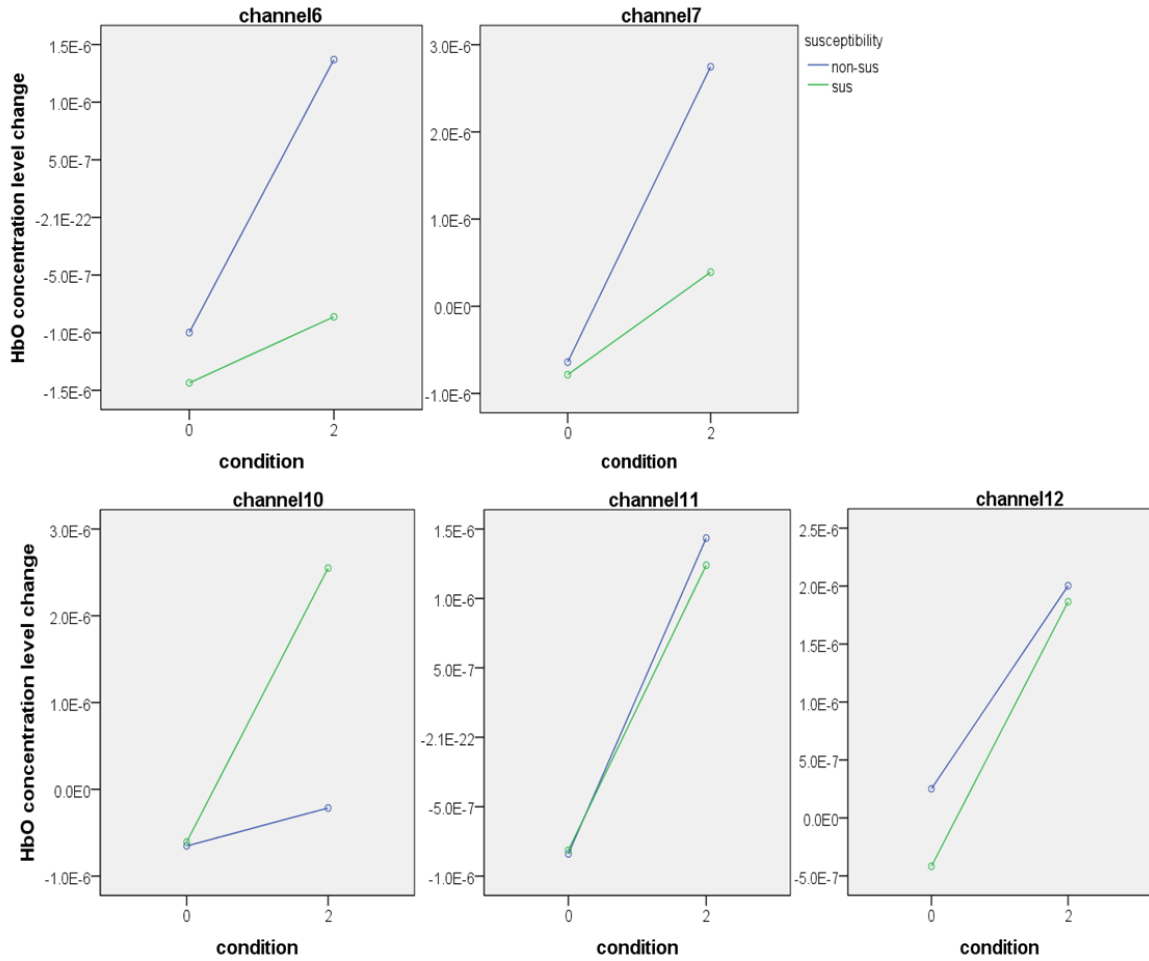


Figure 6.4 The interaction effects of vection (with: condition 0 and without: condition 2) and susceptibility to motion sickness (susceptible: green and resistive: blue) on changes of HbO levels measured in channels 6, 7 (motor/somatosensory area), 10, 11 and 12 (middle temporal lobe to posterior parietal region). Data from 18 subjects.

The channels which were located at the occipital part of the brain and showed significant increase from baseline to vection are illustrated in Figure 6.45. Channel2 ($F= 4.374$, $p= 0.045$), channel3 ($F= 10.826$, $p= 0.003$) and channel4 ($F= 5.366$, $p= 0.028$) show an increase in HbO concentration change during vection, compared with baseline. To better illustrate the data, the motion sickness susceptible and non-susceptible group are shown separately.

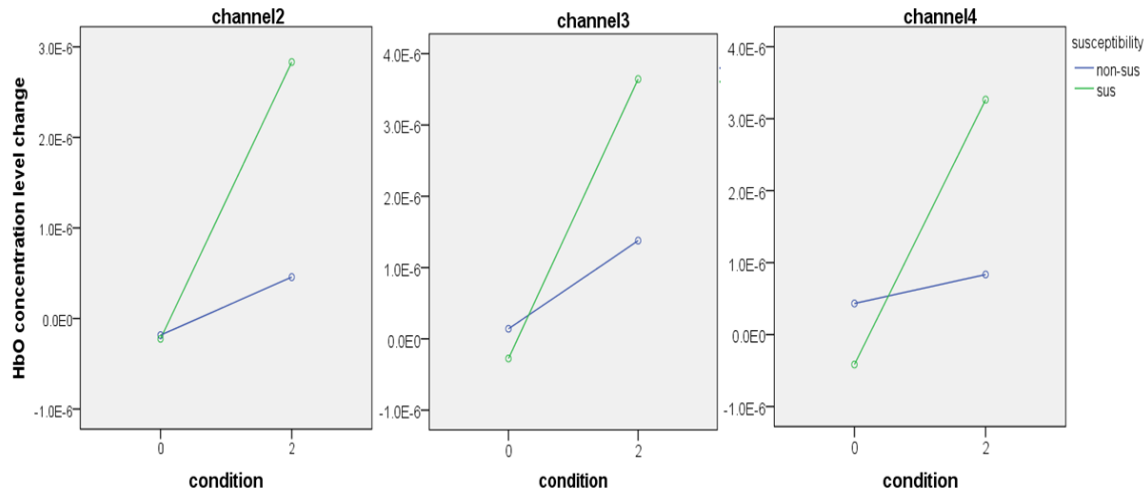


Figure 6.5 The interaction effects of vection (with: condition 0 and without: condition 2) and susceptibility to motion sickness (susceptible: green and resistive: blue) on changes of HbO levels measured on channels 2, 3 and 4 (corresponding to occipital lobe). All three channels are located at the occipital part of the brain. Exact location of the three channels with reference to 10/20 system could be read from Figure 6.3.

The statistical analysis result is shown in Figure 6.5, where the motion sickness susceptible and non-susceptible groups are also separated. Channel6 also shows a significant susceptibility effect ($F=4.51$, $p=0.042$), which means that the overall HbO is higher in non-susceptible group than that in susceptible group.

Channel 8 shows a significant susceptibility effect ($F= 4.77$, $p=0.037$) and a significant interaction effect ($F= 5.3$, $p=0.028$). As illustrated in Figure 6.6, HbO concentration increases from baseline to vection among susceptible people and decreases from baseline to vection among non-susceptible people.

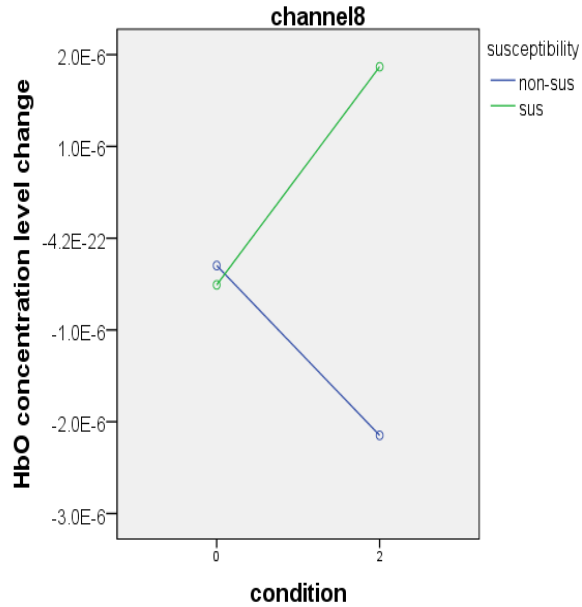


Figure 6.6 The interaction effects of vection (with: condition 0 and without: condition 2) and susceptibility to motion sickness (susceptible: green and resistive: blue) on changes of HbO level measured on channel 8 (corresponding to intraparietal area). Motion sickness susceptible group shows significant increases in HbO concentration change while motion sickness non-susceptible group shows significant reduction in HbO concentration changes. The interaction effects were significant. Data from 18 subjects.

However, not all channels pass the normality test, the Kolmogorov-Smirnov normality test result on each channels is shown in Table 6.2. The most possible reason for failing the normality test should be the limitation in number of subjects.

Table 6.2 Significance level for each channel using Kolmogorov-Smirnov normality test. Data failed Kolmogorov-Smirnov normality test if the p-value is less than 0.05. Channels 2, 8 and 10 failed normality test according to the results in the table.

channel	1	2	3	4	5	6	7	8	9	10	11	12
p-value	0.072	<0.01	0.147	>0.15	>0.15	>0.15	0.119	<0.01	0.093	0.037	0.075	0.138

It could be seen from the Table 6.2 that channel 2, 8 and 10 fail the normality test, thus data from these channels are further processed by Wilcoxon test. As investigating the differences between people with different susceptibility to motion sickness is one of the major targets, the Wilcoxon test is conducted separately in motion sickness susceptible and non-susceptible group.

Wilcoxon sign rank test shows a decrease in channel 8 ($p = 0.016$) among motion sickness non-susceptible people, especially for the channel with non-normal data. However, channel2 and channel10 could not show any significant change according to the test. Meanwhile, Wilcoxon sign rank test shows an increase in channel2 ($p = 0.038$) and channel10 ($p = 0.006$), and no significant increase in HbO concentration change could be found in channel8.

The Wilcoxon test for other channels also reveals the differences between people with different susceptibility. Among motion sickness susceptible group, channel 1($p = 0.038$), 2($p = 0.038$), 3($p = 0.016$), 4($p = 0.029$), and 5($p = 0.022$) on the occipital part of the brain and channel 10($p = 0.006$), 11($p = 0.012$) and 12($p = 0.016$) from the right hemisphere, show a significant increase in HbO from baseline to vection. Among motion sickness non susceptible group, channel 3($p = 0.049$) on the occipital brain, channel 6($p = 0.022$), 7($p = 0.029$) and 11($p = 0.005$) on the right hemisphere show a significant increase while channel 8($p = 0.016$) on the right hemisphere demonstrates a significant decrease in HbO level from baseline to vection.

In this study, the control data collected from plethysmograph did not show any significance for vection effect. This indicates that the significant findings on HbO changes were not caused by the systemic changes in blood pressure.

6.6 Discussion

In this study, the objective was to detect whether brain responses to motion sickness provoking stimuli are different between people with different susceptibility to motion sickness. In order to avoid any individual brain response aroused from nausea, the period and speed of vection stimuli have been carefully tested before adopted in the experiment. The stimulus adopted in this experiment aims at evoking circular vection and avoiding nausea at the same time. 7-point nausea rating and post-exposure simulator sickness questionnaire were collected as reference after each vection exposure. None of the subjects reported any level of exposure or any symptoms in the questionnaire after each trial of vection exposure.

From the statistics results, it could be concluded that channel 2,3,4,6,7,10, 11 and 12 show an increase when people experience vection. Among those channels, channel2, channel3 and channel4 locate at the occipital lobe right above Oz in the 10-20 system. According to the previous studies detecting intracranial structure with reference to 10-20 system (Okamoto *et al.*, 2004), it could be inferred that Oz mostly locates at around Brodmann Area 18 or 19. The activation direction and area in occipital area meet well with the earlier studies where median parieto-occipital cortex was found to be activated in counter-clock/ clock wise rotating dots compared with stationary dots (Brandt *et al.*, 1998).

Other activated channels by vection locate at the right brain hemisphere. C4 and T4 are proved to be located mostly at post/pre-central and middle temporal area (Okamoto *et al.*, 2004). The activated channels locate at the area posterior to the line connecting C4 and T4. Channel 6 and 7 locate around post/pre-central area (C4 in 10-20 system, BA 3, 6 or 1), which is generally marked as somatosensory cortex and motor cortex. The activation in these areas might be motivated by the vection feeling, as subjects feel themselves rotating during the vection. Earlier studies proved that imaginary motion in human could activate motor cortex (Ersland *et al.*,

1996). Channel 10, 11 and 12 locate posterior to middle temporal area (T4 in 10-20 system, BA 21 or 22), thus most likely are located from middle temporal lobe to posterior parietal region. The hemoglobin level changes in those areas could be due to the activation of vestibular related brain cortical areas. Earlier studies of human brain cortices have defined some particular area, such as temporo-peri-Sylvian vestibular cortex in lateral cortical temporoparietal area, which is highly correlated with vestibular function (Kahane *et al.*, 2003). Middle temporal to posterior temporal lobe is found to be activated by vestibular stimulus in earlier studies (Fasold *et al.*, 2002). The activation channels in our study are in alignment with the earlier findings in vestibular cortices.

Channel 6 and channel 8 also show a significant susceptibility effect based on the main effect and interactive effect plot. Channel 8 and channel 9 locate around above posterior temporal lobe, which is generally considered as inferior parietal lobe to intraparietal areas. The statistical result shows that non-susceptible group has a lower oxygen-hemoglobin level than susceptible group in channel 8 and a higher oxygen-hemoglobin level than susceptible group in channel 6. This effect further indicates that non-susceptible group has a higher neural activity level in motor area and is less activated in the area above superior temporal lobe. One of our earlier studies also shows this area is highly related to vestibular functions.

Most importantly, channel 8 shows a significant interactive effect, which indicates the susceptible and non-susceptible group have different changing directions in oxygen-hemoglobin level undervection feeling. The interactive effect shows that oxygen-hemoglobin level in channel 8 increases duringvection among people who are susceptible to motion sickness while decreases among people who are not-susceptible to motion sickness.

Limitation

The limitation in this study lies in the uncertainty of intracranial brain structures. Although placing near-infrared spectroscopy detectors and light transmitter according to 10-20 system is a widely applied procedure among NIRS brain studies (Hock *et al.*, 1997; Matsuda and Hiraki, 2006), variance could exist in underlying brain structures given individual brain differences (MacDonald *et al.*, 2006).

6.7 Summary

This study investigated the brain activation signature among people with different susceptibility to motion sickness when people experience circular vection. Given that people have different susceptibility to motion sickness, motion sickness susceptibility was considered to be the factor of specific interest in this study. The result shows that both visual area and lateral region of human brain would be activated during circular vection among motion sickness susceptible and non-susceptible people. It is also found one channel which is most likely to be located around intra-parietal region responded differently to circular vection among people with different susceptibility to motion sickness.

CHAPTER 7: STUDY FIVE – EXPLORATORY STUDY ON EFFECTS OF ADAPTATION ON VIMS SUSCEPTIBILITY AND REGIONAL BRAIN HEMODYNAMIC RESPONSES

7.1 Introduction

This study is an exploratory test to investigate the cortical response change to VIMS provoking stimuli (circular vection) before and after adaptation among people with different susceptibility to motion sickness. The desensitization and adaption to motion sickness have been developed for decades for both clinical and practical usage, for example pilot and air force training. However the brain signature changes are still poorly documented. This study hypothesizes that brain signature will change in motion sickness susceptible people, and will not change in motion sickness non-susceptible people after the adaptation to VIMS provoking stimuli. Also cortical hemodynamic in motion sickness susceptible group will become similar to that of non-susceptible group after desensitization training.

7.2 Materials and methods

7.2.1 Subjects

Four right handed male subjects participated in this study with the written consent form. Their ages ranged from 23 to 26. None of them had any history of vestibular related disease. This study is proved by the Hong Kong University of Science and Technology. The subjects were carefully selected to cover both motion sickness susceptible and non-susceptible people.

7.2.2 Experiment procedure

Before experiment, subjects were instructed to fill in motion sickness susceptibility questionnaire (MSSQ) and motion sickness susceptibility survey (MSSS). They also got familiarized with the experiment stimuli and environment, and were introduced with experiment procedure. All the subjects were well acknowledged of the procedure and their tasks, and they showed high willingness to participate this experiment.

The experiment was composed of an adaptation training session and two NIRS measurement session before and after the training. Subjects needed to go through NIRS measurement in the first part of the experiment. In the first measurement part, subject watched visual stimuli from a large LCD screen and they needed to fix their eyes on a fixing point located the center of the screen. During the stimuli, subjects sat comfortably and fixed their head on the chin-rest. They watched the stimuli at a distance of 48cm away from a 46 inch LCD screen. NIRS measurement was taken for the entire session.

In the adaptation training session, subjects were repeatedly exposed to vection provoking stimuli every day for around 40 minutes until subjects illustrated adaptation, if any. The training session was conducted in exactly the same environment as in the NIRS measurement session. Subjects were instructed to fix their eyes on a fixation point in the center of the screen during the training session as well. The training exposure was continuous unless subject pressed the stop button. Subjects were instructed press stop once they feel a nausea rating level of 5 or more according to 7-point nausea rating. Experiment would proceed when subjects feel they are ready to continue.

Another NIRS measurement was conducted after the adaptation training session with the same settings and environment as in the first NIRS measurement session.

7.2.3 Stimuli

SONY KDL-46EX720 LCD screen was used to present the stimuli in all sessions, and the field of view (FOV) was 61 degree by 93 degree. The stimulus contained an average of 320 circular patterns on a grey background; half of the patterns were in red and the other half were in black. The FOV for each circular pattern varied from 1 to 2 degree. A gray fixation point was located stationary at the center of the screen all the time, with a FOV of 4 degree. The overall luminance level measured at the subject's eye location was 10lux.

During the NIRS measurement session, the stimuli were presented in block design that contains discrete epochs of baseline and stimuli period. One block was composed of 20s baseline and 30s stimuli and there were three repeated blocks in one trial. Circular patterns moved randomly in all directions in the baseline period, and they rotated at the same angular speed of 5 rotations per minute (RPM) in the stimuli period. Five trials of stimuli were consequently presented to subjects with rest time in between. Each trial contained three blocks and lasted for 155s.

Subjects were instructed to make response in the first trial, by pressing the button at their right hand side once they feel vection and holding on pressing until vection disappears. During the rest two blocks, subjects did not need to make any response. Enough rest was taken after each trial. Subjects reported verbally if they had entered vection in the second and third trial and submitted their nausea rating at the end of visual stimuli. 7-point nausea rating was taken as the standard.

In the adaptation training session, all patterns rotated at the same angular speed of 5 rotation per minute (RPM). Subject could press the stop button anytime to exit the

exposure during the experiment if they felt any uncomfortable feeling such as nausea and headache. During the experiment, the entire environment light was turned off, and surrounding objects were blocked from the subject visual field by a black curtain.



Figure 7.1 A photograph illustrating subjects with NIRS equipment during pilot testings. The experimental setting in this experiment was the same as that in experiment 4B.

During the NIRS measurement session, NIRS measurement was taken from the right hemisphere of brain, and the plethymograph measurement was taken at the ear lobe at the same time. A 2.5cm by 2.5cm light sensor was placed at the right down corner of the LED screen, collecting information of screen luminance change and was covered in black. The data collected by light sensor was used as the alignment standard in synchronizing the NIRS measurement and stimuli.

NIRS measurement parameter settings and optodes location were the same with the earlier NIRS experiment.

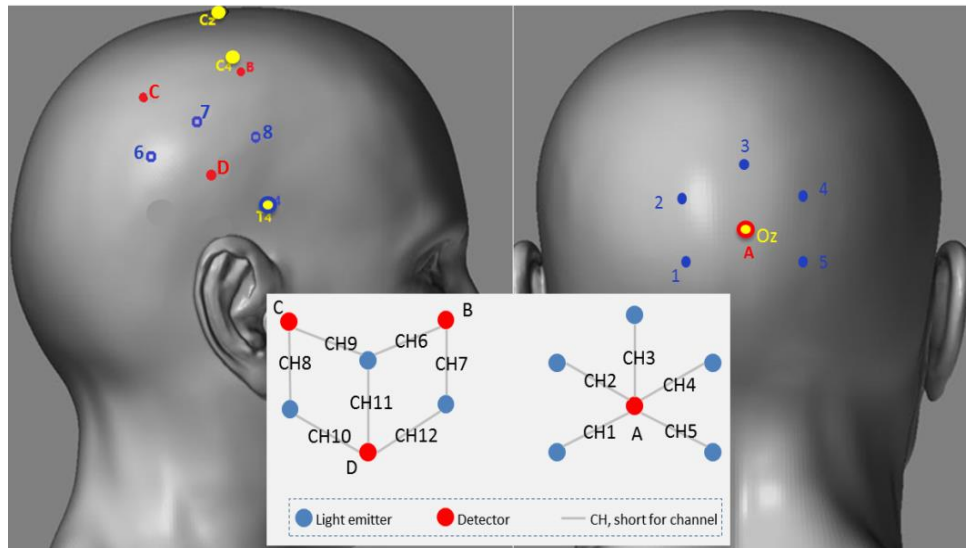


Figure 7.2 An illustration of detectors and light transmitters placement. The red dots represent detector location, blue dots represent light transmitters location and the dots circled in yellow are extra scalp markers. The image in the middle illustrates the locations of the channels in this study (The model for the brain is downloaded from http://i2.photobucket.com/albums/y20/MatrixNAN/RealisticMaleHead_06.jpg, on 10:30pm, UTC+8, May, 17th 2014)

7.2.4 Data processing

Motion sickness rating and training data

The detailed motion sickness susceptibility and motion sickness survey score of the four subjects are listed out in below Table 7.1. The table listed the MSSQ for childhood and adult separately for subjects participated in this experiment. As explained in study three, MSSQ contains two evaluation forms for both childhood and adult. Below table separately lists the MSSQ score for childhood and adult.

Table 7.1 The MSSQ and MSSS score of the subjects in this experiment. This table lists the MSSQ score for both childhood and adult. Subject A had motion sickness in his childhood but never had motion sickness since adult. Subject D was not motion sickness susceptible as a child however became motion sickness susceptible since adult. Subject B and C experienced motion sickness in both childhood and adult period.

	subject A	subject B	subject C	subject D
MSSQ-child	10	9	5.14	0
MSSQ-adult	0	10.125	9	16.2
MSSQ-total	10	19.125	14.14	16.2
MSSS	2	3	3	3

Subject A could be categorized as motion sickness non-susceptible while subject B, C and D are categorized as susceptible using the 50th percentile total score (around 13) as the motion sickness susceptibility standard. A validity test for motion sickness susceptibility test was conducted as well. The exposure time is around 40 minutes and roughly at the same time every day. 7-point nausea rating was collected after each exposure. The detailed exposure time and nausea rating are summarized in the Table 7.2 below:

Table 7.2 The summary of exposure minutes and nausea rating of every subject. The number listed in below table is in the form of exposure minutes (nausea rating). For example, subject A exposed to vection stimuli for 45 minutes and his nausea rating after 45 minutes exposure was 0 in day 1. Subject D reached nausea level of 6 after 6 minutes exposure and he would not continue exposure in day 1. Multiple record on one day means subject took rest between exposures on the same day (generally because subject reported high nausea level).

exposure minutes (nausea rating)	subject A	subject B	subject C	subject D
Day 1	45(0)	45(1)	45(1)	6(6)
Day 2				9.5(5)
	30(0)	30(1)	30(1)	8.55(5)
				11.3(4)
Day 3				18.8(5)
	30(0)	30(0)	30(0)	20.8(5)
Day 4	35(0)	35(0)	35(0)	30(0)
Day 5	40(0)	40(0)	40(0)	40(0)
Day 6	40(0)	40(0)	40(0)	40(0)
Day 7	40(0)	40(0)	40(0)	40(0)

Subject nausea rating was taken as the standard to evaluate if the adaptation to the circular vection occurred. The adaptation training terminated after none of the subjects reported any level of nausea for consecutive 4 days, and the total training lasted for 7 days as a result.

NIRS data processing

NIRS data processing followed same procedure both before and after adaptation training. All channels failed to show heart rate pattern were excluded from the following analysis (Jasdzewski *et al.*, 2003). Blocks contaminated with motion artifact were picked up by two-sided moving standard deviation algorithm and excluded as well (Scholkmann *et al.*, 2010).

NIRS data analysis was conducted through HomER package (Huppert *et al.*, 2006). High frequency noise and low frequency shifts were filtered out by a 3rd Butterworth bandpass filter of 0.001-0.3Hz with no phase distortion (Osharina *et al.*, 2010). The change of oxygen-hemoglobin (HbO) and deoxygen-hemoglobin (Hb) concentration is calculated based on modified Beer-Lambert Law (Arridge *et al.*, 1993). A grant average of hemoglobin concentration change was then calculated by averaging the blocks.

Baseline calculation took data from 10s to 17s within the total 20s baseline period given that it generally takes 5s to 8s for oxygen hemoglobin level to reach its peak after stimulus onset (DeYoe *et al.*, 1994). The period for vection hemoglobin level calculation varied accordingly with individual response time that is determined by finger pressing in the first block of each trial. The averaged hemodynamic level of each channel could be calculated from the NIRS measurement before and after adaptation training.

Considering significant varieties of motion sickness symptoms and adaptations among each individual, Mann-Whitney test was conducted within each subject on the hemoglobin level change during vection before and after adaptation training.

7.3 Result

7.3.1 Adaptation training result

According to the MSSQ score, subject A is categorized as motion-sickness non-susceptible and Subject B, C and D are grouped as motion sickness susceptible. During the period of 7 days exposure, no nausea was reported by subject A. Subject B and subject C had nausea rating of 1 after the first and second exposure. No more nausea was reported by these two subjects after the third training exposure. Subject D abandoned the first training after 6 minutes exposure as he reported serious

nausea and could not continue. The exposure duration before stop gradually became longer in the second and third exposure. And starting from the forth exposure, no nausea was reported by the subject any more. As illustrated in Figure 7.2, all subjects adapted to the vection-provoking stimuli after at most 3 repeated exposures. The training stopped when no subjects reported any nausea for continuously 4 days after 40 minutes exposure to vection stimuli. The adaptation process was similar as that was described in earlier studies (Golding and Stott, 1995, Stern *et al.*, 1989).

7.3.2 Vection behavioral change

During the 7-day training period, the vection intensity was also reported to be reduced among all subjects. Subject A reported almost no feeling of vection after 4 days of exposure. The rest of the subjects reported significant reduction in vection intensity. Below Table 7.3 is extracted from the behavioral measurement before and after adaptation training that was conducted in NIRS measurement sessions, as subject reported whether they had vection in each of the blocks, and the vection duration was recorded during the first block of each trial. Vection occurrence is defined as how many times people feel vection in 5 repeated blocks which contains a total of 15 repeated blocks. The vection duration was averaged using 5 blocks during which subject's vection time were recorded by finger pressing.

Table 7.3 The vection occurrence and duration for each subject before and after adaptation training. Occurrence refers how many blocks that subject reported vection out of a total number of 15 blocks before and after training. Duration refers to how long could subject feel vection on average before and after training. For example, subject A had vection in all 15 blocks and the average vection period was 15.124s before training. After training, he could feel vection in 2 blocks out of total 15 blocks and his average vection period reduced to 5.494s.

	subject A		subject B		subject C		subject D	
vection	occurrence	duration (s)	occurrence	duration (s)	occurrence	duration (s)	occurrence	duration (s)
before training	15/15	15.124	15/15	12.881	15/15	13.194	15/15	8.977
after training	2/15	5.494	14/15	14.567	12/15	3.996	7/15	4.654

Change of vection occurrence and duration are shown in the table. Reduction could be clearly found in subject A and subject D. Subject B couldn't show significant reduction in either occurrence or duration and subject C showed a significant reduction in vection duration only. In addition, all subjects reported a significant reduction in vection intensity after adaptation training. Given that motion sickness is a symptom with great individual difference, the adaptation is also very personalized in terms of behavioral measurement.

7.3.3 Hemodynamic change

From the adaptation training, we could conclude that subject A is not susceptible to the vection provoking stimuli and subject D is very susceptible among all four subjects, subject B and C stays relatively in the middle range. Subject D showed a clear adaptation according to the nausea measure while subject A stayed at none nausea level through the entire adaptation training.

Hemodynamic was illustrated in below Figure 7.3 and Figure 7.4 for each subject. Channel in red means HbO concentration significantly increased during vection while channel in blue stands for significantly decreased. Channel with no color refers to no significant change could be found in HbO level during vection.

Significant change (mann whitney test p-value <0.01) was found in the area which was proved to be different between people with different susceptibility to motion sickness in the earlier experiment in subject D. Hemodynamic change for subject D is illustrated in the Figure 7.3 below. It is found that all channels showed an opposite hemodynamic level change before and after adaptation training for subject D except channel 3, 9, 10, 11 and 12.

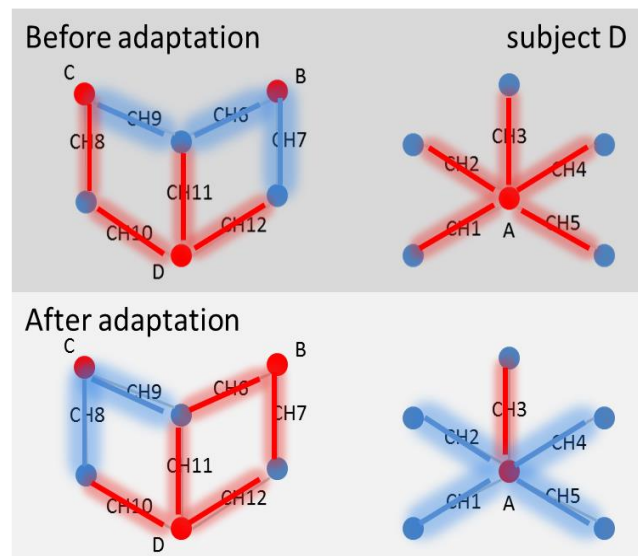


Figure 7.3 An illustration of the changes in the cortical hemodynamic before and after adaptation for subject D. blue dots represent the location of NIR light transmitter and red dots represent the location of NIR detectors. Channels highlighted in red represent HbO level increases in cortical area covered by the channels. Channels highlighted in blue represent HbO level decreases in the cortical area covered by the channels. The purpose of this graph is to illustrate the cortical hemodynamic change before and after adaptation training for motion sickness susceptible subject D.

For subject A, it's found that HbO in channel 2, 6 and 9 reversed changing direction, and HbO change is no longer significant in channel 7, 8 and 10 before and after adaptation training (mann whitney test p-value <0.01). Although no change in nausea rating was reported in the training procedure, Subject A experienced significant reduction in vection occurrence, duration and intensity.

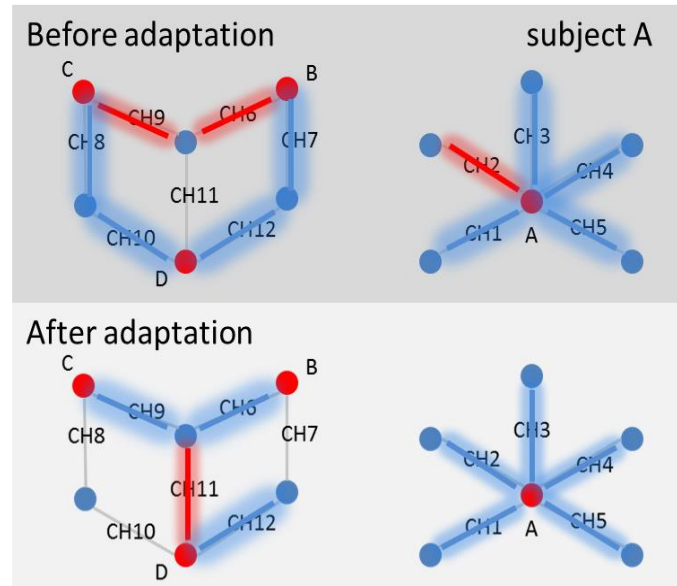


Figure 7.4 An illustration of the changes in the cortical hemodynamic before and after adaptation for subject A. blue dots represent the location of NIR light transmitter and red dots represent the location of NIR detectors. Channels highlighted in Red represent HbO level increases in cortical area covered by the channels. Channels highlighted in blue represent HbO level decreases in the cortical area covered by the channels. Channels not marked in red or blue represent no significant changes were found in the cortical area covered by the channels. The purpose of this graph is to illustrate the cortical hemodynamic change before and after adaptation training for motion sickness susceptible subject A.

Subject B and subject C could not be categorized as typical non-susceptible or susceptible people according to the original nausea rating to vection stimuli. But it could be found clearly that the adaptation was also quite different between subject B and subject C. Subject B was the only one who did not show reduction in both vection occurrence and duration. Subject C showed significant reduction in vection

duration but not vection occurrence. As subject B and subject C was not typical motion sickness susceptible or non-susceptible group, the changes in their hemodynamic were not taken into discussion specifically.

7.4 Discussion

From this study, it is shown that adaptation to motion sickness occurred at a relatively early stage of adaptation training, the most susceptible subject adapted to the vection stimuli starting after three times of exposure and less susceptible people adapted after two times of exposure. The adaption is in accordance with existing studies which also stated that motion sickness adaptation occurs quickly after the start of repeated exposure (Golding and Stott, 1995; Stern *et al.*, 1989; Deshmukh, 2007).

Subject D is the only subject who showed clear adaptation to vection induced motion sickness, and illustrated a directional change in HbO level in channel 8, which was shown to be significantly differed between people with different susceptibility to motion sickness. According to the previous studies detecting intracranial structure in reference with 10-20 system (Okamoto *et al.*, 2004), channel 8 is most likely to be located around posterior temporal lobe. This area is proved to be highly related with vestibular functions both in our earlier study and existing studies (Suzuki *et al.*, 2001; Bottini *et al.*, 2001; Fasold *et al.*, 2002). Channel 6 and 7 locate around post/pre-central area (C4 in 10-20 system, BA 3, 6 or 1), which is generally marked as somatosensory cortex and motor cortex. Both channels show directional changes of HbO level in subject D and A. The area also differs much in terms of significance and direction in subject B and C. As all subjects reported a reduction in vection intensity after adaptation training, result also indicates different changes in vection occurrence and duration. The changes around motor area could be explained by the

vection reduction. Channel 10, 11 and 12 locate posterior to middle temporal area (T4 in 10-20 system, BA 21 or 22), thus most likely to be located from middle temporal lobe to posterior temporal lobe. Channel 10 is found to be significantly related with vestibular input in our earlier study, and we could see HbO change is in the same direction as in subject B, C and D in both before and after adaptation training. And all subject show the same direction of HbO level change after adaptation training.

There are also changes in visual area according to the Figure 7.3, Figure 7.4 and **Error! Reference source not found..** Those are beyond the discussion scope of this research.

7.5 Summary

This study investigates the brain hemodynamic change after adaptation to visually induced motion sickness among people with different susceptibility to motion sickness. Subjects show great varieties in adaption in terms of both behavior and result.

The motion sickness susceptible subject showed significant changes in the area which was found to be distinguished between people with different susceptibility to motion sickness. The motion sickness non-susceptible subject no longer showed significant change in the same area, while the subject no longer showed stable and lasting vection during exposure.

CHAPTER 8: CONCLUSION

Conclusions

This research identifies the cortical areas responding to real physical motion and investigates the interacting effects of motion sickness susceptibility on the cortical response to vection provoking stimuli. This research also investigates whether the cortical response would change after the desensitization training among motion sickness susceptible people through a pilot attempt.

The first two experiments in this thesis determine the cortical areas in which the hemodynamic responsive to real physical motion in human beings. Human vestibular system is activated by physical motion naturally; however existing studies generally use vestibular stimuli (caloric stimuli and galvanic stimuli) rather than real motion to identify the brain cortical response to real physical motion due to the limitation in brain imaging technologies. Consequently, the findings in this thesis are new and original. Among sway, lateral and fore-and-aft motions, sway stimulus produces the widest spread significant activations in cortical hemodynamics responses at areas near motor/sensory motor area, temporal parietal region and intraparietal region. These also correspond to Brodmann areas 3, 4, 6, 1(post/pre-central area), 22, 42 (posterior temporal and temporal parietal lobe), and 39, 40 (both locate at parietal cortex). (Chapters 3 and 4)

The brain hemodynamic changes in response to vection are studied among people with different motion sickness susceptibility. The presence of vection is quantified using vection onset and offset time and the motion sickness susceptibility is measured by questionnaires validated within this thesis (Chapter 5).

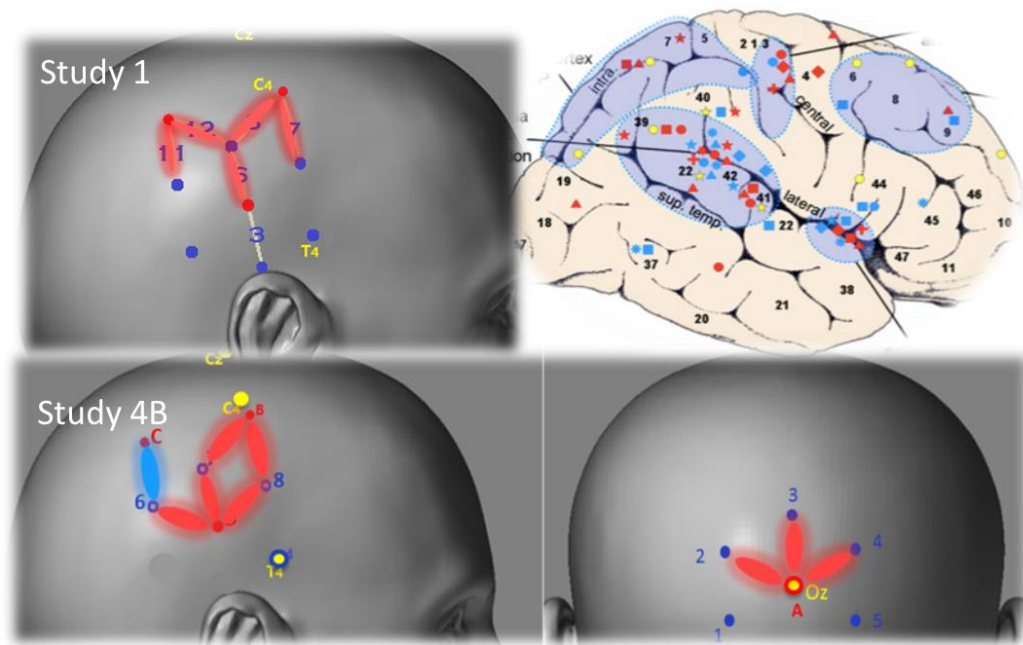


Figure 8.1 A graphical summary of hemodynamic changes in response to the presence ofvection in Study 1 and Study 4B in this thesis. The brain picture on the top righthand corner is adopted from Lopez and Blanke (2011). Red dots on the top righthand corner indicate brain areas which were found to be responsive to caloric stimuli blue dots are those responsive to galvanic stimuli, and yellow dots indicates those responsive to neck vibration. Brodmann area is also shown on the top righthand corner. The purpose of this graph is to illustrate and compare the cortical areas activated in earlier studies (as reported in Lopez and Blanke (2011) and in our studies (Study 1: top lefthand corner; study 4B: lower left and right hand corners).

The major limitations of interpreting the hemodynamic response across different channels are in mapping those channels to the intracranial structures. The identification of the intracranial location is based on studies which provide intracranial reference to 10-20 system (chapter 3 and 6).

According to the previous studies detecting intracranial structure with reference to 10-20 system (Okamoto *et al.*, 2004), Oz mostly locates at around Brodmann Area 18 or 19. C4 and T4 are proved to be located mostly at post/pre-central and middle

temporal area (Okamoto *et al.*, 2004). According to this mapping reference, the cortical activation areas include the sensory motor area, intraparietal region and posterior temporal lobe by swaying motion. Lateral motion activated motor area and intraparietal cortical regions, and, interestingly, no significant cortical areas are found to be activated by fore-and-aft motion.

In study 4B, results indicate that while cortical areas including motor area, visual area and middle/posterior temporal lobe are activated during exposure to vection provoking stimuli, inferior parietal lobe to intra-parietal areas (the channel mark in blue) shows different activation patterns among people with different susceptibility to motion sickness. This finding is consistent with the reciprocal inhibition theory proposed by Brandt *et al.* (1996). This finding is important as it represent the first evidence linking the reciprocal inhibition theory to motion sickness susceptibility (see Chapter 6)

Significant hemodynamic changes are found in inferior parietal lobe to intra-parietal areas within motion sickness susceptible people (Chapter 7). These areas show significant different activations patterns among people with different susceptibility in earlier experiments (see Chapter 6). This pilot study suggests brain hemodynamic signature would change after adaptation training regardless of motion sickness susceptibility. In the meantime, subjects show varied change of behavioral response including occurrence and duration triggered by circular vection. Both brain hemodynamic signature and behavioral response are found to be individualized among different subjects.

Contributions

This research identifies human cortical areas which respond to real physical motion using near infrared spectroscopy. Compared to existing research, cortical areas are

found to respond differently under different motion conditions. As previous studies mainly used non-physical vestibular stimulation, the data reported here is new and original. The findings on hemodynamic changes in different cortical areas during real physical motion could fill the gap of lacking vestibular cortical responses using real physical motion as stimulus. The finding could be integrated with medical and caloric/galvanic studies to illustrate a more detailed locations and functions of cortical areas which are directly related with vestibular system.

Cortical hemodynamic in response tovection provoking stimuli is found to be different among people with different susceptibility to motion sickness. Again, the findings are new and original. The study on effects of VIMS susceptibility is worth repeating with more subjects and it would be a great advantage if fMRI could be utilized as imaging technique. Because one important limitation of our study is the mapping between NIRS channels and brain intracranial structures.

This research also identifies the changes in cortical hemodynamic response after desensitization training among motion sickness susceptible people. Although this pilot attempts only used four participants, data are new and original. The result of this experiment shows how the training could change the hemodynamic response to exactly same stimulus. The adaptation effect lasted long in two of four subjects in our experiment (Both subject felt very minor or novection under same stimulus after they completed the training for months, we lost the tracking of the other two subjects). The training method could be further developed and verified in practical training of pilots and astronauts to gradually build up desensitization training procedure.

BIBLIOGRAPHY

Arridge, S., Schweiger, M., Hiraoka, M., & Delpy, D. (1993). A finite element approach for modeling photon transport in tissue. *Medical Physics*, 20(2), 299-309.

Bear, M. F., Connors, B. W., & Paradiso, M. A. (2007). *Neuroscience* Lippincott Williams & Wilkins.

Benson, A. J. (2002). Motion sickness. *Medical Aspects of Harsh Environments*, 2, 1048-1083.

Blake, R., & Shiffrar, M. (2007). Perception of human motion. *Annu.Rev.Psychol.*, 58, 47-73.

Blamire, A. M., Ogawa, S., Ugurbil, K., Rothman, D., McCarthy, G., Ellermann, J. M., Shulman, R. G. (1992). Dynamic mapping of the human visual cortex by high-speed magnetic resonance imaging. *Proceedings of the National Academy of Sciences of the United States of America*, 89(22), 11069-11073.

Bles, W., Bos, J. E., de Graaf, B., Groen, E., & Wertheim, A. H. (1998). Motion sickness: Only one provocative conflict? *Brain Research Bulletin*, 47(5), 481-487.

Boas, D. A., Dale, A. M., & Franceschini, M. A. (2004). Diffuse optical imaging of brain activation: Approaches to optimizing image sensitivity, resolution, and accuracy. *Neuroimage*, 23, S275-S288.

Boban, M., Črnac, P., Junaković, A., & Malojčić, B. (2014). Hemodynamic monitoring of middle cerebral arteries during cognitive tasks performance. *Psychiatry and Clinical Neurosciences*, 68(11), 795-803.

Borchers, S., Himmelbach, M., Logothetis, N., & Karnath, H. (2011). Direct electrical stimulation of human cortex—the gold standard for mapping brain functions? *Nature Reviews Neuroscience*, 13(1), 63-70.

Borchers, S., Himmelbach, M., Logothetis, N., & Karnath, H. (2012). Direct electrical stimulation of human cortex—the gold standard for mapping brain functions? *Nature Reviews Neuroscience*, 13(1), 63-70.

Bos, J., & Bles, W. (1998). Modelling motion sickness and subjective vertical mismatch detailed for vertical motions. *Brain Research Bulletin*, 47(5), 537-542.

Bottini, G., Karnath, H., Vallar, G., Sterzi, R., Frith, C. D., Frackowiak, R. S., & Paulesu, E. (2001). Cerebral representations for egocentric space Functional–anatomical evidence from caloric vestibular stimulation and neck vibration. *Brain*, 124(6), 1182-1196.

Bozkurt, A., Rosen, A., Rosen, H., & Onaral, B. (2005). A portable near infrared spectroscopy system for bedside monitoring of newborn brain. *Biomedical Engineering Online*, 4(1), 29.

Brandt, T., & Dieterich, M. (1999). The vestibular cortex: Its locations, functions, and disorders. *Annals of the New York Academy of Sciences*, 871(1), 293-312.

Brandt, T., Bartenstein, P., Janek, A., & Dieterich, M. (1998). Reciprocal inhibitory visual-vestibular interaction. visual motion stimulation deactivates the parieto-insular vestibular cortex. *Brain : A Journal of Neurology*, 121 (Pt 9)(Pt 9), 1749-1758.

Brandt, T., Glasauer, S., Stephan, T., Bense, S., Yousry, T. A., Deutschländer, A., & Dieterich, M. (2002). Visual-Vestibular and Visuovisual Cortical Interaction. *Annals of the New York Academy of Sciences*, 956(1), 230-241.

Chance, B., Zhuang, Z., UnAh, C., Alter, C., & Lipton, L. (1993). Cognition-activated low-frequency modulation of light absorption in human brain. *Proceedings of the National Academy of Sciences of the United States of America*, 90(8), 3770-3774.

Cheung, B., & Hofer, K. (2005). Desensitization to strong vestibular stimuli improves tolerance to simulated aircraft motion. *Aviation, Space, and Environmental Medicine*, 76(12), 1099-1104.

Cheung, B., Howard, I., & Money, K. (1991). Visually-induced sickness in normal and bilaterally labyrinthine-defective subjects. *Aviation, Space, and Environmental Medicine*,

Crane, B. T., & Demer, J. L. (1997). Human gaze stabilization during natural activities: Translation, rotation, magnification, and target distance effects. *Journal of Neurophysiology*, 78(4), 2129-2144.

De Waele, C., Baudonnière, P., Lepecq, J., Huy, P. T. B., & Vidal, P. (2001). Vestibular projections in the human cortex. *Experimental Brain Research*, 141(4), 541-551.

Demer, J. L., Oas, J. G., & Baloh, R. W. (1993). Visual-vestibular interaction in humans during active and passive, vertical head movement. *Journal of Vestibular Research: Equilibrium & Orientation*,

Deshmukh, S. (2007). Desensitisation of airsickness in trainee pilots by physical exercise therapy. *Ind J Aerospace Med: Special Commemorative Volume may*, , 38.

Deutschländer, A., Bense, S., Stephan, T., Schwaiger, M., Brandt, T., & Dieterich, M. (2002). Sensory system interactions during simultaneous vestibular and visual stimulation in PET. *Human Brain Mapping*, 16(2), 92-103.

DeYoe, E. A., Bandettini, P., Neitz, J., Miller, D., & Winans, P. (1994). Functional magnetic resonance imaging (fMRI) of the human brain. *Journal of Neuroscience Methods*, 54(2), 171-187.

Dichgans, J., & Brandt, T. (1978). Visual-vestibular interaction: Effects on self-motion perception and postural control. *Perception* (pp. 755-804) Springer.

Dichgans, J., & Brandt, T. (1972). Visual-vestibular interaction and motion perception. *Bibliotheca Ophthalmologica : Supplementa Ad Ophthalmologica*, 82, 327-338.

Dieterich, M., Bense, S., Lutz, S., Drzezga, A., Stephan, T., Bartenstein, P., & Brandt, T. (2003). Dominance for vestibular cortical function in the non-dominant hemisphere. *Cerebral Cortex*, 13(9), 994-1007.

Dobie, T. G., May, J. G., Gutierrez, C., & Heller, S. S. (1991). *The Transfer of Adaptation between Actual and Simulated Rotary Stimulation*,

Ebenholtz, S. M., Cohen, M. M., & Linder, B. J. (1994). The possible role of nystagmus in motion sickness: A hypothesis. *Aviation, Space, and Environmental Medicine*, 65(11), 1032-1035.

Emri, M., Kisely, M., Lengyel, Z., Balkay, L., Marian, T., Miko, L., Toth, A. (2003). Cortical projection of peripheral vestibular signaling. *Journal of Neurophysiology*, 89(5), 2639-2646. doi:10.1152/jn.00599.2002 [doi]

Ersland, L., Rosén, G., Lundervold, A., Smievoll, A. I., Tillung, T., & Sundberg, H. (1996). Phantom limb imaginary fingertapping causes primary motor cortex activation: An fMRI study. *Neuroreport*, 8(1), 207-210.

Eyeson-Annan, M., Peterken, C., Brown, B., & Atchison, D. (1996). Visual and vestibular components of motion sickness. *Aviation, Space, and Environmental Medicine*, 67(10), 955-962.

Farmer, A. D., Ban, V. F., Coen, S. J., Sanger, G. J., Barker, G. J., Gresty, M. A., Hellström, P. M. (2015). Visually induced nausea causes characteristic changes in cerebral, autonomic and endocrine function in humans. *The Journal of Physiology*, 593(5), 1183-1196.

Fasold, O., von Brevern, M., Kuhberg, M., Ploner, C. J., Villringer, A., Lempert, T., & Wenzel, R. (2002). Human vestibular cortex as identified with caloric stimulation in functional magnetic resonance imaging. *Neuroimage*, 17(3), 1384-1393.

Ferrari, M., Giannini, I., Sideri, G., & Zanette, E. (1985). Continuous non invasive monitoring of human brain by near infrared spectroscopy. *Oxygen transport to tissue VII* (pp. 873-882) Springer.

Gagnon, L., Yücel, M. A., Dehaes, M., Cooper, R. J., Perdue, K. L., Selb, J., Boas, D. A. (2012). Quantification of the cortical contribution to the NIRS signal over the motor cortex using concurrent NIRS-fMRI measurements. *Neuroimage*, 59(4), 3933-3940.

Germon, T. J., Evans, P. D., Barnett, N. J., Wall, P., Manara, A. R., & Nelson, R. J. (1999). Cerebral near infrared spectroscopy: Emitter-detector separation must be increased. *British Journal of Anaesthesia*, 82(6), 831-837.

Gilden, D., Blake, R., & Hurst, G. (1995). Neural adaptation of imaginary visual motion. *Cognitive Psychology*, 28(1), 1-16.

Golding, J. F. (1998). Motion sickness susceptibility questionnaire revised and its relationship to other forms of sickness. *Brain Research Bulletin*, 47(5), 507-516.

Golding, J. F. (2006). Motion sickness susceptibility. *Autonomic Neuroscience*, 129(1), 67-76.

Golding, J. F., Kadzere, P., & Gresty, M. A. (2005). Motion sickness susceptibility fluctuates through the menstrual cycle. *Aviation, Space, and Environmental Medicine*, 76(10), 970-973.

Golding, J. F., & Stott, J. R. (1995). Effect of sickness severity on habituation to repeated motion challenges in aircrew referred for airsickness treatment. *Aviation, Space, and Environmental Medicine*, 66(7), 625-630.

Grill-Spector, K., & Malach, R. (2004). The human visual cortex. *Annu.Rev.Neurosci.*, 27, 649-677.

Grosbras, M., Beaton, S., & Eickhoff, S. B. (2012). Brain regions involved in human movement perception: A quantitative voxel-based meta-analysis. *Human Brain Mapping*, 33(2), 431-454.

Guldin, W., & Grüsser, O. (1998). Is there a vestibular cortex? *Trends in Neurosciences*, 21(6), 254-259.

Guo, C., Tsoi, C. W., Wong, Y. L., Yu, K. C., & So, R. (2013). Visually induced motion sickness during computer game playing. *Contemporary Ergonomics and Human Factors 2013: Proceedings of the International Conference on Ergonomics & Human Factors 2013, Cambridge, UK, 15-18 April 2013*, 51.

Gupta, V. K. (2005). Motion sickness is linked to nystagmus-related trigeminal brain stem input: A new hypothesis. *Medical Hypotheses*, 64(6), 1177-1181.

Hock, C., Villringer, K., Müller-Spahn, F., Wenzel, R., Heekeren, H., Schuh-Hofer, S., Dirnagl, U. (1997). Decrease in parietal cerebral hemoglobin oxygenation during performance of a verbal fluency task in patients with alzheimer's disease monitored by means of near-infrared spectroscopy (NIRS)—correlation with simultaneous rCBF-PET measurements. *Brain Research*, 755(2), 293-303.

Hofmann, M. J., Herrmann, M. J., Dan, I., Obrig, H., Conrad, M., Kuchinke, L., Fallgatter, A. J. (2008). Differential activation of frontal and parietal regions during visual word recognition: An optical topography study. *Neuroimage*, 40(3), 1340-1349.

- Homan, R. W., Herman, J., & Purdy, P. (1987). Cerebral location of international 10–20 system electrode placement. *Electroencephalography and Clinical Neurophysiology*, 66(4), 376-382.
- Hoshi, Y., & Tamura, M. (1997). Fluctuations in the cerebral oxygenation state during the resting period in functional mapping studies of the human brain. *Medical and Biological Engineering and Computing*, 35(4), 328-330.
- Hoshi, Y. (2003). Functional near-infrared optical imaging: Utility and limitations in human brain mapping. *Psychophysiology*, 40(4), 511-520.
- Hoshi, Y., & Tamura, M. (1997). Near-infrared optical detection of sequential brain activation in the prefrontal cortex during mental tasks. *Neuroimage*, 5(4), 292-297.
- Howarth, P. A., & Hodder, S. G. (2008). Characteristics of habituation to motion in a virtual environment. *Displays*, 29(2), 117-123.
- Huppert, T. J., Diamond, S. G., Franceschini, M. A., & Boas, D. A. (2009). HomER: A review of time-series analysis methods for near-infrared spectroscopy of the brain. *Applied Optics*, 48(10), D280-D298.
- Huppert, T., Hoge, R., Diamond, S., Franceschini, M. A., & Boas, D. A. (2006). A temporal comparison of BOLD, ASL, and NIRS hemodynamic responses to motor stimuli in adult humans. *Neuroimage*, 29(2), 368-382.
- Jasdzewski, G., Strangman, G., Wagner, J., Kwong, K., Poldrack, R., & Boas, D. (2003). Differences in the hemodynamic response to event-related motor and visual paradigms as measured by near-infrared spectroscopy. *Neuroimage*, 20(1), 479-488.
- Jasper, H. (1958). The 10/20 international electrode system. *EEG and Clinical Neurophysiology*, 10, 371-375.

Jobsis, F. F. (1977). Noninvasive, infrared monitoring of cerebral and myocardial oxygen sufficiency and circulatory parameters. *Science (New York, N.Y.)*, 198(4323), 1264-1267.

Kahane, P., Hoffmann, D., Minotti, L., & Berthoz, A. (2003). Reappraisal of the human vestibular cortex by cortical electrical stimulation study. *Annals of Neurology*, 54(5), 615-624.

Kato, T., Kamei, A., Takashima, S., & Ozaki, T. (1993). Human visual cortical function during photic stimulation monitoring by means of near-infrared spectroscopy. *Journal of Cerebral Blood Flow and Metabolism : Official Journal of the International Society of Cerebral Blood Flow and Metabolism*, 13(3), 516-520. doi:10.1038/jcbfm.1993.66 [doi]

Kennedy, R. S., & Frank, L. H. (1985). *A Review of Motion Sickness with Special Reference to Simulator Sickness*,

Keshavarz, B., & Hecht, H. (2012). Visually induced motion sickness and presence in videogames: The role of sound. *Proceedings of the Human Factors and Ergonomics Society Annual Meeting*, , 56(1) 1763-1767.

Keshavarz, B., Riecke, B. E., Hettinger, L. J., & Campos, J. L. (2015). Vection and visually induced motion sickness: How are they related? *Frontiers in Psychology*, 6, 472.

Klosterhalfen, S., Kellermann, S., Pan, F., STÖCKHORST, U., Hall, G., & ENCK, P. (2005). Effects of ethnicity and gender on motion sickness susceptibility. *Aviation, Space, and Environmental Medicine*, 76(11), 1051-1057.

Klosterhalfen, S., Muth, E. R., Kellermann, S., Meissner, K., & Enck, P. (2008). Nausea induced by vection drum: Contributions of body position, visual pattern, and gender. *Aviation, Space, and Environmental Medicine*, 79(4), 384-389.

Koban, L., Ninck, M., Li, J., Gisler, T., & Kissler, J. (2010). Processing of emotional words measured simultaneously with steady-state visually evoked potentials and near-infrared diffusing-wave spectroscopy. *BMC Neuroscience*, 11(1), 85.

Kohl, R. L. (1983). Sensory conflict theory of space motion sickness: An anatomical location for the neuroconflict. *Aviation, Space, and Environmental Medicine*,

Lobel, E., Kleine, J. F., Le Bihan, D., Leroy-Willig, A., & Berthoz, A. (1998). Functional MRI of galvanic vestibular stimulation. *Journal of Neurophysiology*, 80(5), 2699-2709.

Lobel, E., Kleine, J. F., Bihan, D. L., Leroy-Willig, A., & Berthoz, A. (1998). Functional MRI of galvanic vestibular stimulation. *Journal of Neurophysiology*, 80(5), 2699-2709.

Lopez C, Blanke O. The thalamocortical vestibular system in animals and humans[J]. *Brain research reviews*, 2011, 67(1): 119-146.

MacDonald, S. W., Nyberg, L., & Bäckman, L. (2006). Intra-individual variability in behavior: Links to brain structure, neurotransmission and neuronal activity. *Trends in Neurosciences*, 29(8), 474-480.

Mansouri, C., & Kashou, N. H. (2012). New window on optical brain imaging; medical development, simulations and applications.

Marcelli, V., Esposito, F., Aragri, A., Furia, T., Riccardi, P., Tosetti, M., . . . Di Salle, F. (2009). Spatio-temporal pattern of vestibular information processing after brief caloric stimulation. *European Journal of Radiology*, 70(2), 312-316.

Matsuo, K., Kato, N., & Kato, T. (2002). Decreased cerebral haemodynamic response to cognitive and physiological tasks in mood disorders as shown by near-infrared spectroscopy. *Psychological Medicine*, 32(06), 1029-1037.

Meissner, K., Enck, P., Muth, E., Kellermann, S., & Klosterhalfen, S. (2009). Cortisol levels predict motion sickness tolerance in women but not in men. *Physiology & Behavior*, 97(1), 102-106.

Money, K. (1969). *Motion Sickness*,

Murkin, J. M., & Arango, M. (2009). Near-infrared spectroscopy as an index of brain and tissue oxygenation. *British Journal of Anaesthesia*, 103 Suppl 1, i3-13. doi:10.1093/bja/aep299 [doi]

Nolan, H., Butler, J., Whelan, R., Foxe, J., Bülthoff, H., & Reilly, R. (2012). Neural correlates of oddball detection in self-motion heading: A high-density event-related potential study of vestibular integration. *Experimental Brain Research*, 219(1), 1-11.

Obrig, H., Neufang, M., Wenzel, R., Kohl, M., Steinbrink, J., Einhüpl, K., & Villringer, A. (2000). Spontaneous low frequency oscillations of cerebral hemodynamics and metabolism in human adults. *Neuroimage*, 12(6), 623-639.

O'Hanlon, J. F., & McCauley, M. E. (1973). *Motion Sickness Incidence as a Function of the Frequency and Acceleration of Vertical Sinusoidal Motion*,

Okamoto, M., Dan, H., Sakamoto, K., Takeo, K., Shimizu, K., Kohno, S., Kohyama, K. (2004). Three-dimensional probabilistic anatomical cranio-cerebral correlation via the international 10–20 system oriented for transcranial functional brain mapping. *Neuroimage*, 21(1), 99-111.

Okamoto, M., Dan, H., Shimizu, K., Takeo, K., Amita, T., Oda, I., Suzuki, T. (2004). Multimodal assessment of cortical activation during apple peeling by NIRS and fMRI. *Neuroimage*, 21(4), 1275-1288.

Oman, C. M. (1990). Motion sickness: A synthesis and evaluation of the sensory conflict theory. *Canadian Journal of Physiology and Pharmacology*, 68(2), 294-303.

Osharina, V., Ponchel, E., Aarabi, A., Grebe, R., & Wallois, F. (2010). Local haemodynamic changes preceding interictal spikes: A simultaneous electrocorticography (ECoG) and near-infrared spectroscopy (NIRS) analysis in rats. *Neuroimage*, 50(2), 600-607.

Owen, N., Leadbetter, A. G., & Yardley, L. (1998). Relationship between postural control and motion sickness in healthy subjects. *Brain Research Bulletin*, 47(5), 471-474.

Paillard, A., Quarck, G., Paolino, F., Denise, P., Paolino, M., Golding, J. F., & Ghulyan-Bedikian, V. (2013). Motion sickness susceptibility in healthy subjects and vestibular patients: Effects of gender, age and trait-anxiety. *Journal of Vestibular Research*, 23(4, 5), 203-209.

Pelphrey, K. A., Mitchell, T. V., McKeown, M. J., Goldstein, J., Allison, T., & McCarthy, G. (2003). Brain activity evoked by the perception of human walking: Controlling for meaningful coherent motion. *The Journal of Neuroscience : The Official Journal of the Society for Neuroscience*, 23(17), 6819-6825. doi:23/17/6819 [pii]

Philbeck, J. W., Behrmann, M., Biega, T., & Levy, L. (2006). Asymmetrical perception of body rotation after unilateral injury to human vestibular cortex. *Neuropsychologia*, 44(10), 1878-1890.

Reason, J. (1968). Relations between motion sickness susceptibility, the spiral after-effect and loudness estimation. *British Journal of Psychology*, 59(4), 385-393.

Reason, J. T. (1978). Motion sickness adaptation: A neural mismatch model. *Journal of the Royal Society of Medicine*, 71(11), 819-829.

Riecke, B. E., Schulte-Pelkum, J., Caniard, F., & Bühlhoff, H. H. (2005). Influence of auditory cues on the visually-induced self-motion illusion (circular vection) in virtual reality. *Proceedings of Eighth Annual Workshop Presence*,

Rine, R. M., Schubert, M. C., & Balkany, T. J. (1999). Visual-vestibular habituation and balance training for motion sickness. *Physical Therapy*, 79(10), 949-957.

Rokszin, A., Márkus, Z., Braunitzer, G., Berényi, A., Benedek, G., & Nagy, A. (2010). Visual pathways serving motion detection in the mammalian brain. *Sensors*, 10(4), 3218-3242.

Sang, Y. P., Fleur, D., Golding, J. F., & Gresty, M. A. (2003). Suppression of sickness by controlled breathing during mildly nauseogenic motion. *Aviation, Space, and Environmental Medicine*, 74(9), 998-1002.

Scholkmann, F., Spichtig, S., Muehlemann, T., & Wolf, M. (2010). How to detect and reduce movement artifacts in near-infrared imaging using moving standard deviation and spline interpolation. *Physiological Measurement*, 31(5), 649.

Seemungal, B. M., Guzman-Lopez, J., Arshad, Q., Schultz, S. R., Walsh, V., & Yousif, N. (2013). Vestibular activation differentially modulates human early visual cortex and V5/MT excitability and response entropy. *Cerebral Cortex (New York, N.Y.: 1991)*, 23(1), 12-19. doi:10.1093/cercor/bhr366 [doi]

Simpson, J. I., Leonard, C., & Soodak, R. (1988). The accessory optic system analyzer of Self-Motiona. *Annals of the New York Academy of Sciences*, 545(1), 170-179.

Smart, L. J., Jr, Stoffregen, T. A., & Bardy, B. G. (2002). Visually induced motion sickness predicted by postural instability. *Human Factors*, 44(3), 451-465.

Smither, J. A., Mouloua, M., & Kennedy, R. (2008). Reducing symptoms of visually induced motion sickness through perceptual training. *The International Journal of Aviation Psychology*, 18(4), 326-339.

So, R. H., Finney, C. M., & Goonetilleke, R. S. (1999). Motion sickness susceptibility and occurrence in hong kong chinese. *Contemporary Ergonomics*, , 88-92.

So, R. H., & Ujike, H. (2010). Visually induced motion sickness, visual stress and photosensitive epileptic seizures: What do they have in common?—Preface to the special issue. *Applied Ergonomics*, 41(4), 491-493.

Stephan, T., Deutschländer, A., Nolte, A., Schneider, E., Wiesmann, M., Brandt, T., & Dieterich, M. (2005). Functional MRI of galvanic vestibular stimulation with alternating currents at different frequencies. *Neuroimage*, 26(3), 721-732.

Stephan, T., Hübner, K., & Brandt, T. (2009). Stimulus profile and modeling of continuous galvanic vestibular stimulation in functional magnetic resonance imaging. *Annals of the New York Academy of Sciences*, 1164(1), 472-475.

Stern, R. M., Hu, S., Vasey, M. W., & Koch, K. L. (1989). Adaptation tovection-induced symptoms of motion sickness. *Aviation, Space, and Environmental Medicine*,

Strangman, G., Boas, D. A., & Sutton, J. P. (2002). Non-invasive neuroimaging using near-infrared light. *Biological Psychiatry*, 52(7), 679-693.

Stroud, K. J., Harm, D. L., & Klaus, D. M. (2005). Preflight virtual reality training as a countermeasure for space motion sickness and disorientation. *Aviation, Space, and Environmental Medicine*, 76(4), 352-356.

Sunaert, S., Van Hecke, P., Marchal, G., & Orban, G. A. (1999). Motion-responsive regions of the human brain. *Experimental Brain Research*, 127(4), 355-370.

Suzuki, M., Kitano, H., Ito, R., Kitanishi, T., Yazawa, Y., Ogawa, T., Kitajima, K. (2001). Cortical and subcortical vestibular response to caloric stimulation detected by functional magnetic resonance imaging. *Cognitive Brain Research*, 12(3), 441-449.

Tak, S., & Ye, J. C. (2014). Statistical analysis of fNIRS data: A comprehensive review. *Neuroimage*, 85, 72-91.

Ujike, H. (2009). Estimation of visually induced motion sickness from velocity component of moving image. *International Conference on Virtual and Mixed Reality*, 136-142.

Uliano, K., Lambert, E., Kennedy, R., & Sheppard, D. (1986). *The Effects of Asynchronous Visual Delays on Simulator Flight Performance and the Development of Simulator Sickness Symptomatology*,

Wenzel, R., Bartenstein, P., Dieterich, M., Danek, A., Weindl, A., Minoshima, S., Brandt, T. (1996). Deactivation of human visual cortex during involuntary ocular oscillations. A PET activation study. *Brain : A Journal of Neurology*, 119 (Pt 1)(Pt 1), 101-110.

Werkhoven, P., Snippe, H. P., & Alexander, T. (1992). Visual processing of optic acceleration. *Vision Research*, 32(12), 2313-2329.

Young, L. R., & Merfeld, D. (1994). Visual-vestibular interaction.

APPENDIX A: NEAR-INFRARED SPECTROSCOPY MEASUREMENT SYSTEM

Imagent ISS is utilized as the optical imaging system which generates near-infrared light and takes measurement in the series of experiments in this research. Imagent ISS is a multichannel frequency-domain based near-infrared spectroscopy measurement system. It captures the intensity change of diffusely scattered near-infrared light, and the changes of oxygenated hemoglobin (HbO) and deoxygenated hemoglobin (Hb) concentration could be calculated based on the modified Beer-Lambert Law.



Figure A.1 Imagent ISS: near-infrared spectroscopy system. The Imagent ISS was adopted for NIRS measurement in all our experiments. The system has 4 NIR detectors and 8 pairs of NIR transmitters (one pair contains transmitters of two wavelengths).

Imagent ISS adopts a standard modulation frequency of 110MHz, and the light power is about 1mW on average. The signals are collected separately in two working

wavelengths, 690 and 830nm. Our Imagent ISS system has 16 laser-diodes, half is in 690nm and the other half is in 830nm. Each 690nm and 830nm laser-diodes are coupled to function as one light source. It also has four photomultiplier tube detectors. These detectors are time multiplexed and are sensitive to Pico watts.

In this research, Imagent system works as the hemodynamic measurement system, different pair up of detectors and light transmitters is adopted in experiments to meet different needs of measurement. Sampling frequency is set to be 12.5Hz.

The optical fibers are used to transmit near infrared light from light source to measurement site. One end of optical fiber is coupled to laser-diodes using SMA905 connector, and the other end of optical fibers are left bare. In Imagent ISS system, the numerical aperture of optical fibers needs to be high, as it is less sensitive to bending. And the core diameter of optical fiber needs to be larger than 400 μm in order to couple to laser-diodes. The numerical aperture is around 0.5 and the core diameter is 400 μm in our experiment. The detector is made up of hundreds of optical fibers with tiny core diameters (around 20 μm). Its numerical aperture is around 0.55 to 0.6. The core diameter of the detector is 3mm.

APPENDIX B: MOTION SIMULATOR

The motion simulator locates at CLP Power Wind/Water Tunnel Facility in the Hong Kong University of Science and Technology. A 4m x 3m fully enclosed test platform was supported on two pairs of custom-built sliding bearings riding on the precision machined and leveled rails. It could move ± 800 mm along the long axis and ± 400 mm along the short axis. The motion could be bi-directional narrow band random motions. The maximum acceleration could be generated is around 30 milli-g and the frequency range is 0.05 to 1 Hz.



Figure B.1 A photo of the motion simulator used in the study. The motion simulator could move along the fore-and-aft axis (x) and lateral axis (y). It is designed and built in house at HKUST. The actuation is electromagnetic.

The motion in this experiment is achieved by inputting the coordination file for both axis. The motion parameters must be set within the range of motion simulator capability. Smoothing function should be applied to avoid discrepancy in acceleration

especially during the starting and ending period of motion because jerks could be sensed if acceleration is not continuous.

APPENDIX C: MSSQ-SHORT

1. Please State Your Age Years.

2. Please State Your Sex (tick box) Male Female
[] []

This questionnaire is designed to find out how susceptible to motion sickness you are, and what sorts of motion are most effective in causing that sickness. Sickness here means feeling queasy or nauseated or actually vomiting.

Your CHILDHOOD Experience Only (before 12 years of age), for each of the following types of transport or entertainment please indicate:

3. As a CHILD (before age 12), how often you Felt Sick or Nauseated (tick boxes):

	Not Applicable - Never Travelled	Never Felt Sick	Rarely Felt Sick	Sometimes Felt Sick	Frequently Felt Sick
Cars					
Buses or Coaches					
Trains					
Aircraft					
Small Boats					
Ships, e.g. Channel Ferries					
Swings in playgrounds					
Roundabouts in playgrounds					
Big Dippers, Funfair Rides					

Your Experience over the LAST 10 YEARS (approximately), for each of the following types of transport or entertainment please indicate:

4. Over the LAST 10 YEARS, how often you Felt Sick or Nauseated (tick boxes):

	Not Applicable - Never Travelled	Never Felt Sick	Rarely Felt Sick	Sometimes Felt Sick	Frequently Felt Sick
Cars					
Buses or Coaches					
Trains					
Aircraft					
Small Boats					
Ships, e.g. Channel Ferries					
Swings in playgrounds					
Roundabouts in playgrounds					
Big Dippers, Funfair Rides					

Scoring the MSSQ- Short

Section A (Child) (Question 3)

Score the number of types of transportation not experienced (i.e., total the number of ticks in the 't' column, maximum is 9).

Total the sickness scores for each mode of transportation, i.e. the nine types from 'cars' to 'big dippers' (use the 0-3 number score key at bottom, those scores in the 't' column count as zeroes).

MSA = (total sickness score child) x (9) / (9 - number of types not experienced as a child)

Note 1. Where a subject has not experienced any forms of transport a division by zero error occurs. It is not possible to estimate this subject's motion sickness susceptibility in the absence of any relevant motion exposure.

Note 2. The Section A (Child) score can be used as a pre-morbid indicator of motion sickness susceptibility in patients with vestibular disease.

Section B (Adult) (Question 4)

Repeat as for section A but using the data from section B.

MSB = (total sickness score adult) x (9) / (9 - number of types not experienced as an adult)

Raw Score MSSQ-Short

Total the section A (Child) MSA score and the section B (Adult) MSB score to give the MSSQ-Short raw score (possible range from minimum 0 to maximum 54, the maximum being unlikely)

MSSQ raw score = MSA + MSB

Percentile Score MSSQ-Short

The raw to percentile conversions are given below in the Table of Statistics & Figure, use interpolation where necessary.

Alternatively a close approximation is given by the fitted polynomial where y is percentile; x is raw score
 $y = a.x + b.x^2 + c.x^3 + d.x^4$
 a = 5.1160923 b = -0.055169904
 c = -0.00067784495 d = 1.0714752e-005

Table of Means and Percentile Conversion Statistics for the MSSQ-Short (n=257)

Percentiles Conversion	Raw Scores MSSQ-Short		
	Child Section A	Adult Section B	Total A+B
0	0	0	0
10	.0	.0	.8
20	2.0	1.0	3.0
30	4.0	1.3	7.0
40	5.6	2.6	9.0
50	7.0	3.7	11.3
60	9.0	6.0	14.1
70	11.0	7.0	17.9
80	13.0	9.0	21.6
90	16.0	12.0	25.9
95	20.0	15.0	30.4
100	23.6	21.0	44.6
Mean	7.75	5.11	12.90
Std. Deviation	5.94	4.84	9.90

Table note: numbers are rounded

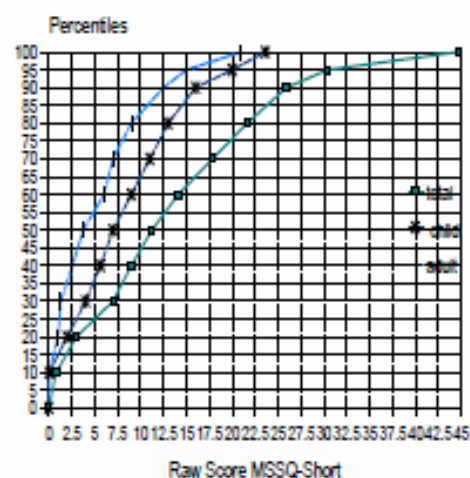


Figure: Cumulative distribution Percentiles of the Raw Scores of the MSSQ-Short (n=257 subjects).

Reference Note

For more background information and references to the original Reason & Brand MSSQ and to its revised version the 'MSSQ-Long', see:
 Golding JF. Motion sickness susceptibility questionnaire revised and its relationship to other forms of sickness. *Brain Research Bulletin*, 1998; 47: 507-516.
 Golding JF. (2006) Predicting Individual Differences in Motion Sickness Susceptibility by Questionnaire. *Personality and Individual differences*, 41: 237-248.

APPENDIX D: CONSENT FORM

Consent Form For Human Factors Experiment Participation

1. Name _____ Age _____
2. Are you feeling ill in any way? Yes/No
3. Do you suffer from diabetes epilepsy (癲癇症) or other neurological diseases? Yes/No
4. Are you under medical treatment? Yes/No
5. Have you had any intake of alcohol (飲酒) during past 24 hours? Yes / No
6. Have you had injuries or over-exercises during the past 24 hours that will affect your postural stability or perception? Yes / No

If your answer is "Yes" to question (2) to (6), please give details to the Experimenter.

DECLARATION

I consent to take part in the experiment. My replies to the above questions are correct to the best of my belief, and I understand that they will be treated as confidential by the experimenter.

I understand that I may at any time withdraw from the experiment and that I am under no obligation to give reasons for withdraw declared above.

I undertake to obey the regulations of the laboratory and instructions of the experimenter regarding safety only to my right to withdraw declared above.

The purpose and methods of the experiment have been explained to me and I have had the opportunity to ask questions.

I know I will get **50HKD/h** for compensation of participation.

Signature of Subject _____ Date _____

This experiment conforms to the requirement of the University Research Ethic Committee.

Signature of Experimenter _____ Date _____

Starting time _____ Finish time _____

APPENDIX E: DATA ANALYZE PROCEDURE

After the NIRS data collection, the raw data are processed in following procedure.

Step 1: Converting from raw data to HomER package.

HomER data package contains six fields which are used in HbO concentration calculation. The fields are 'd', 't', 'aux', 's', 'ml' and 'SD'. The field 'd' contains DC data which were picked up directly from the NIRS measurement data. The data selection was conducted according to the detector-light emitter pair settings. For example, A-DC5 will be selected if detector A is paired with light emitter 5. The field 't' contains the time stamp of each data collection point, which is determined by NIRS sampling frequency. The field 'aux' records the auxiliary measurement. In our experiments, the plethymograph data was recorded in aux field. The field 's' marks the stimulus onset time which is in reference with the field 't'. The field 'ml' contains the pair-up information between the light and emitter. The field 'SD' records the wavelength of near-infrared light, and the coordinates of all the light emitters and detectors. The selected data are packed into .nirs package and are ready to be loaded to HomER.

After loading package to HomER, each channel could be viewed separately with light emitter- detector location and stimulus which were defined in package. Below figure is an illustration of collected NIRS data for the green channel marked in the right panel (Figure E.1). The graph on the left side shows how light intensity change with time. The horizontal axis represents the time in seconds and the vertical axis represents the light intensity level. In this package, green vertical line marks the

onset of stimuli in each block. The graph on the right side shows how detectors and light transmitters are located. 'O' represents the detector location and 'X' represents the light transmitter locations. Both axis are in centimeters.

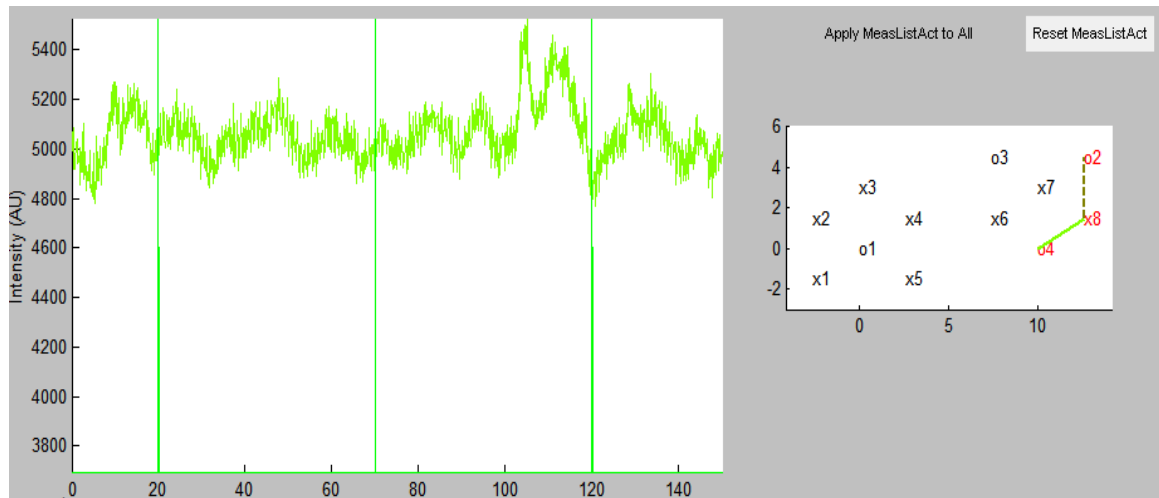


Figure E.1 The raw discrete time history a single wavelength near-infra red (NIR) light intensity data measured by the detector ('O4') when transmitter X8 was emitting NIR of 830nm wavelength. Data were plotted in the HomER analysis software. The Purpose is to illustrate what the raw data look like. The diagram on the right illustrate the relative location of channels

Step 2: heart rate pattern screening

The heart rate pattern could be illustrated from the NIRS data directly. Below figure shows how the heart rate pattern looks like from raw data (Figure E.2). The data is taken from a single channel of a subject. There're two methods to conduct heart rate pattern screening. One is to check the raw data directly, the other method is to look at the powder density function of the raw data.

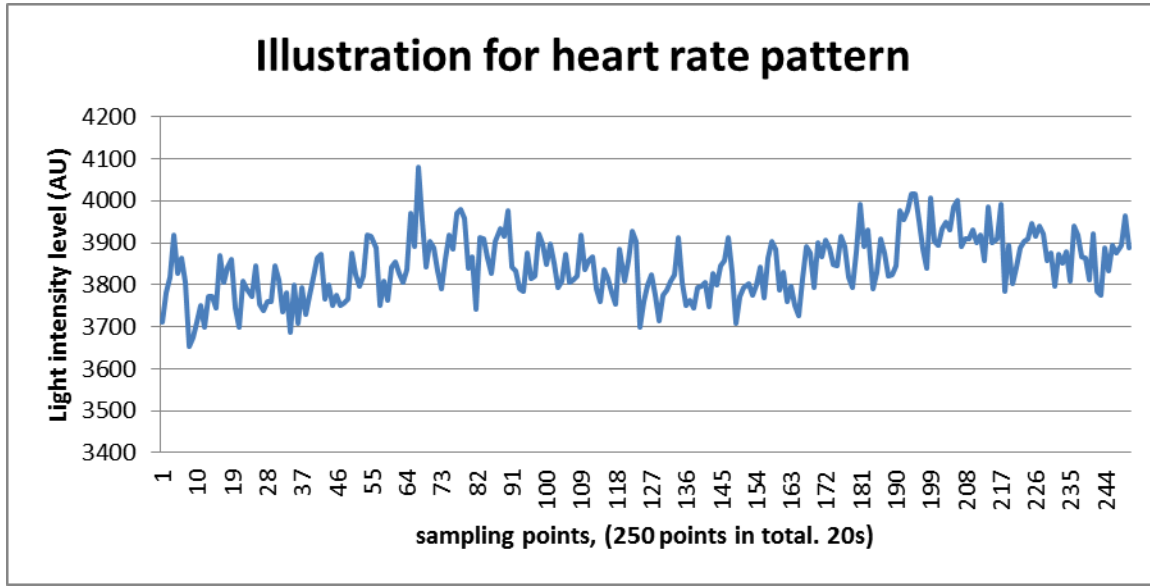


Figure E.2 This figure shows the heart rate pattern look-alike wave forms as observed in the raw NIR light intensity data. The purpose of the figure is to illustrate how the heart rate signals were picked up by the NIR raw data. If a channel did not have heart rate signal, we concluded that the channel is dead. The most possible reason was hair blockage.

Step 3: Artifact recognition:

The motion artifact recognition in this experiment is detected by two-sided standard moving deviation (Scholkmann *et al.*, 2010). Motion artifact is mostly caused by sudden shift of light emitters and detectors. Below figure shows the artifact selection of the channel loaded in HomER (Figure E.3). The peaks raise above the black line is considered to be caused by motion artifact. The blocks containing motion artifact will be excluded from the future analysis. The equation for calculating two-sided standard moving deviation is listed as below:

$$s(t) = \frac{1}{2k+1} \left[\sum_{j=-k}^k x^2(t+j) - \frac{1}{2k+1} \left(\sum_{j=-k}^k x(t+j) \right)^2 \right]^{\frac{1}{2}}$$

$S(t)$ is the standard moving deviation at time t , k standards for the half-window length from which the whole window is made up. The whole window included one center point at time t and two half windows which are taken from the left and right side of t . so the whole window length is $2K + 1$. x is the raw data collection from NIRS measurement.

Windowing of moving standard deviation is based on outliers detection during a smoothing process. If the window length is set to be very short, it is extensively sensitive to sudden shifts and less sensitive to large trend shift. And the larger the window length is, the lower identification ability for sudden shifts could be achieved as the data will be smoother. However, the long window is very useful in detecting the large trend shifts. In our experiment, the window length is set to be 2 seconds.

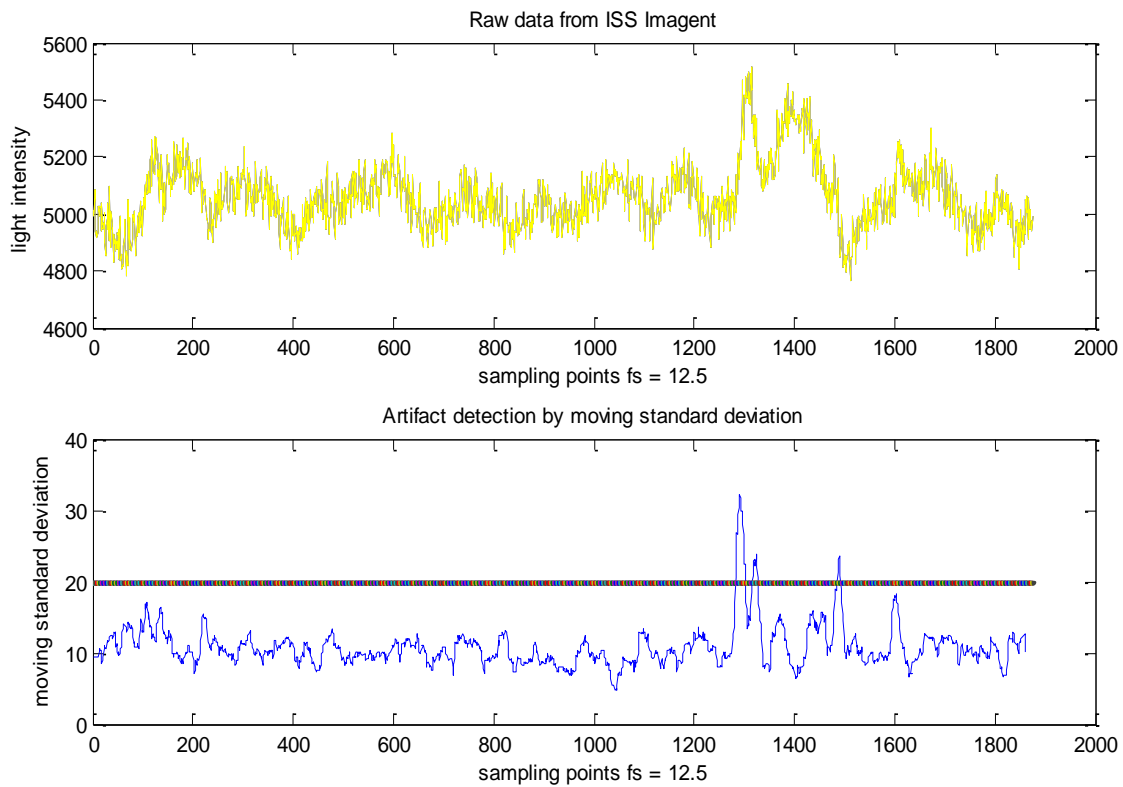


Figure E.3 An illustration of the artifact detection procedure for one single channel. The top figure shows the raw light intensity data and the figure below shows the moving standard deviation (SD). As the SD value went above the threshold as represented by the horizontal line represents the threshold calculated from the raw data. The points raised above the threshold are treated as artifact contaminated sampling points. The threshold was data driven and was set at 2.5 times of the average SD within a time window of 2s. A sensitivity analysis was conducted on using a threshold of 2 times SD, 1.5 times SD and the main finding did NOT change.

The block containing motion artifact will be removed. A block is removed by disabling the stimuli indication line from the GUI (in red dot lines). Below figure shows the third block is disabled, as motion artifact was detected using the two-sided moving standard deviation method (Figure E.4).

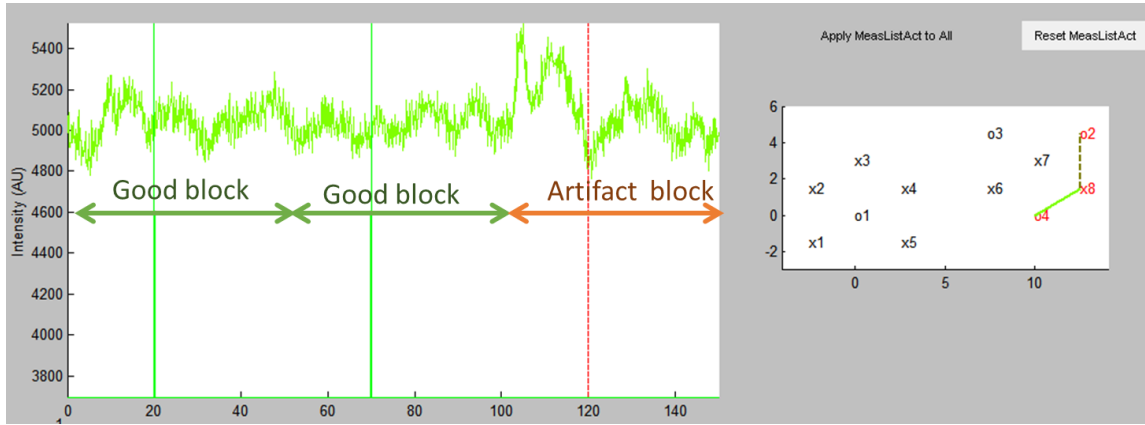


Figure E.4 The blocks could be disabled from HomER software directly. Those blocks would not be taken into average in further calculation steps (meanwhile those blocks could be shown in the plots of raw sampling points). The purpose of this figure is to show HomER illustration of raw sampling points and how the channel is excluded from the further calculation in HomER .

The concentration of HbO and Hb is calculated in HomER. The raw intensity is first normalized (normalized data will go through filtering as in step 4), and change in optical density is then calculated separately for each wavelength. Finally the HbO and Hb concentration could be derived from below equation:

$$\Delta OD_{\text{Lambda}\#1} = \varepsilon_{\text{Hb}}^{\text{Lambda}\#1} * L * [\text{Hb}] + \varepsilon_{\text{HbO}_2}^{\text{Lambda}\#1} * L * [\text{HbO}_2]$$

$$\Delta OD_{\text{Lambda}\#2} = \varepsilon_{\text{Hb}}^{\text{Lambda}\#2} * L * [\text{Hb}] + \varepsilon_{\text{HbO}_2}^{\text{Lambda}\#2} * L * [\text{HbO}_2]$$

Step 4: Filtering and averaging

The raw data will go through filter in HomER, in our experiment, we used Butterworth 3rd order filter in HomER settings. The Butterworth filtering could be set up from HomER GUI directly.

The averaging between different blocks could be calculated either from same data file or across multiple data files. Disabled blocks were excluded from calculating the average. Below figure illustrates different data files could be loaded at the same time, and all valid blocks in those data files could be taken into average calculating in one shot. In experiment one, valid blocks from single data file were taken into average HbO/Hb calculation. In the experiment 4A and 5, valid blocks from multiple data files were taken into the averaging of HbO/Hb concentration change.

Below figure shows the illustration of average HbO level change (Figure E.5). The horizontal axis illustrates the time, which is related with how stimulus was recorded in the field 's'. In our experiments, the starting of stimulus on set was marked with time zero. The calculated HbO concentration of all channels could be exported from HomER software directly. The output will be utilized in future statistical analysis.

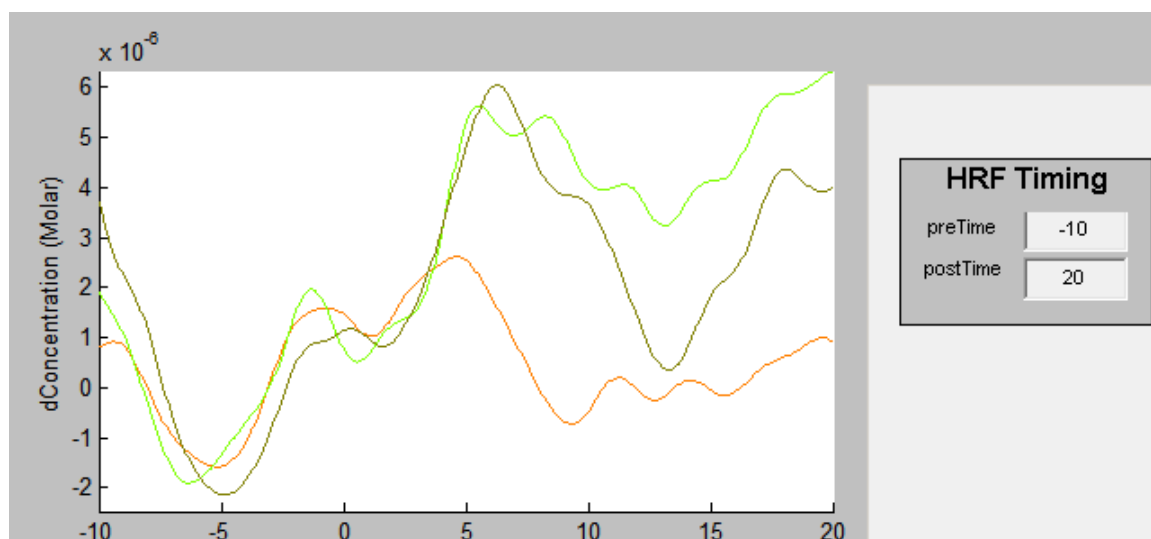


Figure E.5 An illustration of averaged change of HbO across all blocks excluding motion artifact contaminated blocks. Time 0 in the horizontal axis represents stimulus onset. The unit in the horizontal axis is in seconds. The different color curves represent data from different channels.

Step 5: statistical analysis

ANOVA analysis and Wilcoxon sign-rank test would be conducted on the HbO concentration change. According to the experiment design, level of factors and response are further organized into SPSS. Wilcoxon sign-rank test would be also conducted if data showed poor normality.